

JSCSEN 74(2)103–221(2009)

Journal of the Serbian Chemical Society

Electronic
version

VOLUME 74

No 2

BELGRADE 2009

Available on line at



www.shd.org.rs/JSCS

The full search of JSCS
is available through

DOAJ DIRECTORY OF
OPEN ACCESS
JOURNALS
www.doaj.org





CONTENTS

Organic Chemistry and Biochemistry

- A. Husain, M. Mumtaz Alam and N. Siddiqui: Synthesis, reactions and biological activity of 3-arylidene-5-(4-methylphenyl)-2(3H)-furanones 103
- V. Tešević, N. Nikićević, S. Milosavljević, D. Bajić, V. Vajs, I. Vučković, Lj. Vujisić, I. Dorđević, M. Stanković and M. Veličković: Characterization of volatile compounds of “Drenja”, an alcoholic beverage obtained from the fruits of cornelian cherry 117
- M. Arfan, N. Raziq, I. Aljančić and S. Milosavljević: Secondary metabolites of *Hypericum monogynum* from Pakistan (Short communication) 129
- P. M. Mishra and A. Sree: Comparison of the antibacterial activity, volatiles and fatty acid composition of lipids of *Phycopsis* species collected at different locations from the Bay of Bengal (Orissa coast)..... 133

Inorganic Chemistry

- K. Shahid, S. Shahzadi and S. Ali: Synthesis, coordination and biological aspects of organotin(IV) derivatives of 4-[(2,4-dinitrophenyl)amino]-4-oxo-2-butenoic acid and 2-[(2,4-dinitrophenyl)amino]carbonyl}benzoic acid 141

Theoretical Chemistry

- S. Radenković and I. Gutman: Stability order of isomeric benzenoid hydrocarbons and Kekulé structure count (Short communication)..... 155

Physical Chemistry

- M. Mazloum-Ardakani, S. Lotfi, J. Ghasemi, A. Shababi and M. Noroozi: Spectrophotometric determination of the acidity constants of calcon in water and mixed water-organic solvents..... 159
- G. Rajarajan, N. Jayachandramani, S. Manivarman, J. Jayabharathi and V. Thanikachalam: Kinetics and mechanism of the oxidation of some substituted aldonitrone by quinolinium chlorochromate in aqueous DMF medium in the absence and presence of oxalic acid 171

Electrochemistry

- B. Bogdanović, M. Felderhoff and G. Streukens: Hydrogen storage in complex metal hydrides (Review)..... 183
- H. Jia, S. Chen, B. Yuan, C. Wang and L. Li: Mapping the concentration changes during the dynamic processes of crevice corrosion by digital holographic reconstruction (Short communication) 197

Metallurgy

- M. Britchi, N. Ene, M. Olteanu and C. Radovici: Titanium diffusion coatings on austenitic steel obtained by the pack cementation method 203
- V. B. Cvetkovski, V. T. Conić, M. Vuković and M. V. Cvetkovska: Mesophilic leaching of copper sulphide sludge..... 213

Published by the Serbian Chemical Society
Karnegijeva 4/III, 11000 Belgrade, Serbia
Printed by the Faculty of Technology and Metallurgy
Karnegijeva 4, P.O. Box 35-03, 11120 Belgrade, Serbia



J. Serb. Chem. Soc. 74 (2) 103–115 (2009)
JSCS–3813

Synthesis, reactions and biological activity of 3-arylidene-5-(4-methylphenyl)-2(3H)-furanones[‡]

ASIF HUSAIN*, M. MUMTAZ ALAM and NADEEM SIDDIQUI

*Department of Pharmaceutical Chemistry, Faculty of Pharmacy, Jamia Hamdard
(Hamdard University), New Delhi - 110 062, India*

(Received 10 March, revised 20 September 2008)

Abstract: 3-Arylidene-5-(4-methylphenyl)-2(3H)-furanones **2a–m** were prepared from 3-(4-methyl-benzoyl)propanoic acid **1** and several aromatic aldehydes. Some of the selected furanones were reacted with ammonia gas and benzylamine to give corresponding 3-arylidene-1,3-dihydro-5-(4-methylphenyl)-2H-pyrrol-2-ones **3a–h** and 3-arylidene-1-benzyl-1,3-dihydro-5-(4-methylphenyl)-2H-pyrrol-2-ones **4a–f**, respectively, which were characterized on the basis of IR, ¹H-NMR, mass spectral data and elemental analysis results. These compounds were tested for their anti-inflammatory and antibacterial activities. The compounds, which showed significant anti-inflammatory activity, were further screened for their analgesic and ulcerogenic activities. Three new compounds (**2e**, **2h** and **4d**), out of twenty-seven showed very good anti-inflammatory activity in the carrageenan induced rat paw edema test, with significant analgesic activity in the acetic acid induced writhing test together with negligible ulcerogenic action. The antibacterial activity is expressed as the corresponding MIC values.

Keywords: furanone; pyrrolone; anti-inflammatory; analgesic; antibacterial activity.

INTRODUCTION

The chemistry of furanones has attracted more attention in the last few decades due to their reactivity and novel biological activities. Butenolides, a family of α,β -unsaturated lactones, also known as furanones, are ubiquitous chemical moieties found in many natural products. The furanone system, as present in many natural compounds, is associated with important biological actions.¹ Even the simpler butyrolactone, 3,3-diethylbutyrolactone, shows anticonvulsant activity.² While the furanones exhibit antibiotic activity,³ they have been reported^{4–8} to also have anti-inflammatory, analgesic, anthelmintic, antiviral and anticancer properties. The reactivity of the γ -lactone ring present in furanone derivatives has

* Corresponding author. E-mail: drasifhusain@yahoo.com

[‡] Partially presented at the 12th APTI Annual National Convention, India.

doi: 10.2298/JSC0902103H

been further exploited for the synthesis of nitrogen heterocycles of potential pharmacological interest.^{9,10}

Herein, the syntheses and reactions of 3-arylidene-5-(4-methylphenyl)-2(3*H*)-furanones following the literature procedure^{10,11} with a slight modification and a study of biological activities of the resulting products are reported. Previously, the anti-inflammatory activity of a number of 2-arylidene-4-substituted phenyl-but-3-en-4-olides was studied and the results were encouraging.^{8,12}

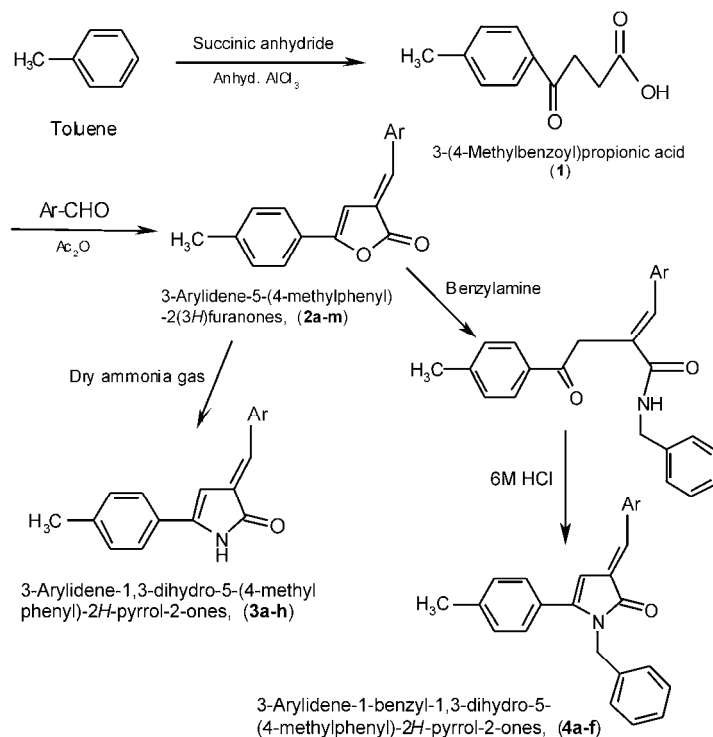
3-(4-Methylbenzoyl)propanoic acid **1** is an example of the aroylpropanoic acid class of non-steroidal anti-inflammatory drugs (NSAIDs). Aroylpropanoic acids are good anti-inflammatory agents; however, they have been reported^{13–15} to have gastrointestinal side effects, as do other commonly used NSAIDs. In view of these observations, it was therefore considered worthwhile to study various furanone derivatives of 3-(4-methylbenzoyl)propanoic acid for their anti-inflammatory, analgesic and ulcerogenic actions. These furanones were further exploited for the synthesis of nitrogen heterocycles (pyrrolone and benzylpyrrolone). In view of the reported antimicrobial activity of furanones and pyrrolones, these compounds were also screened for their antibacterial activity with encouraging results.

RESULTS AND DISCUSSION

Chemistry

Overall, twenty-seven new compounds (**2a–m**, **3a–h** and **4a–f**) were prepared as outlined in Scheme 1. The 3-arylidene-5-(4-methylphenyl)-2(3*H*)-furanones **2a–m** were synthesized from 3-(4-methylbenzoyl)propanoic acid **1** by reacting with aromatic aldehydes in the presence of triethylamine in acetic anhydride following modified Perkin reaction conditions. The required 3-(4-methylbenzoyl)propanoic acid was prepared by condensing dry toluene with succinic anhydride in presence of anhydrous aluminum chloride, following Friedel-Crafts acylation reaction conditions. 3-arylidene-1,3-dihydro-5-(4-methylphenyl)-2*H*-pyrrol-2-ones **3a–h** were prepared by reacting the furanones with ammonia gas in absolute ethanol. The 3-arylidene-1-benzyl-1,3-dihydro-5-(4-methylphenyl)-2*H*-pyrrol-2-ones **4a–f** were synthesized by reacting the appropriate furanone with benzylamine in dry benzene to give *N*-benzyl- γ -ketoamides, which were then cyclized in 6 M HCl to give the corresponding benzylpyrrolones. Calculations of the δ values using incremental parameters for the hydrogen (semicyclic double bond) seems to suggest the (*E*)-configuration. The structures assigned to the compounds are supported by the IR, ¹H-NMR and mass spectral data and elemental analysis results given below.

3-(4-Methylbenzoyl)propanoic acid (**1**). Yield: 65 %; m.p. 106 °C. ¹H-NMR (CDCl₃, δ , ppm): 2.37 (3H, *s*, CH₃), 2.65 and 3.26 (*t*, each 2×CH₂), 7.27 and 7.85 (*d*, each A₂B₂, *p*-substituted phenyl).



Scheme 1. Protocol for synthesis of furanones (**2a-m**), pyrrolones (**3a-h**) and benzylpyrrolones (**4a-f**).

3-Benzylidene-5-(4-methylphenyl)-2(3H)-furanone (2a). Yield: 72 %; m.p. 90 °C. Anal. Calcd. for C₁₈H₁₄O₂: C, 82.42; H, 5.38. Found: C, 82.35; H, 5.34. IR (KBr, cm⁻¹): 1772 (lactone C=O), 1611 (ArC=C), 821 (ArC-H). ¹H-NMR (CDCl₃, δ, ppm): 2.34 (3H, s, CH₃), 6.59 (1H, s, furanone ring), 7.28 (1H, s, olefinic H), 7.3 and 7.56 (d, each A₂B₂, tolyl ring), 7.42 (3H, m, H-3,4,5, phenyl), 7.61 (2H, m, H-2,6, phenyl). MS (m/z): 262 (M⁺), 119, 91.

3-(2-Methoxybenzylidene)-5-(4-methylphenyl)-2(3H)-furanone (2b). Yield: 74 %; m.p. 132–134 °C. Anal. Calcd. for C₁₉H₁₆O₃: C, 78.06; H, 5.52. Found: C, 77.88; H, 5.46. IR (KBr, cm⁻¹): 1762 (lactone C=O), 1604 (ArC=C), 812 (ArC-H). ¹H-NMR (CDCl₃, δ, ppm): 2.35 (3H, s, CH₃), 3.85 (3H, s, OCH₃), 6.83 (1H, s, furanone ring), 6.94 (1H, m, H-3, arylidene ring), 7.29 (1H, s, olefinic H), 7.11 and 7.53 (d, each A₂B₂, tolyl ring), 7.39 (2H, m, H-4,5, arylidene ring), 7.67 (1H, dd, H-6, arylidene ring). MS (m/z): 292 (M⁺), 119, 91.

3-(3-Methoxybenzylidene)-5-(4-methylphenyl)-2(3H)-furanone (2c). Yield: 71 %; m.p. 140–142 °C. Anal. Calcd. for C₁₉H₁₆O₃: C, 78.06; H, 5.52. Found: C, 77.75; H, 5.44. IR (KBr, cm⁻¹): 1771 (lactone C=O), 1617 (ArC=C), 822 (ArC-H). ¹H-NMR (CDCl₃, ppm): 2.37 (3H, s, CH₃), 3.88 (3H, s, OCH₃), 6.88 (1H, s, furanone ring), 7.13 (1H, m, H-4, arylidene ring), 7.49 (3H, m, H-2,5,6 arylidene

ring), 7.63 (1H, *s*, olefinic H), 7.26 and 7.59 (*d*, each A₂B₂, tolyl ring). MS (*m/z*): 292 (M⁺), 119, 107, 91.

3-(4-Methylbenzylidene)-5-(4-methylphenyl)-2(3H)-furanone (2d). Yield: 68 %; m.p. 122 °C. Anal. Calcd. for C₁₉H₁₆O₂: C, 82.58; H, 5.84. Found: C, 82.36; H, 5.78. IR (KBr, cm⁻¹): 1720 (lactone C=O), 1601 (ArC=C), 806 (ArC-H). ¹H-NMR (CDCl₃, δ, ppm): 2.37 and 2.44 (*s*, each 2×CH₃), 6.71 (1H, *s*, furanone ring), 6.97 and 7.25 (*d*, each A₂B₂, tolyl ring), 7.35 (1H, *s*, olefinic H), 7.56 (4H, *m*, H-2,3,5,6 arylidene ring). MS (*m/z*): 276 (M⁺), 119, 91.

5-(4-Methylphenyl)-3-(2,3,4-trimethoxybenzylidene)-2(3H)-furanone (2e). Yield: 65 %; m.p. 168–170 °C. Anal. Calcd. for C₂₁H₂₀O₅: C, 71.58; H, 5.72. Found: C, 71.43; H, 5.75. IR (KBr, cm⁻¹): 1766 (lactone C=O), 1611 (ArC=C), 817 (ArC-H). ¹H-NMR (CDCl₃, δ, ppm): 2.41 (*s*, CH₃), 3.94 (*s*, 3×OCH₃), 6.71 (1H, *s*, furanone ring), 7.16 and 7.62 (*d*, each A₂B₂, tolyl ring), 7.35 (1H, *s*, olefinic H), 7.69 (2H, *m*, H-5,6 arylidene ring). MS (*m/z*): 352 (M⁺), 119, 91.

3-(4-Acetoxybenzylidene)-5-(4-methylphenyl)-2(3H)-furanone (2f). Yield: 69 %; m.p. 156–158 °C. Anal. Calcd. for C₂₀H₁₆O₄: C, 74.99; H, 5.03. Found: C, 75.10; H, 5.12. IR (KBr, cm⁻¹): 1729 (lactone C=O), 1612 (ArC=C), 819 (ArC-H). ¹H-NMR (CDCl₃, δ, ppm): 2.14 (3H, *s*, OCOCH₃), 2.31 (3H, *s*, CH₃), 6.98 (1H, *s*, furanone ring), 7.02 (2H, *m*, H-2,6 arylidene ring), 7.28 (1H, *s*, olefinic H), 7.11 and 7.56 (*d*, each A₂B₂, tolyl ring), 7.42 and 7.63 (*d*, each A₂B₂, arylidene ring). MS (*m/z*): 320 (M⁺), 119, 91, 77.

3-(3-Acetoxybenzylidene)-5-(4-methylphenyl)-2(3H)-furanone (2g). Yield: 73 %; m.p. 144–146 °C. Anal. Calcd. for C₂₀H₁₆O₄: C, 74.99; H, 5.03. Found: C, 74.86; H, 5.06. IR (KBr, cm⁻¹): 1733 (lactone C=O), 1609 (ArC=C), 827 (ArC-H). ¹H-NMR (CDCl₃, δ, ppm): 2.15 (3H, *s*, OCOCH₃), 2.35 (3H, *s*, CH₃), 6.98 (1H, *s*, furanone ring), 7.11 (1H, *m*, H-4, arylidene ring), 7.53 (3H, *m*, H-2,5,6, arylidene ring), 7.48 (1H, *s*, olefinic H), 7.26 and 7.60 (*d*, each A₂B₂, tolyl ring). MS (*m/z*): 320 (M⁺), 119, 91.

3-(4-Acetoxy-3-ethoxybenzylidene)-5-(4-methylphenyl)-2(3H)-furanone (2h). Yield: 66 %; m.p. 132–134 °C. Anal. Calcd. for C₂₂H₂₀O₅: C, 72.52; H, 5.53. Found: C, 72.26; H, 5.38. IR (KBr, cm⁻¹): 1748 (lactone C=O), 1618 (ArC=C), 808 (ArC-H). ¹H-NMR (CDCl₃, δ, ppm): 1.45 (3H, *t*, OCH₂CH₃), 2.34 (3H, *s*, OCOCH₃), 2.37 (3H, *s*, CH₃), 4.08 (2H, *q*, OCH₂CH₃), 6.94 (1H, *s*, furanone ring), 7.19 (2H, *m*, H-5,6 arylidene ring), 7.31 (1H, *m*, H-2 arylidene ring), 7.46 (1H, *s*, olefinic H), 7.17 and 7.66 (*d*, each A₂B₂, tolyl ring). MS (*m/z*): 364 (M⁺), 119, 91.

3-(2-Furanylmethylene)-5-(4-methylphenyl)-2(3H)-furanone (2i). Yield: 63 %; m.p. 160–162 °C. Anal. Calcd. for C₁₆H₁₂O₃: C, 76.18; H, 4.79. Found: C, 75.93; H, 4.66. IR (KBr, cm⁻¹): 1779 (lactone C=O), 1635 (ArC=C), 820 (ArC-H). ¹H-NMR (CDCl₃, δ, ppm): 2.41 (3H, *s*, CH₃), 7.04 (1H, *s*, furanone ring), 7.43

(3H, *m*, furylidene ring), 7.61 (1H, *s*, olefinic H), 7.18 and 7.72 (*d*, each A₂B₂, tolyl ring). MS (*m/z*): 252 (M⁺), 119, 91.

3-(3,4-Methylenedioxybenzylidene)-5-(4-methylphenyl)-2(3H)-furanone (2j). Yield: 67 %; m.p. 174–176 °C. Anal. Calcd. for C₁₉H₁₄O₄: C, 74.50; H, 4.61. Found: C, 74.38; H, 4.50. IR (KBr, cm⁻¹): 1755 (lactone C=O), 1616 (ArC=C), 814 (ArC-H). ¹H-NMR (CDCl₃, δ, ppm): 2.35 (3H, *s*, CH₃), 4.08 (2H, *s*, OCH₂O), 6.93 (1H, *s*, furanone ring), 7.16 (2H, *m*, H-5,6 arylidene ring), 7.33 (1H, *m*, H-2 arylidene ring), 7.51 (1H, *s*, olefinic H), 7.12 and 7.67 (*d*, each A₂B₂, tolyl ring). MS (*m/z*): 306 (M⁺), 121, 119, 91.

3-(9-Anthrylmethylene)-5-(4-methylphenyl)-2(3H)-furanone (2k). Yield: 72 %; m.p. 166 °C. Anal. Calcd. for C₂₆H₁₈O₂: C, 86.17; H, 5.01. Found: C, 85.91; H, 4.96. IR (KBr, cm⁻¹): 1778 (lactone C=O), 1611 (ArC=C), 818 (ArC-H). ¹H-NMR (CDCl₃, δ, ppm): 2.32 (3H, *s*, CH₃), 6.67 (1H, *s*, furanone ring), 7.24 (1H, *s*, olefinic H), 7.35 and 7.66 (*d*, each A₂B₂, tolyl ring), 7.53 (4H, *m*, H-2,3,6,7, anthryl), 8.05 (4H, *m*, H-1,4,5,8, anthryl), 8.24 (1H, *s*, H-10, anthryl). MS (*m/z*): 362 (M⁺), 181, 119.

3-[4-(Diethylamino)benzylidene]-5-(4-methylphenyl)-2(3H)-furanone (2l). Yield: 68 %; m.p. 126–128 °C; Anal. Calcd. for C₂₂H₂₃NO₂: C, 79.25; H, 6.95; N, 4.20. Found: C, 79.18; H, 7.02; N, 4.16. IR (KBr, cm⁻¹): 1751 (lactone C=O), 1608 (ArC=C), 820 (ArC-H). ¹H-NMR (CDCl₃, δ, ppm): 2.33 (3H, *s*, CH₃), 3.35 (6H, *s*, 2×-CH₂CH₃), 3.78 (4H, *s*, 2×-CH₂CH₃), 7.23 (1H, *s*, furanone ring), 7.21 and 7.63 (*d*, each A₂B₂, tolyl ring), 7.32 and 7.56 (*d*, each A₂B₂, arylidene ring), 7.72 (1H, *s*, olefinic H). MS (*m/z*): 333 (M⁺), 119, 91, 77.

3-(Cinnamoylmethylene)-5-(4-methylphenyl)-2(3H)-furanone (2m). Yield: 70 %; m.p. 158 °C. Anal. Calcd. for C₂₀H₁₆O₂: C, 83.31; H, 5.59. Found: C, 83.16; H, 5.45. IR (KBr, cm⁻¹): 1782 (lactone C=O), 1618 (ArC=C), 819 (ArC-H). ¹H-NMR (CDCl₃, δ, ppm): 2.36 (3H, *s*, CH₃), 6.70 (1H, *s*, furanone ring), 7.31 and 7.57 (*d*, each A₂B₂, tolyl ring), 7.64–7.82 (7H, *m*, arylidene ring + 2 olefinic protons). MS (*m/z*): 288 (M⁺), 119, 91.

3-Benzylidene-1,3-dihydro-5-(4-methylphenyl)-2H-pyrrol-2-one (3a). Yield: 65 %; m.p. 128–130 °C. Anal. Calcd. for C₁₈H₁₅NO: C, 82.73; H, 5.79; N, 5.36. Found: C, 82.61; H, 5.66; N, 5.23. IR (KBr, cm⁻¹): 3384 (N-H), 1756 (C=O), 1616 (ArC=C), 799 (ArC-H). ¹H-NMR (CDCl₃, δ, ppm): 2.41 (3H, *s*, CH₃), 6.44 (1H, *s*, pyrrolone ring), 7.33 (1H, *s*, olefinic H), 7.27 and 7.43 (*d*, each A₂B₂, tolyl ring), 7.46 (3H, *m*, H-3,4,5, arylidene ring), 7.62 (2H, *m*, H-2,6, arylidene ring), 7.97 (1H, *s*, NH). MS (*m/z*): 261 (M⁺), 118, 91, 77.

1,3-Dihydro-3-(2-methoxybenzylidene)-5-(4-methylphenyl)-2H-pyrrol-2-one (3b). Yield: 68 %; m.p. 174 °C. Anal. Calcd. for C₁₉H₁₇NO₂: C, 78.33; H, 5.88; N, 4.81. Found: C, 78.08; H, 5.56; N, 4.85; IR (KBr, cm⁻¹): 3445 (N-H), 1699 (C=O), 1509 (ArC=C), 809 (ArC-H). ¹H-NMR (CDCl₃, δ, ppm): 2.32 (3H, *s*, CH₃), 3.77 (3H, *s*, OCH₃), 6.92 (1H, *s*, pyrrolone ring), 7.09 (1H, *m*, H-3,

arylidene ring), 7.27 and 7.54 (*d*, each A₂B₂, tolyl ring), 7.45 (2H, *m*, H-4,5, arylidene ring), 7.68 (1H, *s*, olefinic H), 7.71 (1H, *dd*, H-6, arylidene ring), 8.11 (1H, *s*, NH). MS (*m/z*): 291 (M⁺), 118, 91.

1,3-Dihydro-3-(3-methoxybenzylidene)-5-(4-methylphenyl)-2H-pyrrol-2-one (3c). Yield: 65 %; m.p. 188 °C. Anal. Calcd. for C₁₉H₁₇NO₂: C, 78.33; H, 5.88; N, 4.81. Found: C, 78.16; H, 5.53; N, 4.78. IR (KBr, cm⁻¹): 3462 (N–H), 1697 (C=O), 1613 (ArC=C), 817 (ArC–H). ¹H-NMR (CDCl₃, δ, ppm): 2.39 (3H, *s*, CH₃), 3.83 (3H, *s*, OCH₃), 6.86 (1H, *s*, pyrrolone ring), 7.19 (1H, *m*, H-4, arylidene ring), 7.31 and 7.74 (*d*, each A₂B₂, tolyl ring), 7.53 (3H, *m*, H-2,5,6, arylidene ring), 7.65 (1H, *s*, olefinic H), 7.95 (1H, *s*, NH). MS (*m/z*): 291 (M⁺), 118, 91.

1,3-Dihydro-3-(4-methoxybenzylidene)-5-(4-methylphenyl)-2H-pyrrol-2-one (3d). Yield: 62 %; m.p. 156–158 °C. Anal. Calcd. for C₁₉H₁₇NO: C, 82.88; H, 6.22; N, 5.09. Found: C, 82.50; H, 6.25; N, 4.88. IR (KBr, cm⁻¹): 3471 (N–H), 1725 (C=O), 1616 (ArC=C), 801 (ArC–H). ¹H-NMR (CDCl₃, δ, ppm): 2.37 and 2.43 (*s*, each 2×CH₃), 6.72 (1H, *s*, pyrrolone ring), 7.07 and 7.51 (*d*, each A₂B₂, tolyl ring), 7.62 (1H, *s*, olefinic H), 7.68 (4H, *m*, H-2,3,5,6 arylidene ring), 8.11 (1H, *s*, NH). MS (*m/z*): 275 (M⁺), 118, 91.

1,3-Dihydro-5-(4-methylphenyl)-3-(2,3,4-trimethoxybenzylidene)-2H-pyrrol-2-one (3e). Yield: 64 %. m.p. 172–174 °C. Anal. Calcd. for C₂₁H₂₁NO₄: C, 71.78; H, 6.02; N, 3.99. Found: C, 71.56; H, 5.83; N, 4.12. IR (KBr, cm⁻¹): 3458 (N–H), 1708 (C=O), 1631 (ArC=C), 813 (ArC–H). ¹H-NMR (CDCl₃, δ, ppm): 2.34 (*s*, CH₃), 3.91 (*s*, 3×OCH₃), 7.41 (1H, *s*, pyrrolone ring), 7.16 and 7.86 (*d*, each A₂B₂, tolyl ring), 7.51 (1H, *s*, olefinic H), 7.75 (2H, *m*, H-5,6 arylidene ring), 8.19 (1H, *s*, NH). MS (*m/z*): 351 (M⁺), 118, 91.

1,3-Dihydro-3-(4-hydroxybenzylidene)-5-(4-methylphenyl)-2H-pyrrol-2-one (3f). Yield: 61 %; m.p. 152–154 °C. Anal. Calcd. for C₁₈H₁₅NO₂: C, 77.96; H, 5.45; N, 5.05. Found: C, 77.78; H, 5.24; N, 5.12. IR (KBr, cm⁻¹): 3424 (N–H), 1713 (C=O), 1596 (ArC=C), 830 (ArC–H). ¹H-NMR (CDCl₃, δ, ppm): 2.41 (3H, *s*, CH₃), 6.94 (1H, *s*, pyrrolone ring), 7.64 (1H, *s*, olefinic H), 7.23 and 7.51 (*d*, each, A₂B₂, tolyl ring), 7.37 and 7.68 (*d*, each, A₂B₂, arylidene ring), 8.18 (*s*, 1H, NH). MS (*m/z*): 277 (M⁺), 118, 91, 77.

1,3-Dihydro-3-(3-hydroxybenzylidene)-5-(4-methylphenyl)-2H-pyrrol-2-one (3g). Yield: 58 %; m.p. 146–148 °C. Anal. Calcd. for C₁₈H₁₅NO₂: C, 77.96; H, 5.45; N, 5.05. Found: C, 77.82; H, 5.31; N, 5.16. IR (KBr, cm⁻¹): 3419 (N–H), 1745 (C=O), 1616 (ArC=C), 821 (ArC–H). ¹H-NMR (CDCl₃, δ, ppm): 2.28 (*s*, 3H, CH₃), 6.92 (*s*, 1H, pyrrolone ring), 7.21 (*m*, 1H, H-5, arylidene ring), 7.22 and 7.61 (*d*, each, A₂B₂, tolyl ring), 7.73 (*s*, 1H, olefinic H), 8.03 (*m*, 1H, H-4, arylidene ring), 8.15 (*d*, 1H, H-2, arylidene ring), 8.58 (*s*, 1H, NH). MS (*m/z*): 277 (M⁺), 118, 91.

1,3-Dihydro-3-(4-hydroxy-3-ethoxybenzylidene)-5-(4-methylphenyl)-2H-pyrrol-2-one (3h). Yield: 60 %; m.p. 182–184 °C. Anal. Calcd. for C₂₀H₁₉NO₃: C, 77.96; H, 5.45; N, 5.05. Found: C, 77.82; H, 5.31; N, 5.16.

74.75; H, 5.96; N, 4.36. Found: C, 74.60; H, 5.72; N, 4.24. IR (KBr, cm^{-1}): 3396(N-H), 1738 (C=O), 1629 (ArC=C), 827 (ArC-H). $^1\text{H-NMR}$ (CDCl_3 , δ , ppm): 1.44 (3H, *t*, OCH_2CH_3), 2.35 (3H, *s*, OCOCH_3), 2.39 (3H, *s*, CH_3), 4.08 (2H, *q*, OCH_2CH_3), 6.95 (1H, *s*, pyrrolone ring), 7.31 (2H, *m*, H-5,6 arylidene ring), 7.43 (1H, *m*, H-2 arylidene ring), 7.18 and 7.88 (*d*, each A_2B_2 , tolyl ring), 7.64 (1H, *s*, olefinic H), 8.05 (1H, *s*, NH). MS (m/z): 321 (M^+), 118, 91.

1-Benzyl-3-benzylidene-1,3-dihydro-5-(4-methylphenyl)-2H-pyrrol-2-one (4a). Yield: 65 %; m.p. 122–124 °C. Anal. Calcd. for $\text{C}_{25}\text{H}_{21}\text{NO}$: C, 85.44; H, 6.02; N, 3.99. Found: C, 85.38; H, 5.90; N, 4.12. IR (KBr, cm^{-1}): 1750 (C=O), 1616 (ArC=C), 799 (ArC-H). $^1\text{H-NMR}$ (CDCl_3 , δ , ppm): 2.34 (3H, *s*, CH_3), 4.85 (2H, *s*, CH_2), 6.16 (1H, *s*, pyrrolone ring), 6.97 and 7.63 (*d*, each A_2B_2 , tolyl ring), 7.3 (6H, *m*, $2\times\text{H-3,4,5}$ benzyl + phenyl), 7.43 (1H, *s*, olefinic H), 7.27 and 7.43 (*d*, each A_2B_2 , tolyl ring), 7.5 (4H, *m*, $2\times\text{H-2,6}$ benzyl + phenyl). MS (m/z): 351 (M^+), 260, 118, 91, 77.

1-Benzyl-1,3-dihydro-3-(3-methoxybenzylidene)-5-(4-methylphenyl)-2H-pyrrol-2-one (4b). Yield: 67 %; m.p. 132–134 °C. Anal. Calcd. for $\text{C}_{26}\text{H}_{23}\text{NO}_2$: C, 81.86; H, 6.08; N, 3.67. Found: C, 81.65; H, 6.15; N, 3.73; IR (KBr, cm^{-1}): 1729 (C=O), 1598 (ArC=C), 817 (ArC-H). $^1\text{H-NMR}$ (CDCl_3 , δ , ppm): 2.39 (3H, *s*, CH_3), 3.83 (3H, *s*, OCH_3), 6.86 (1H, *s*, pyrrolone ring), 7.19 (1H, *m*, H-4 arylidene ring), 7.31 and 7.74 (*d*, each A_2B_2 , tolyl ring), 7.53 (3H, *m*, H-2,5,6 arylidene ring), 7.65 (1H, *s*, olefinic H), 7.95 (1H, *s*, NH). MS (m/z): 381 (M^+), 118, 91.

1-Benzyl-1,3-dihydro-3-(4-methoxybenzylidene)-5-(4-methylphenyl)-2H-pyrrol-2-one (4c). Yield: 61 %; m.p. 118–120 °C. Anal. Calcd. for $\text{C}_{26}\text{H}_{23}\text{NO}$: C, 85.45; H, 6.34; N, 3.83. Found: C, 85.41; H, 6.22; N, 4.02. IR (KBr, cm^{-1}): 1737 (C=O), 1616 (ArC=C), 793 (ArC-H). $^1\text{H-NMR}$ (CDCl_3 , δ , ppm): 2.34 (3H, *s*, CH_3), 4.85 (2H, *s*, CH_2), 6.16 (1H, *s*, pyrrolone ring), 6.97 and 7.63 (*d*, each A_2B_2 , tolyl ring), 7.3 (6H, *m*, $2\times\text{H-3,4,5}$ benzyl + phenyl), 7.43 (1H, *s*, olefinic H), 7.27 and 7.43 (*d*, each A_2B_2 , tolyl ring), 7.5 (4H, *m*, $2\times\text{H-2,6}$ benzyl + phenyl). MS (m/z): 365 (M^+), 274, 118, 91, 77.

1-Benzyl-1,3-dihydro-5-(4-methylphenyl)-3-(2,3,4-trimethoxybenzylidene)-2H-pyrrol-2-one (4d). Yield: 58 %; m.p. 138–140 °C. Anal. Calcd. for $\text{C}_{28}\text{H}_{27}\text{NO}_4$: C, 76.17; H, 6.16; N, 3.17. Found: C, 75.94; H, 6.12; N, 3.10. IR (KBr, cm^{-1}): 1716 (C=O), 1606 (ArC=C), 819 (ArC-H). $^1\text{H-NMR}$ (CDCl_3 , δ , ppm): 2.34 (3H, *s*, CH_3), 3.68 (*s*, $3\times\text{OCH}_3$), 4.82 (2H, *s*, CH_2), 6.45 (1H, *s*, pyrrolone ring), 6.97 and 7.62 (*d*, each A_2B_2 , tolyl ring), 7.24 (3H, *m*, H-3,4,5 benzyl), 7.41 (1H, *s*, olefinic H), 7.52 (2H, *m*, H-2,6 benzyl), 7.73 (2H, *m*, H-5,6 arylidene ring). MS (m/z): 441 (M^+), 118, 91, 77.

1-Benzyl-1,3-dihydro-3-(3,4-methylenedioxybenzylidene)-5-(4-methylphenyl)-2H-pyrrol-2-one (4e). Yield: 61 %; m.p. 182–184 °C. Anal. Calcd. for $\text{C}_{26}\text{H}_{21}\text{NO}_3$: C, 78.97; H, 5.35; N, 3.51. Found: C, 78.83; H, 5.31; N, 3.48. IR (KBr, cm^{-1}): 1749 (C=O), 1610 (ArC=C), 815 (ArC-H). $^1\text{H-NMR}$ (CDCl_3 , δ

ppm) 4.85 (2H, *s*, CH₂), 6.01 (2H, *s*, -OCH₂O-), 6.52 (1H, *s*, pyrrolone ring), 6.95 (1H, *d*, H-5 arylidene ring), 7.12 and 7.76 (*d*, each A₂B₂, tolyl, ring) 7.17 (7H, *m*, 5H phenyl + H-2,6 arylidene), 7.25 (5H, *m*, benzyl), 7.66 (1H, *s*, olefinic H). MS (*m/z*): 395 (M⁺), 304, 91, 77.

3-(9-Anthrylmethylene)-1-benzyl-1,3-dihydro-5-(4-methylphenyl)-2H-pyrrol-2-one (4f). Yield: 69 %; m.p. 146–148 °C. Anal. Calcd. for C₃₃H₂₅NO: C, 87.78; H, 5.58; N, 3.10. Found: C, 87.61; H, 5.50; N, 3.14. IR (KBr, cm⁻¹): 1756 (C=O), 1614 (ArC=C), 821 (ArC-H). ¹H-NMR (CDCl₃, δ, ppm): 2.31 (3H, *s*, CH₃), 6.61 (1H, *s*, pyrrolone ring), 7.31 and 7.76 (*d*, each A₂B₂, tolyl ring), 7.24 (1H, *s*, olefinic H), 7.54 (4H, *m*, H-2,3,6,7 anthryl), 8.03 (4H, *m*, H-1,4,5,8 anthryl), 8.23 (1H, *s*, H-10, anthryl). MS (*m/z*): 451 (M⁺), 119, 91.

In general, the infrared spectral data of the furanones **2a–m** revealed bands at 1782–1720 (lactone C=O), 1635–1601 (ArC=C) and 827–806 (ArC-H). The pyrrolones **3a–h** showed bands at 3471–3384 (pyrrolone N-H), 1745–1697 (C=O), 1631–1596 (ArC=C) and 830–799 (ArC-H). The benzylpyrrolones **4a–f** revealed bands at 1756–1716 (lactam C=O), 1616–1598 (ArC=C) and 821–793 (ArC-H). In the ¹H-NMR spectral data, all the compounds showed a singlet of three protons at around δ 2.3 ppm, accounted for by the methyl group of the tolyl ring. Two singlets of one proton each were present at around δ 6.5 and 7.4 ppm, which could be assigned to the ring β H and the olefinic hydrogen of the arylidene substituent. Other peaks were observed at the appropriate positions. Some points could be made regarding the fragmentation pattern observed in the electron impact mass spectrum. The 3-arylidene-5-(4-methylphenyl)-2(3H)-furanones **2a–m** gave an M⁺ peak in reasonable intensities. The major fragment appears to be CH₃-C₆H₄-C≡O⁺ (*m/z* 119), arising from the heterocyclic oxygen and γ carbon with its substituent. Subsequently, it loses CO to give (C₇H₇)⁺ (*m/z* 91). A peak at *m/z* 77, corresponding to (C₆H₅)⁺, appeared. Occasionally, the aryl ring of the arylidene moiety also appeared as Ar⁺. In the case of pyrrolones **3a–h**, the major fragmentation is through CH₃-C₆H₄-C≡N⁺H (*m/z* 118), which is followed by loss of HCN to give (C₇H₇)⁺ (*m/z* 91). In case of benzylpyrrolones **4a–f**, loss of 91 mass units, corresponding to the benzyl moiety from the molecular ion, was observed together with peaks at *m/z* 91, 77. The other pathway is *via* CH₃-C₆H₄-C≡N⁺H (*m/z* 118), arising from C-2 and its substituent, which appears to be novel. This also loses HCN to give (C₇H₇)⁺ (*m/z* 91).

Biological evaluation

Anti-inflammatory activity. The anti-inflammatory activity test showed that compound **2h** exhibited the maximum anti-inflammatory activity (69.05 % inhibition), two compounds, **2e** and **4d**, also showed good activity with 61.90 and 64.28 % inhibition, respectively. The standard drug diclofenac exhibited 78.57 % inhibition. Compound **2b**, **2f**, **4b**, **4c** and **4f** showed significant activity ranging from 40.47–54.76 %. The results are presented in Table I.

The structure activity relationship showed that substitution of the oxygen atom of the furanone ring with NH (pyrrolones) resulted in a marked decrease in the anti-inflammatory activity, while substitution of the oxygen atom with the benzylamine moiety (benzylpyrrolones) markedly increased the activity. Compounds having trimethoxyl functions at the 2,3,4-position of the arylidene moiety were found to have better anti-inflammatory activity than those having one or no methoxyl function.

TABLE I. Biological data of the synthesized compounds

Compd.	Anti-inflammatory activity ^a		Analgesic activity ^a		Ulcerogenic activity ^a (severity index)
	Change in edema volume ^b , mL	Inhibition %	No. of writhing episodes ^b	Protection %	
2b	0.22±0.01	47.62	16.3±0.42	27.87	0.50±0.18
2d	0.28±0.02	33.33	nt	–	nt
2e	0.16±0.02	61.90	7.6±0.36	66.37	0.75±0.11
2f	0.20±0.01	52.38	12.6±0.22	44.24	0.583±0.08
2h	0.13±0.02	69.05	6.3±0.33	72.27	0.666±0.11
2k	0.27±0.01	35.72	nt ^c	–	nt
2l	0.26±0.02	38.10	nt	–	nt
3b	0.34±0.02	19.05	nt	–	nt
3d	0.36±0.02	14.28	nt	–	nt
3e	0.31±0.01	26.19	nt	–	nt
3f	0.29±0.01	30.95	nt	–	nt
4b	0.19±0.02	54.76	8.3±0.33	63.28	0.75±0.17
4c	0.24±0.01	42.86	14.5±0.42	35.84	0.416±0.15
4d	0.15±0.01	64.28	6.6±0.33	70.79	0.833±0.16
4f	0.25±0.02	40.47	17.3±0.33	23.31	0.583±0.20
Control	0.42±0.02	–	22.6±0.42	–	0.00
Diclofenac	0.09±0.03	78.57	7.3±0.42	67.69	2.33±0.21

^aNumber of animals in each group was 6; ^bvalues as ±S.E.M.; ^cnt = not tested

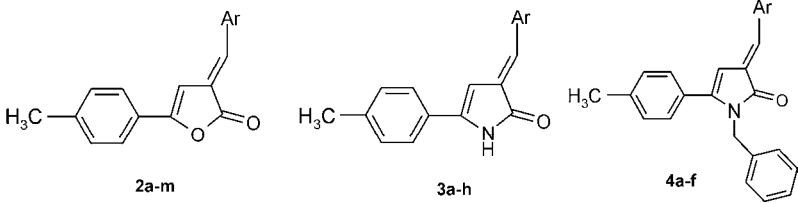
Analgesic activity. The analgesic activity as evaluated by the acetic acid-induced writhing test in albino mice showed that compound **2h** exhibited the maximum analgesic activity (72.27 %) while the standard drug diclofenac showed 67.69 % activity. Compound **2e**, **4b** and **4d** also showed good analgesic activity, ranging from 63.28–70.79 % (Table I).

Acute ulcerogenesis. The tested compounds tested a significant reduction in ulcerogenic activity, ranging from 0.416 to 0.833, whereas the standard drug diclofenac showed a high severity index (2.33). The results indicate that compounds are almost devoid of ulcerogenic action (Table I).

Antibacterial activity. Compounds **2h**, **3e** and **3h** showed significant activity against *S. aureus* with MIC values of 12.5 (**2h** and **3e**) and 6.5 µg/ml (**3h**) (Table II). Of these compounds, compound **3e** also showed good activity against *E. coli* with MIC value of 15 µg/ml. Compounds **2f**, **2l**, **3b**, **3c**, **3f**, and **4d** exhibited

appreciable antibacterial activity against both the bacterial strains with *MIC* values ranging from 20–50 µg/ml. Analyses of the results indicate that the introduction of a NH in place of the oxygen atom in the furanone ring (pyrrolones) enhanced the antibacterial action whereas the benzylpyrrolones were weak in their antibacterial action.

TABLE II. Physical data and *in vitro* antibacterial screening of the synthesized compounds



Compd.	Ar	M.p. °C	Mol. formula/ <i>M_r</i>	<i>MIC</i> / µg mL ⁻¹	
				<i>S. aureus</i>	<i>E. coli</i>
2a	Phenyl-	90	C ₁₈ H ₁₄ O ₂ /262.31	– ^a	–
2b	2-Methoxyphenyl-	132–134	C ₁₉ H ₁₆ O ₃ /292.33	>100	–
2c	3-Methoxyphenyl-	140–142	C ₁₉ H ₁₆ O ₃ /292.33	>100	>100
2d	4-Methylphenyl-	122	C ₁₉ H ₁₆ O ₂ /276.33	–	–
2e	2,3,4-Trimethoxyphenyl-	168–170	C ₂₁ H ₂₀ O ₅ /352.38	50	>100
2f	4-Acetoxyphenyl-	156–158	C ₂₀ H ₁₆ O ₄ /320.34	50	50
2g	3-Acetoxyphenyl-	144–146	C ₂₀ H ₁₆ O ₄ /320.34	100	50
2h	4-Acetoxy-3-ethoxyphenyl-	132–134	C ₂₂ H ₂₀ O ₅ /364.39	12.5	25
2i	2-Furyl-	160–162	C ₁₆ H ₁₂ O ₃ /252.27	–	–
2j	3,4-Methylenedioxyphenyl-	174–176	C ₁₉ H ₁₄ O ₄ /306.32	>100	>100
2k	9-anthryl-	166	C ₂₆ H ₁₈ O ₂ /362.43	–	–
2l	4-(Diethylamino)phenyl-	126–128	C ₂₂ H ₂₃ NO ₂ /333.43	20	25
2m	Cinnamoyl-	158	C ₂₀ H ₁₆ O ₂ /288.34	–	–
3a	Phenyl-	128–130	C ₁₈ H ₁₅ NO/261.32	50	>100
3b	2-Methoxyphenyl-	174	C ₁₉ H ₁₇ NO ₂ /291.35	50	50
3c	3-Methoxyphenyl-	188	C ₁₉ H ₁₇ NO ₂ /291.35	25	50
3d	4-Methylphenyl-	156–158	C ₁₉ H ₁₇ NO/275.35	>100	–
3e	2,3,4-Trimethoxyphenyl-	172–174	C ₂₁ H ₂₁ NO ₄ /351.4	12.5	15
3f	4-Hydroxyphenyl-	152–154	C ₁₈ H ₁₅ NO ₂ /277.32	50	25
3g	3-Hydroxyphenyl-	146–148	C ₁₈ H ₁₅ NO ₂ /277.32	>100	>100
3h	4-Hydroxy-3-ethoxyphenyl-	182–184	C ₂₀ H ₁₉ NO ₃ /321.37	6.5	25
4a	Phenyl-	122–124	C ₂₅ H ₂₁ NO/351.44	–	–
4b	3-Methoxyphenyl-	132–134	C ₂₆ H ₂₃ NO ₂ /381.47	>100	–
4c	4-Methylphenyl-	118–120	C ₂₆ H ₂₃ NO/365.47	–	–
4d	2,3,4-Trimethoxyphenyl-	138–140	C ₂₈ H ₂₇ NO ₄ /441.52	25	25
4e	3,4-Methylenedioxyphenyl-	182–184	C ₂₆ H ₂₁ NO ₃ /395.46	50	>100
4f	9-Anthryl-	146–148	C ₃₃ H ₂₅ NO/451.56	–	–
Nitrofurazone		–	–	12.5	6.5

^aInsignificant antibacterial activity

EXPERIMENTAL

Chemistry

Melting points were taken in open capillary tubes and are uncorrected. Microanalysis of the compounds was performed on a Perkin-Elmer model 240 analyzer and the values were found to be within ± 0.4 % of the theoretical values. The $^1\text{H-NMR}$ spectra were recorded on a Varian E-360 MHz or a Bruker spectropsin DPX-300 MHz; The chemical shifts, δ , are reported in ppm downfield from tetramethylsilane (TMS), which was used as the internal standard. The mass spectra were recorded on a Jeol JMS-D 300 instrument fitted with a JMS 2000 data system at 70 eV. The progress of the reactions was monitored by TLC, which was performed on silica gel (Merck No. 5554).

Preparation of 3-(4-Methylbenzoyl)propanoic acid (1)

To a mixture of succinic anhydride (0.10 mol) in dry toluene (50 mL) in a round bottom flask was added, in portions, anhydrous aluminum chloride (0.1125 mol). The reaction mixture was refluxed for two hours after which the excess toluene was removed by steam distillation. The residue was purified by dissolving in sodium hydroxide solution, filtering, followed by addition of hydrochloric acid. The so obtained solid mass was filtered, washed with cold water, dried and crystallized from methanol to give fine crystals of **1**, which gave effervescence with sodium bicarbonate solution, confirming the presence of the carboxylic group.

General procedure for the synthesis of 3-arylidene-5-(4-methylphenyl)-2(3H)-furanones (2a-m)

A solution of 3-(4-methylbenzoyl)propanoic acid (0.71 g, 3.0 mmol) and the required aromatic aldehyde (equimolar, 3.0 mmol) in acetic anhydride (15 mL) with triethylamine (1–2 drops) was refluxed for 2–4 h under anhydrous conditions. After completion of the reaction, the contents were poured onto crushed ice in small portions under stirring. A colored solid mass separated out, which was filtered, washed with water and crystallized from a mixture of methanol:chloroform (1:1) to give **2a-m**.

General procedure for the synthesis of 3-arylidene-1,3-dihydro-5-(4-methylphenyl)-2H-pyrrol-2-ones (3a-h)

Dry ammonia gas was passed into an anhydrous ethanolic solution of the required furanone (1.0 g) for one hour at room temperature, the ethanol was distilled off under reduced pressure and the so obtained solid mass was crystallized from methanol/acetone to give **3a-h**.

General procedure for the synthesis of 3-arylidene-1-benzyl-1,3-dihydro-5-(4-methylphenyl)-2H-pyrrol-2-ones (4a-f)

Synthesis of these compounds involved the following two steps:

The synthesis of N-benzyl- γ -ketoamides. The required furanone (3.0 mmol) and benzylamine (4.0 mmol) were refluxed in dry benzene for two hours. On completion of the reaction, the excess benzene was distilled off and the solid mass so obtained was washed with petroleum ether and dried. The compounds obtained were used without crystallization.

Lactamization of the N-benzyl- γ -ketoamides. The required *N*-benzyl- γ -ketoamide (3.0 mmol) was refluxed in 6 M hydrochloric acid (20 ml) for one hour. The contents were then cooled and the so obtained solid mass was collected, washed with water and crystallized from methanol to give **4a-f**.

Biological evaluation

Anti-inflammatory activity. Some of the selected compounds were evaluated for their *in vivo* anti-inflammatory activity by the carrageenan induced rat paw edema method.¹⁶ The pro-

tocol of the animal experiments was approved by the Institutional Animal Ethics Committee (IAEC). The compounds were tested at 20 mg/kg oral dose and were compared with the standard drug diclofenac (10 mg/kg). The foot volume of the rats was measured before and after 4 h of carrageenan injection by a plethysmograph. The percentage inhibition of inflammation was calculated according to the following formula: Anti-inflammatory activity (% inhibition) = $1 - V_t/V_c \times 100$, where V_t and V_c are the edema volumes in the drug-treated and the control groups, respectively.

Analgesic activity. The compounds which showed anti-inflammatory activity > 40 % were further tested for their analgesic activity. The analgesic activity of the synthesized compounds **2b**, **2e**, **2f**, **2h**, **4b**, **4c**, **4d** and **4f** was evaluated by the acetic acid induced writhing test¹⁷ in albino mice. A 1.0 % aqueous acetic acid solution (*i.p.* injection; 0.10 ml) was used as the writhing induced agent. The compounds were tested at 20 mg/kg oral dose and were compared with the standard drug diclofenac (10 mg/kg). The analgesic activity was expressed in terms of % protection. Analgesic activity (%) = $(n - n'/n) \times 100$ where n = mean number of writhes of the control group and n' = mean number of writhes of the test group.

Acute ulcerogenesis. The compounds which were tested for analgesic activity were further screened for their ulcerogenic action. The test was performed according to Cioli *et al.*¹⁴ The ulcerogenic activity was evaluated after *p.o.* administration of the test compounds or diclofenac at a dose of 60 mg/kg.

Antibacterial activity. The antibacterial studies were carried out on the synthesized compounds against the microorganism *viz.* *Staphylococcus aureus* and *Escherichia coli* in meat peptone agar medium at a concentration of 100 µg/ml by the cup plate method. Compounds inhibiting growth of one or more of the above microorganisms were further tested for minimum inhibitory concentration (MIC). The test was carried out according to the turbidity method.¹⁸

Acknowledgement. Financial support provided by the AICTE (under the RPS-scheme) is gratefully acknowledged. We are thankful to Mrs. Shaukat Shah, in-charge the animal house, Jamia Hamdard, for providing animals for the pharmacological studies and Prof. P. K. Pillai, Head, Department of Microbiology, Majeedia Hospital, for helping in performing the antibacterial activity tests.

ИЗВОД

СИНТЕЗА, РЕАКЦИЈЕ И БИОЛОШКА АКТИВНОСТ 3-АРИЛИДЕН-5-(4-МЕТИЛФЕНИЛ)-2(3H)-ФУРАНОНА

ASIF HUSAIN, M. MUMTAZ ALAM и NADEEM SIDDIQUI

*Department of Pharmaceutical Chemistry, Faculty of Pharmacy, Jamia Hamdard
(Hamdard University), New Delhi - 110 062, India*

3-Арилиден-5-(4-метилфенил)-2(3H)-фуранони **2a–m** добијени су из 3-(4-метилбензоил)пропанске киселине **1** и неколико ароматичних алдехида. Одабрани фуранони реагују са амонијачним гасом и бензиламином градећи одговарајуће 3-арилиден-1,3-дихидро-5-(4-метилфенил)-2H-пирол-2-оне **3a–h**, односно 3-арилиден-1-бензил-1,3-дихидро-5-(4-метилфенил)-2H-пирол-2-оне **4a–f**, који су окарактерисани на основу IR, ¹H-NMR и MS података, као и елементалне анализе. Ова једињења су тестирана на анти-инфламаторну и анти-бактеријску активност. Једињења која су показала значајну анти-инфламаторну активност су затим даље тестирана на аналгетску и улцерогену активност. Три нова једињења, **2e**, **2h** и **4d**, од укупно 27, показала су врло добру анти-инфламаторну активност у карагеаном-индукованом тесту едема шапе пацова, уз изражену аналгетску активност у тесту грчења индукованог сир-

ћетном киселином, као и занемарљиву улцерогену активност. Антибактеријска активност изражена је помоћу одговарајућих MIC вредности.

(Примљено 10. марта, ревидирано 20. септембра 2008)

REFERENCES

1. Y. S. Rao, *Chem. Rev.* **76** (1976) 625
2. W. E. Klunk, D. F. Covey, J. A. Ferrendelli, *Mol. Pharmacol.* **22** (1982) 431
3. S. C. Harvey, *Ramington's Pharmaceutical Science*, Mack Publishing Company, Easton, PA, 1985, p. 1189
4. S. S. Shin, Y. Byun, K. M. Lim, J. K. Choi, K. W. Lee, J. H. Moh, J. K. Kim, Y. S. Jeong, J. Y. Kim, Y. H. Choi, H. J. Koh, Y. H. Park, Y. I. Oh, M. S. Noh, S. Chung, *J. Med. Chem.* **47** (2004) 792
5. C. K. Lau, C. Brideau, C. C. Chan, S. Charleson, W. A. Cromlish, D. Ethier, J. Y. Gauthier, R. Gordon, J. Guay, S. Kargman, C. S. Li, P. Prasit, D. Riendeau, M. Therien, D. M. Visco, L. Xu, *Bioorg. Med. Chem. Lett.* **15** (1999) 3187
6. E. Lattmann, D. Kinchington, S. Dunn, H. Singh, W. O. Ayuko, M. J. Tisdale, *J. Pharm. Pharmacol.* **56** (2004) 1163
7. N. D. Heindel, J. A. Minatelli, *J. Pharm. Sci.* **70** (1981) 84
8. M. S. Y. Khan, A. Husain, *Pharmazie* **57** (2002) 448
9. S. A. Khattab, M. Hosny, *Indian J. Chem.* **19B** (1980) 1038
10. S. M. El-Kousy, A. M. El-Torgoman, A. A. El-Basiounyl, A. I. Hashem, *Pharmazie* **43** (1988) 80
11. R. Filler, E. J. Piasek, H. A. Leipold, *Org. Synth.* **5** (1973) 80
12. A. Husain, S. M. Hasan, A. Kumar, M. M. Alam, *Asian J. Chem.* **17** (2005) 1579
13. B. Testa, P. Jenner, *Drug Metabolism, Chemical and Biochemical Aspect*, Marcel Dekker Inc., New York, 1976
14. V. Cioli, S. Putzolu, V. Rossi, P. Sorza Barcellona, C. Corradino, *Toxicol. Appl. Pharmacol.* **50** (1979) 283
15. C. Kohler, E. Tolman, W. Wooding, L. Ellenbogen, *Thromb. Res.* **20** (1980) 123
16. C. A. Winter, E. A. Risley, G. W. Nuss, *Proc. Soc. Exp. Biol.* **111** (1962) 544
17. E. Seigmund, R. Cadmus, G. Lu, *Proc. Soc. Exp. Biol.* **95** (1957) 729
18. *Medical Microbiology, Vol. 2*, R. Cruickshank, J. P. Dugid, D. P. Marmion, R. H. A. Swain, (Eds.), Churchill, London, 1975.



J. Serb. Chem. Soc. 74 (2) 117–128 (2009)
JSCS–3814

Characterization of volatile compounds of “Drenja”, an alcoholic beverage obtained from the fruits of cornelian cherry

VELE TEŠEVIĆ^{1*#}, NINOSLAV NIKIĆEVIĆ², SLOBODAN MILOSAVLJEVIĆ^{1#},
DANICA BAJIĆ^{3#}, VLATKA VAJS^{3#}, IVAN VUČKOVIĆ^{3#}, LJUBODRAG VUJISIĆ^{3#},
IRIS ĐORĐEVIĆ^{4#}, MIROSLAVA STANKOVIĆ⁵ and MILOVAN VELIČKOVIĆ²

¹Faculty of Chemistry, University of Belgrade, Studentski trg 16, 11000 Belgrade, ²Faculty of Agriculture, University of Belgrade, Nemanjina 6, 11080 Zemun, ³Institute for Chemistry, Technology and Metallurgy, University of Belgrade, Njegoševa 12, 11000 Belgrade, ⁴Faculty for Veterinary Medicine, University of Belgrade, Bulevar oslobođenja 18, 11000 Belgrade and ⁵Physical Chemistry Laboratory, Institute of Nuclear Science “Vinča”, 11001 Belgrade, Serbia

(Received 17 June, revised 8 September 2008)

Abstract: In this study, volatile compounds were analyzed in five samples of home-made spirit beverage made by the distillation of fermented fruits of cornelian cherry (*Cornus mas* L.). The major volatile compounds, besides ethanol, identified and quantified were: methanol, acetaldehyde, 1-propanol, ethyl acetate, 2-methyl-1-propanol, 1-butanol, amyl alcohols, 1-hexanol and 2-phenylethanol. The minor volatiles were submitted to liquid–liquid extraction with dichloromethane and analyzed by gas chromatography and gas chromatography/mass spectrometry (GC/MS). A total of 84 compounds were identified. The most abundant compounds were straight-chain free fatty acids, ethyl esters of C₆–C₁₈ acids, limonene, 2-phenylethanol and 4-ethylphenol. Most of the compounds found in the “Drenja” spirits investigated in this study are similar to those present in other alcoholic beverages.

Keywords: *Cornus mas*; alcoholic beverage; fruit spirits; Cornelian cherry spirit; volatiles; GC/MS.

INTRODUCTION

Volatile compounds play an important role in the organoleptic characteristics of alcoholic beverages. In the complex mixture of alcoholic beverages, flavor compounds are present in small amounts. Several hundred compounds from different families, such as alcohols, esters, aldehydes, ketones, volatile acids, terpenes, *etc.*, contribute to the flavor of a spirit. This great variety of volatile com-

* Corresponding author. E-mail: vtesevic@chem.bg.ac.yu

Serbian Chemical Society member.

doi: 10.2298/JSC0902117T

pounds with different polarities, volatilities and wide range of concentration ensures that the flavor of a spirit is very complex. The combination of all these compounds constitutes the character of spirit and differentiates one spirit from another.

Cornus is a very large genus comprising forty species in the form of shrubs and trees native to central and southern Europe and parts of western Asia.¹ Only a few species are grown for their fruits, with the cornelian cherry (*Cornus mas* L.) being the main representative. The sour and sweet juice of Cornelian cherry fruits contains a high amount of vitamin C. Furthermore, the fruits are rich in sugar, organic acids and tannin.² There are several reports about their use in traditional medicine and as a food preservative. For example, *C. officinalis*, a widely grown *Cornus* sp., is used in Chinese herbal medicine and is known for its tonic, analgesic and diuretic activities.³ The fruits from several *Cornus* spp. are used to improve liver and kidney functions. It is also reported to have antibacterial, antihistamine, anti-allergic, antimicrobial and antimalarial activities.⁴ In Europe, cornelian cherry fruits are used for food and cosmetic applications.⁵

The fruits of the cornelian cherry can be dark red, cherry red, pink or yellow. They can be oval, pear shaped or bottle shaped. The average fruit weight ranges from 5.0 to 8.0 g. The fruits are eaten fresh, dried, and pickled like olives, or they are used to produce jam, jelly, marmalade, syrup or wine.⁶ “Drenja” distillate is the spirit beverage that comes from the distillation of fermented fruits of the cornelian cherry tree. This spirit is a traditional alcoholic beverage from various regions of Balkan Peninsula. Although plum, Williams pear, apricot and quince fruit spirits are by far more known, “Drenja” fruit spirit is worthy of attention by experts and consumers. “Drenja” fruit spirit has a very impressive and attractive aroma being luxurious with a little enigmatic velvety sense to the taste. This type of fruit spirit is quite different in comparison with other fruit brandies. The beverage is colorless or colored if matured in oak vessels.

The objective of this work was to characterize, using the GC and GC/MS techniques, the major and minor volatile compounds of the not yet studied “Drenja” alcoholic beverage, obtained from cornelian cherry fruits.

EXPERIMENTAL

Samples

In order to perform this study, five samples (I–V) of “Drenja” spirit from homemade sources were analyzed. They were collected directly from the producers and all samples were produced by the same procedure.

Five samples of “Drenja” distillates were collected in Šipovljane close to the town Drvar (Bosnia and Herzegovina) in September, 2006. According to the local producers, the fermentation period lasted from 5 to 6 weeks. The household-produced brandies were the result of the spontaneous fermentation of cornelian cherry fruits with epiphytic microbiota participation. The distillation was realized using a traditional copper alembic of 80 L, which is a simplified type of the Charentais alembic. The fermented raw material was transferred to the

vessel up to 3/4 of its capacity in order to be distilled. Before the beginning of heating, the alembic was hermetically closed with dough in order to prevent any vapor leakage. First distillation of the fermented mashes was performed without separation of the head. Redistillation was performed using the same device, but with the separation of 1 % of head, the heart (the heart average strength of alcohol was 60 % v/v) and a tail. The heart containing 60 % v/v of ethanol was diluted with distilled water down to 45 % v/v. All samples were placed in glass bottles and stored in the dark at 4 °C until they were analyzed. All tested samples were colorless and distinguished by a characteristic aroma and flavor.

Alcoholic strength

The ethanol content in the distillates was determined using the pycnometric method according to the European Union.⁷

Analysis of volatile compounds in "Drenja"

Analysis of major volatile compounds in "Drenja" appears to correspond to the EU reference method for volatile compounds.⁷ For determination of the major volatile compounds samples were injected directly into the gas chromatograph. The main components (methanol, acetaldehyde, 1-propanol, ethyl acetate, 2-methyl-1-propanol, 1-butanol, amyl alcohols, 1-hexanol and 2-phenylethanol), were identified by comparing their retention times with those of authentic compounds. Their concentrations were calculated from peak areas in GC chromatograms using 4-methyl-1-pentanol as internal standard.

An internal standard solution (1 mL) containing 5 g/L of 4-methyl-1-pentanol in ethanol was added to 10 mL sample of "Drenja". A two microliter aliquot was injected into a Hewlett Packard 5890 gas chromatograph. The compounds were separated on a Chrompack CP-Wax 52 CB fused silica column (polyethylene glycol stationary phase; 50 m×0.32 mm i.d. with 1.2 µm film thickness). The injection mode was split (1:1), and the injector temperature was 233 °C. The GC oven temperature was programmed from 40 to 222 °C at a rate of 4.3 °C/min with a final isotherm of 20 min. The carrier gas was hydrogen at a flow rate 1.02 mL/min. Detector (FID) temperature: 300 °C. H₂ flow rate: 40 mL/min. Air flow rate: 400 mL/min. Auxiliary gas (N₂) flow rate: 30 mL/min.

Extraction and concentration of minor volatile constituents

Two hundred milliliters of "Drenja" distillate was mixed with 200 mL of ultrapure water and then extracted with 40 mL of dichloromethane. NaCl (20 g) was added, and the mixture was stirred magnetically for 30 min. The layers were separated in a separation funnel, and the organic layer was dried (2 h) over anhydrous sodium sulfate. The extract was concentrated to 1.0 mL under nitrogen and directly analyzed by GC FID and GC/MS.

Gas chromatographic analysis was performed using a gas chromatograph HP 5890 equipped with a flame ionization detector (FID) and a split/splitless injector. The separation was achieved on a HP-5 fused silica capillary column, 30 m×0.25 mm i.d., 0.25 µm film thickness. The GC oven temperature was programmed from 50 °C (6 min) to 285 °C at a rate of 4.3 °C/min. Hydrogen was used as carrier gas at a flow rate of 1.6 mL/min at 45 °C. The injector temperature was 250 °C and the detector temperature 280 °C. The injection volume of the beverage extracts was 1.0 µL using the splitless mode. GC/MS analysis was performed using an Agilent 6890 gas chromatograph coupled with Agilent 5973 Network mass selective detector (MSD), operating in the positive ion electron impact (EI) mode. The separation was achieved on an Agilent 19091S-433 HP-5MS fused silica capillary column, 30 m×0.25 mm i.d., 0.25 µm film thickness. The GC oven temperature was programmed from 60 to 285 °C at a rate of 4.3 °C/min. Helium was used as the carrier gas, with an inlet pressure of 25 kPa and

flow rate of 1 mL/min at 210 °C. The injector temperature was 250°C, employing the splitless injection mode. The MS scan conditions were: source temperature: 200 °C; interface temperature: 250 °C; energy of electron beam: 70 eV; mass scan range: 40–350 amu (atomic mass units). Identification of the components was based on retention indices and comparison with reference spectra (Wiley and NIST databases). Percentages (relative) of the identified compounds were computed from the corresponding GC peak areas.

Chemicals and reagents

All standards used in this study were supplied by Sigma-Aldrich (St. Louis, MO). 4-Methyl-1-pentanol was employed as an internal standard. Ethanol, NaCl, anhydrous sodium sulfate and dichloromethane were purchased from Merck (Darmstadt, Germany).

Statistical analysis

Each component was present in samples I–V and the mean \pm SE for each value was calculated. The statistical analysis was performed using Origin software package version 7.0. The error bars in the figures indicate the standard error of the mean. The statistical significance of difference between the data pairs was evaluated by analysis of variance (one-way Anova) followed by the Tukey test. A statistical difference was considered significant at $p < 0.01$. The concentrations of the volatile components were recalculated on the basis of 100 % v/v ethanol (AA) and are expressed as g/hL AA.

RESULTS AND DISCUSSION

The main components of the distillate were ethanol and water, with a series of volatile substances that distil together and comprise a smaller portion of the spirit. These volatile substances, together with the components that are present in higher proportions, give distinctive flavor characteristics to the “Drenja”. The nature and composition of these components depend on the characteristics of the raw material, and on the fermentation and distillation processes.

A typical chromatogram for the “Drenja” samples is shown in Fig. 1. The chromatograms of the other samples showed the same pattern as those in Fig. 1,

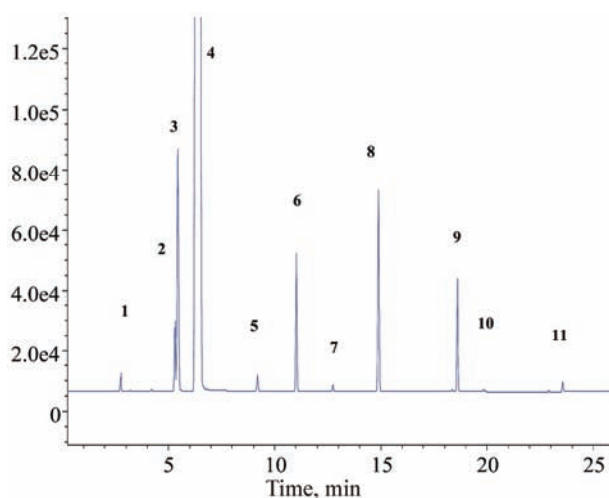


Fig. 1. Gas chromatogram obtained after direct injection of “Drenja” distillate: **1**: acetaldehyde; **2**: ethyl acetate; **3**: methanol; **4**: ethanol; **5**: 1-propanol; **6**: 2-methyl-1-propanol; **7**: 1-butanol; **8**: 2/3-methyl-1-butanol **9**: 4-methyl-1-pentanol (internal standard); **10**: 1-hexanol; **11**: 2-phenylethanol.

although the peak heights were different in each case. The retention times for the major compounds and their concentrations are summarized in Table I. The alcohols found were ethanol, methanol, 1-propanol, 2-methyl-1-propanol, 1-butanol, 1-hexanol, 2-phenylethanol and a mixture of 2-methyl-1-butanol and 3-methyl-1-butanol. As these isomers can be resolved only under specific chromatographic conditions, they are usually reported together as 2/3-methyl-1-butanol.

TABLE I. Concentrations of the major volatile compounds in "Drenja" samples (g/hL AA, unless otherwise indicated)

Compound	Sample					Average $SE(yEr\pm)^a$
	I	II	III	IV	V	
Ethanol (% vol)	45.0	42.6	45.0	46.2	45.0	44.76±0.59
Acetaldehyde	1.71	31.32	28	28.46	5.31	18.96±6.36
Ethyl acetate	306.6	159.0	205.3	211.2	107.1	197.84±33.01
Methanol	242	752	743	556	772	613±100.6
1-Propanol	30.0	16.9	25.3	13.2	25.3	22.14±3.07
2-Methyl-1-propanol	45.8	112.4	90.2	80.7	144.9	94.8±16.49
1-Butanol	3.2	4.9	4.8	2.8	7.1	4.56±0.76
2/3 Methyl-1-butanol	148.9	238.5	204.2	179.6	263.5	206.94±20.39
1-Hexanol	35.6	12.5	13.4	48.5	3.1	22.62±8.39
High alcohols (total)	224.7	372.7	324.5	276.3	440.8	327.80±37.47
2-Phenylethanol	28.6	32.6	36.2	39.1	12.2	29.74±4.72

^aStandard error of the predicted y-value for each x in a regression

Comparisons of the differences in pairs of the major components present in "Drenja" are given in Table II, from which it can be seen that there are usually significant statistical differences ($p < 0.01$; $p < 0.05$). No significant differences were found between acetaldehyde and 1-propanol, 1-butanol, 1-hexanol and 2-phenylethanol; between 2-methyl-1-propanol and 1-hexanol and 2-phenylethanol; between ethyl acetate and 2/3 methyl-1-butanol; between 2/3 methyl-1-butanol and 1-hexanol; and between 1-hexanol and 2-phenyl ethanol.

Ethanol

The fermentation of fruit mashes relies on the conversion of fruit sugars to ethanol by yeast. The Embden–Meyerhof–Parnas Pathway (EMP) is a well-known process for the conversion of sugars to ethanol by yeast. This pathway proceeds by degrading the sugar to acetaldehyde, which is then reduced to ethanol. The yield of ethanol is dependent upon the initial concentration of the total sugar present in the fruit, which is measured as the total dissolved sugar present in the liquid mash. All samples exhibited ethanol contents ranging from 42.6 to 46.2 % v/v. The EC regulation 1576/89 established general manufacturing procedures of marc distillates and fixed common analytical composition limits, *i.e.*, 86 % v/v of ethanol as the highest proof for the crude distillate and 37.5 % v/v as the minimal proof at bottling.⁸

TABLE II. Statistical significance of the difference between data pairs; the statistical significance of the difference between the data pairs was evaluated by analysis of the variance (one-way Anova) followed by the Tukey test. Analysis of the variance followed by the least significance at $p < 0.01$

Compound	Acetalde- hyde	Ethyl acetate	Methanol	1-Propanol	2-Methyl-1- -propanol	1-Butanol	2/3 Methyl-1- -butanol	1-He- xanol	High alcohols	2-Phenyl- ethanol
Ethanol	$p < 0.01$	$p < 0.01$	$p < 0.01$	$p < 0.01$	$p < 0.05$	$p < 0.01$	$p < 0.01$	$p < 0.05$	$p < 0.01$	$p < 0.05$
Acetaldehyde		$p < 0.01$	$p < 0.01$	N.s. ^a	$p < 0.01$	N.s.	$p < 0.01$	N.s.	$p < 0.01$	N.s.
Ethyl acetate			$p < 0.01$	$p < 0.01$	$p < 0.05$	$p < 0.01$	N.s.	$p < 0.01$	$p < 0.05$	$p < 0.01$
Methanol				$p < 0.01$	$p < 0.01$	$p < 0.01$	$p < 0.01$	$p < 0.01$	$p < 0.05$	$p < 0.01$
1-Propanol				$p < 0.01$	$p < 0.01$	$p < 0.01$	$p < 0.01$	N.s.	$p < 0.01$	N.s.
2-Methyl-1- propanol					$p < 0.01$	$p < 0.01$	$p < 0.01$	$p < 0.01$	$p < 0.01$	$p < 0.01$
1-Butanol						$p < 0.01$	$p < 0.01$	N.s.	$p < 0.01$	$p < 0.01$
2/3 Methyl-1- butanol							$p < 0.01$	$p < 0.01$	$p < 0.05$	$p < 0.01$
1-Hexanol								$p < 0.01$	$p < 0.01$	N.s.
High alcohols (total)									$p < 0.01$	$p < 0.01$

^aNo statistical difference ($p > 0.05$)

Methanol

Methanol is a very important compound in the production of fruit brandies and it is similar to ethanol in taste and smell; however, it is toxic and potentially dangerous if present in high concentrations.⁹ Methanol production is associated with the enzymatic degradation of the methoxy groups of pectin, as well as the acidic degradation of pectin. The methanol content in the analyzed samples ranged between 242 and 772 g/hL AA (maximum legal limit 1000 g/hL of 100 % vol. ethanol).⁸ In comparisons with other fruit pomace distillates (apple, cherry, pear and plum),¹⁰ "Drenja" has a similar level of methanol. Filajdić and Djuković found 1.41–8.85 g/hL AA methanol in Yugoslavian plum brandies, with higher levels occurring in home-made brandies.¹¹ Relatively low methanol concentrations have been determined in grape distillates (0.13–0.67 g/hL AA) owing to the small amounts of pectins in the raw materials.¹²

Acetaldehyde

The most common aldehyde present in distilled fruit spirits is acetaldehyde. It is a compound arising from the fermented raw materials, and its level increases during distillation and aging.¹³ It is also considered to be mainly the result of spontaneous or microbial-mediated oxidation. In cornelian cherry spirits, as with other distilled fruit spirits, acetaldehyde is usually seen as an undesirable aroma and discarded with the head fraction. European-style spirits are defined by law; however, the regulation provides no limits for acetaldehyde for any of the distilled spirits, which are manufactured by fermentation with retention of the organoleptic properties of their raw materials (*e.g.*, rum, whisky, brandy and fruit spirit). The concentration of acetaldehyde was found to range from 1.71 to 31.32 g/hL AA (Table I). Other spirit beverages usually contain very different acetaldehyde levels, ranging from 153–1073 mg/hL AA in some grape brandies, *e.g.*, Greek Tsipouro and Portuguese Bagaceiras (1330 mg/hL AA).^{12,14}

Ethyl acetate

Ethyl acetate is one of the most important esters due to its unpleasant flavor at higher concentrations. High ethyl acetate concentrations are indicative of prolonged storage of the raw material and probable acetic bacterial spoilage. It was generally found at higher levels than the usual values for Tsipouro,¹² melon,¹⁵ and Mezcal,¹⁶ but lower than Bagaceiras¹⁴ and Orujo.¹⁷ Filajdić and Djuković found a very high ethyl acetate content (4648 mg/hL AA) in home-made plum brandies.¹¹

Higher alcohols

Higher alcohols (also known as fusel alcohols) are secondary yeast metabolites, which can have both positive and negative impacts on the aroma and flavor

of a spirit. Excessive concentrations of higher alcohols can result in a strong, pungent smell and taste, whereas optimal levels impart fruity characters (Table I).

Higher alcohols are present in alcoholic beverages and are formed in small amounts by yeast, from sugars and from amino acids metabolism (Ehrlich mechanism) during the alcoholic fermentation process. The most common fusel alcohols in distilled spirits include: 2-butanol, isobutanol, 1-butanol, 1-propanol and amyl alcohols. Branched-chain higher alcohols, amyl alcohol, active amyl alcohol and isobutanol were the main fusel alcohols in “Drenja”. The amyl alcohols (2/3 methyl-1-butanol) content of the analyzed samples was in the range of 148.9–263.5 g/hL AA. 2-Methyl-1-propanol concentrations were in the range of 45.8–144.9 g/hL AA. The content of higher alcohols in the studied samples was similar to that of various distillates, such as Bagaceiras,¹⁴ Tsipouro¹² and Mouro.¹⁸ The minimum of total higher alcohols are fixed by the Regulating Commission at 200 g/hL AA of pure alcohol and all samples were within these limits.

1-Propanol

1-Propanol has a pleasant, sweetish odor, but excessive concentrations will introduce solvent notes that mask all the positive notes in distillates.¹⁹ The concentration of 1-propanol was found to range from 13.2 to 30.0 g/hL AA (Table I).

1-Hexanol

1-Hexanol is not an alcoholic fermentation product. When the fruits are not ripe enough, high 1-hexanol concentrations in spirits are observed.²⁰ The 1-hexanol concentrations in the studied samples ranged between 3.1 and 48.5 g/hL AA. Previous studies revealed much lower 1-hexanol contents (20–83 mg/hL AA) in Yugoslavian plum brandies.¹¹ However, high hexanol concentrations (64–316 mg/hL AA) were determined in Portuguese Bagaceiras, as well as in apple, pear and grape pomace spirits (102–154 mg/hL AA).¹⁴

2-Phenylethanol

2-Phenylethanol introduces a pleasant aroma, resembling that of roses, to distillates and derives from L-phenylalanine through the metabolic reaction of *Saccharomyces cerevisiae* during carbonic anaerobiosis.²¹ The high concentrations of 2-phenylethanol (12.2–39.1 g/hL AA) imparts a positive influence on the “Drenja” aroma. High levels of 2-phenylethanol have been found in, *e.g.*, Greek Tsipouro 12 (28–234 mg/hL AA) and spirits produced from blueberries, probably resulting from a high concentration of phenylalanine in the raw material.¹⁸

Minor compounds in “Drenja”

The minor volatile compounds identified in these spirits are presented in Table III. A total of 84 free aroma compounds were identified, including alcohols, esters, monoterpenes, carbonyl compounds, lactones, free acids, volatile phenols and acetals.

TABLE III. Relative percentages of the minor volatile compounds in "Drenja" samples (I–V)

Compound	<i>R_f</i> ^a	I	II	III	IV	V
Ethyl lactate	810.5	tr ^b	tr		tr	
Butyl acetate	812	tr			tr	
Furfural	830	1.14	1.89	1.85	1.22	5.49
1.1-Diethoxybutane				0.54	tr	
Hex-3-(<i>Z</i>)-en-1-ol	847		tr		tr	
Isopentyl acetate	876	2.03	3.70	0.62	1.06	1.73
Acetic acid, pentyl ester	847		0.82			
Hexan-1-ol	859	5.14	3.34	3.05	6.78	2.75
1.1-Diethoxy-3-methyl propane		0.28		0.77		
2-Methyl-butiric acid					1.56	
Phenylethyl acetate		0.33			0.22	tr
Ethyl pentanoate	900		1.28			
Methyl hexanoate	925		0.70			0.43
1.1-Diethoxy-3-methylbutane	955	0.65			1.61	
1.1-Diethoxypentane		0.54	0.83	1.68	1.32	1.24
Butyl propionate					0.90	0.65
Oct-1-en-3-ol	978	1.73	tr	2.67	4.62	1.28
Benzaldehyde	961	1.51			0.77	
Ethyl hexanoate	996	1.28	1.96	1.47	1.68	1.90
<i>p</i> -Cymene	1026	0.87	tr	0.53	2.20	
Limonene	1031	2.33	1.00	2.74	6.85	3.24
1.1-Diethoxyhexane		0.43	0.17			
Benzyl alcohol	1032	0.90	tr	1.20		1.37
Nonanal	1075	0.11		0.87	0.16	
2-Phenylacetaldehyde	1042	0.21	tr	0.23		0.13
Octanol	1070	0.32	0.82	0.12	0.78	0.88
<i>cis</i> -Linalool oxide	1074	1.12	0.12	0.32	0.13	1.10
<i>trans</i> -Linalool oxide	1088	1.10	0.59	1.23	0.76	0.64
Linalool	1096	1.11	0.26	1.32	1.52	0.76
Nonanal	1098		0.13			
Methyl benzoate	1098	0.32		0.43		0.34
2-Phenylethanol	1110	10.64	8.86	9.16	8.82	16.00
Methyl octanoate	1125	0.21	0.30			
Nerol oxide	1153	0.52	0.26	0.56	0.31	0.76
Benzyl acetate	1163	tr		0.76		0.34
1-Nonanol	1171	0.18	tr	0.34	0.21	0.64
4-Ethylphenol		0.60	3.44	3.21	3.65	1.78
Diethyl succinate		2.47		0.54	0.34	0.65
Ethyl benzoate	1170	4.81		0.85	1.05	0.99
Octanoic Acid	1175	3.48	10.17	3.58	2.13	4.21
Ethyl octanoate	1195	3.24	5.82	5.68	7.58	10.53
α -Terpineol	1189	0.93	0.67	0.77	0.54	0.98
Decanal	1204	0.21	0.14	0.21	0.11	0.11
Ethyl phenylacetate	1244	0.68	0.43	0.33	0.31	0.76
Phenylethyl acetate	1256	2.39	0.12	0.43	0.13	0.88
Methyl salicylate	1190	0.85	0.21	0.12	0.34	0.12

TABLE III. Continued

Compound	<i>R</i> ^a	I	II	III	IV	V
Ethyl salicylate	1267	0.48	0.23	0.12	0.32	0.15
Decan-1-ol	1272	0.21	tr		0.11	
Nonanoic acid	1275	1.02	2.59			
Methyl decanoate	1326	0.76	tr	0.87		1.09
Eugenol	1356	0.23		0.76	0.11	0.66
Ethyl (4 <i>E</i>)-decanoate	1382		tr			
Decanoic acid		3.47		4.25	5.91	4.28
Ethyl decanoate	1394	2.20	18.40	5.13	6.37	10.72
Caryophyllene	1418	0.64	0.44	0.65	0.56	0.34
Vanillin	1391	0.22	tr		0.17	0.12
Isoamyl octanoate	1446		0.39			
Ethyl (Z)-cinnamate	1466	0.89	0.48	0.87	0.39	0.76
α -Humulene	1454		tr			
1-Dodecanol	1473	0.12	0.14		0.11	
α -Murolene	1499		0.14			
Methyl dodecanoate	1527	0.13	0.16		0.23	
δ -Cadinene	1524	0.56	0.55	0.32	0.54	0.65
Nerolidol	1534	0.54		0.34	0.33	0.23
Dodecanoic acid	1568	2.28	1.35	1.89	1.56	1.21
Ethyl dodecanoate	1576	2.60	7.48	5.33	3.51	4.36
3-Methylbutyl pentadecanoate	1642	0.14	0.12	0.22	0.10	0.13
α -Cadinol	1653	0.23	0.33			
Tetradecan-1-ol	1676	0.21	tr			
Farnesol(2 <i>Z</i> ,6 <i>E</i>)	1694	0.33	0.13			
Methyl tetradecanoate	1727	0.32	0.26	2.94	0.21	5.27
Tetradecanoic acid		0.44	0.49	0.11	0.32	0.21
Ethyl tetradecanoate	1793	0.58	0.94	2.00	0.66	0.88
Isopropyl miristate	1809	0.22	tr	0.57		
Phenethyl octanoate	1849	0.12	0.18			
Methyl hexadecanoate	1927	1.22	1.46	1.34	1.20	1.86
Hexadecanoic acid	1968	1.00	0.54	0.87	0.65	0.76
Ethyl hexadecanoate	1993	3.90	1.90	3.74	1.15	3.42
Methyl linoleate	2092	0.18	0.24	0.54	0.21	
Methyl oleate	2093	1.22	0.46	0.21	0.33	
9.12-Octadecadienoic acid	2094	0.51	0.40	0.11	0.32	
Ethyl linoleate	2177	6.50	3.22	6.06	2.40	4.34
Ethyl oleate	2180	2.80	2.41	4.60	3.10	2.77
Ethyl stearate	2194		0.35			
Total		89.70	93.41	92.02	90.31	90.89

^aRetention index on DB-5 according to *n*-paraffins; ^btrace (less than 0.1 %)

Ethyl esters and fatty acids are the main components of “Drenja” aroma and have an important sensorial influence in these distilled alcoholic beverages. Ethyl esters contribute to the flavor with a pleasant fruity and flowery smell,²¹ indicative of the quality of the spirit.^{22,23} Ethyl hexanoate supplies the aroma of fruit (banana, green apple, *etc.*) and its presence, along with other ethyl esters, is beneficial for the spirit. The ethyl esters, hexanoate, octanoate, decanoate and dodeca-

noate, which are produced during the fermentation, pass into the spirits and their content increases during aging.²⁴ The dominant esters are the ethyl esters of fatty acids and acetates of higher alcohols. Ethyl hexanoate and ethyl octanoate predominated in the analyzed "Drenja" distillates. Long-chain fatty acids, octanoic, nonanoic, dodecanoic, tetradecanoic and hexadecanoic acid, have a smaller influence on the flavor of distillates.^{23,25} Table III shows that the most abundant among the present acids were octanoic, nonanoic, decanoic, dodecanoic and hexadecanoic acid.

The terpene profile was similar in all the distillates. Six monoterpenes were detected in the "Drenja" distillates: limonene, *cis*- and *trans*-linalool oxide, linalool, nerol oxide and α -terpineol. Of these, only limonene was previously reported as a constituent of the volatile fraction of cornelian cherry fruit.²² The terpene profile of the "Drenja" distillates may be the result of heat-catalyzed, acid hydrolysis of glycosylated terpenol precursors during distillation.

CONCLUSIONS

In the "Drenja" distillates, volatile compounds that pose health hazards or organoleptic faults, such as methanol or acetaldehyde, were found at levels lower than those established by the EU. Quantitatively, the higher alcohols were the largest group of the volatile composition in the "Drenja" distillates. There were statistically significant differences ($p < 0.01$; $p < 0.05$) in the major components present in the studied "Drenja" compared with ethanol. The ethyl esters and fatty acids formed enzymatically during the fermentation process constitute important groups of aroma compounds that contribute to the "fruity" note to the sensory properties of "Drenja" distillates. Moreover, the compounds that contribute to the typical flavor characteristics of the "Drenja" distillate, such as 2-phenylethanol, limonene and 4-ethylphenol, are desirable for this specific distillate. It seems that the complex and luxurious aroma of "Drenja" spirits depends on the subtle balance of the various mentioned functionalized compounds.

Acknowledgments. This research was supported by a grant from the Ministry of Science and Technological Development of the Republic of Serbia (Project No. 142053).

ИЗВОД

КАРАКТЕРИЗАЦИЈА ИСПАРЉИВИХ КОМПОНЕНТИ «ДРЕЊЕ», АЛКОХОЛНОГ ПИЋА ДОБИЈЕНОГ ИЗ ПЛОДОВА ДРЕЊИНЕ (*Cornus mas*)

ВЕЛЕ ТЕШЕВИЋ¹, НИНОСЛАВ НИКИЋЕВИЋ², СЛОБОДАН МИЛОСАВЉЕВИЋ¹, ДАНИЦА БАЈИЋ³,
ВЛАТКА ВАЈС³, ИВАН ВУЧКОВИЋ³, ЉУБОДРАГ ВУЈИСИЋ³, ИРИС ЋОРЂЕВИЋ⁴,
МИРОСЛАВА СТАНКОВИЋ⁵ и МИЛОВАН ВЕЛИЧКОВИЋ²

¹Хемијски факултет, Универзитет у Београду, Студентски тирз 16, 11000 Београд, ²Пољопривредни факултет, Универзитет у Београду, Немањина 6, 11080 Земун, ³Институт за хемију, технологију и металургију, Универзитет у Београду, Њежицева 12, 11000 Београд, ⁴Факултет за ветеринарске науке, Универзитет у Београду, Булевар ослобођења, 11000 Београд и ⁵Институт за нуклеарне науке "Винча", Лабораторија за физичку хемију, 11000 Београд

У раду су анализиране испарљиве компоненте у пет узорака алкохолних пића, домаће израде, добијених дестилацијом ферментисаних плодова дрењине (*Cornus mas* L.). Главна

испарљива једињења, која су одређена и квантификована, су: метанол, 1-пропанол, етил-ацетат, 2-метил-1-пропанол, 1-бутанол, изоамил-алкохоли, 1-хексанол и 2-фенилетанол. Мање заступљена испарљива једињења су екстрахована дихлорметаном и анализирана комбинацијом гасне хроматографије и масене спектрометрије (GC/MS). Идентификована су укупно 84 једињења. Најзаступљенија једињења била су етил естри масних киселина са C₆–C₁₈, слободне масне киселине, лимонен, 2-фенилетанол и 4-етилфенол. Већина једињења нађена у “дрењи” су слична онима која су присутна и у другим алкохолним пићима.

(Примљено 17. јуна, ревидирано 8. септембра 2008)

REFERENCES

1. E. Sezai, *J. Fruit. Ornam. Plant Res.* **12** (2004) 87
2. F. Demir, I. H. Kalyoncu, *J. Food Eng.* **60** (2003) 335
3. K. D. Kean, K. J. Hwan, *Arch. Pharm. Res.* **21** (1998) 787
4. J. Mau, C. Chen, P. Hsieh, *J. Agric. Food Chem.* **49** (2001) 183
5. N. P. Seeram, R. Schutzki, A. Chandra. M. G. Nair, *J. Agric. Food Chem.* **50** (2002) 2519
6. T. Karadeniz, *J. Amer. Pom. Soc.* **56** (2002) 164
7. EEC, *Council Regulation 2870/00 laying down Community reference methods for the analysis of spirit drinks, Off. J. Eur. Commun.* **L333** (2000)
8. EEC, *Council Regulation 110/2008 on the definition, description and presentation of spirit drinks, Off. J. Eur. Commun.* **L39** (2008)
9. A. Paine, A. D. Dayan, *Hum. Exp. Toxicol.* **20** (2001) 563
10. C. Bauer, H. Wachter, N. Christoph, A. Robmann, A. Ludwig, *Z. Lebensm. Unters. Forsch. A* **204** (1997) 445
11. M. Filajdić, J. Djuković, *J. Sci. Food. Agric.* **24** (1973) 835
12. A. A. Apostolopoulou, A. I. Flouros, P. G. Demertzis, K. Akrida-Demertzi, *Food Control* **16** (2005) 157
13. M. L. Silva, F. X. Malcata, *Am. J. Enol. Vitic.* **49** (1998) 56
14. M. L. Silva, F. X. Malcata, G. Revel, *J. Food Compos. Anal.* **9** (1996) 72
15. L. F. Hernandez-Gomez, J. Ubeda, A. Briones, *Food Chem.* **82** (2003) 539
16. A. L. Rodriguez, H. L. Gonzalez, A. P. Barba de la Rosa, P. E. Minakata, M. G. Lopez, *J. Agric. Food Chem.* **54** (2006) 1337
17. S. Cortes, M. L. Gil, E. Fernandez, *Food Control* **16** (2005) 383
18. E. H. Soufleros, S. A. Mygdalia, P. Natskoulis, *Food Chem.* **86** (2004) 625
19. M. Fundira, M. Blom, I. S. Pretorius, P. van Rensburg, *J. Agric. Food Chem.* **50** (2002) 1535
20. R. Cantagrel, L. Lurton, J. P. Vidal, B. Galy, in *Fermented Beverage Production*. A. G. H. Lea, J. R. Piggott, Eds., Blackie Academic & Professional, London, 1997, p. 208
21. S. Karagiannis, P. Lanaridis, *J. Food Sci.* **67** (2002) 369
22. E. H. Soufleros, I. Pissa, D. Petridis, M. Lygerakis, K. Mermelas, *Food Chem.* **75** (2001) 487
23. V. Tešević, N. Nikićević, A. Jovanović, D. Djoković, Lj. Vujisić, I. Vučković, M. Bonić, *Food Technol. Biotechnol.* **43** (2005) 367
24. M. L. Silva, F. X. Malcata, *Z. Lebensm. Unters. Forsch. A* **208** (1999) 134
25. M. Dolezal, J. Velisek, P. Famfulikova, *Biologically-Active Phytochemicals in Food*, Special Publication, The Royal Society of Chemistry, Cambridge, 2001, p. 241.



J. Serb. Chem. Soc. 74 (2) 129–132 (2009)
JSCS–3815

SHORT COMMUNICATION

Secondary metabolites of *Hypericum monogynum* from Pakistan

MOHAMMAD ARFAN^{1*}, NAILA RAZIQ¹, IVANA ALJANČIĆ^{2#}
and SLOBODAN MILOSAVLJEVIĆ^{3#}

¹Institute of Chemical Science, Peshawar University, 25000 Peshawar, Pakistan,

²Institute for Chemistry, Technology and Metallurgy, University of Belgrade, Njegoševa 12,
11000 Belgrade and ³Faculty of Chemistry, University of Belgrade,
Studentski trg 16, 11000 Belgrade, Serbia

(Received 26 May, revised 15 October 2008)

Abstract: 4-Chlorobenzoic acid (**1**), quercitrin (**2**), astilbin (**3**), along with β -sitosterol, γ -sitosterol, friedelin and β -amyrin were isolated from the aerial parts of *Hypericum monogynum*. Whereas compound **1** was isolated for the first time from natural sources, flavanonol **3** was not found before in these species.

Keywords: *Hypericum monogynum*; Clusiaceae; 4-chlorobenzoic acid; quercitrin; astilbin.

INTRODUCTION

The genus *Hypericum* L. (family Clusiaceae) comprises about 460 species distributed worldwide in temperate regions. *Hypericum* species were already known to ancient communities as useful medicinal plants. The best known among them is *Hypericum perforatum* (St. John's wort), the use of which as a remedy was described and recommended throughout the Middle Ages. Several groups of bioactive natural products, e.g., naphthodianthrones, phloroglucinols, phenylpropanoids, flavonol glycosides, biflavones, tannins, proanthocyanidins and xanthenes have been identified from the genus. Biological tests of the flavonoids isolated from the genus *Hypericum* demonstrated inhibition of lipoxigenase,¹ antidepressant² and scavenging³ activity, while the flavonoid glycoside exhibited antifungal activity.⁴ In Pakistan, twenty species of this genus are known. *Hypericum monogynum* Miller (Syn. *Hypericum chinense* L.) is distributed mainly in S.E. China and Taiwan. It is cultivated in many parts of the world, including the plains of W. Pakistan. This species is used in traditional medicine as an alternative, antidote and astringent, as well as in the treatment of miasmatic diseases.⁵

* Corresponding author. E-mail: m_arfan@upesh.edu.pk

Serbian Chemical Society member.

doi: 10.2298/JSC0902129A

Continuing our chemical examination of the flora of the North-West region of Pakistan and the search for compounds of pharmacological interest, an examination of the aerial parts of *H. monogynum* Miller, originating from Peshawar is now reported.

Previous examinations of *H. monogynum* involved the constituents of the aerial parts⁶ and volatiles.⁷ In a sample from China, Wang *et al.*⁶ identified 10 compounds: quercetin, quercitrin, hyperoside, rutin, (–)-epicatechin, 3,5-dihydroxy-1-methoxyxanthone, 3,4-*O*-isopropylidene shikimic acid, shikimic acid, daucosterol and oleanolic acid.

RESULTS AND DISCUSSION

A combination of different preparative chromatographic techniques and selective extractions with different solvents applied on the MeOH extract of the aerial parts of *H. monogynum* afforded seven compounds: 4-chlorobenzoic acid (**1**),⁸ quercitrin (**2**),⁹ astilbin (**3**) (Fig. 1),¹⁰ β -sitosterol,¹¹ γ -sitosterol,¹² friedelin and β -amyryn.¹³ The occurrence of **2**, also found in the same species before,⁶ as well as flavanonol rhamnoside **3**, detected previously in several species of the genus, among them *H. perforatum*,¹⁴ is not unexpected. Quercitrin (**2**) was demonstrated to be a potent antileishmanial compound, with a low toxicity profile and exhibited antioxidant activity in the DPPH test.¹⁵ The co-occurring flavanonol **3** was shown to exhibit diverse biological activities, such as lipolytic, anti-oxidative, anti-allergic, anti-inflammatory and insecticidal.¹⁶ To the best of our knowledge, *p*-chlorobenzoic acid has not been found from plant sources before. As shown in an investigation of the plant-growth activity of substituted benzoic and phenoxyacetic acids, including **1**,¹⁰ benzoic acids substituted with an electronegative atom capable of displacement by an electron-rich plant substrate exhibit plant-growth activity.¹⁷

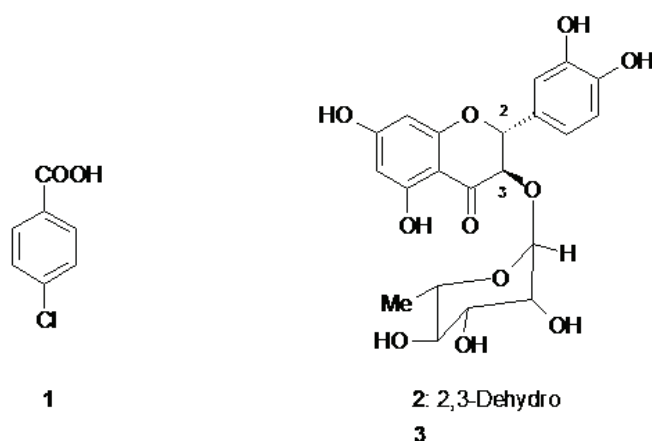


Fig. 1. Structures of 4-chlorobenzoic acid (**1**), quercitrin (**2**) and astilbin (**3**).

EXPERIMENTAL

General

The spectra were recorded with the following instruments: UV, Cintra 40, GBC UV-Vis spectrometer; IR, Perkin-Elmer FT-IR spectrometer 1725X; ^1H - and ^{13}C -NMR, Bruker DMX 600 (600 MHz for ^1H) in CD_3OD with TMS as the internal reference; DCI MS (150 eV, isobutane), Finnigan MAT mass spectrometer 8230, double focusing (BE geometry). Silica gel 60 and polyamide SC_6 were used for column chromatography. Silica gel 60 F_{254} and RP-8 $\text{F}_{254\text{s}}$ precoated aluminum sheets (0.25 mm, Merck) were used for TLC control.

Plant material

The aerial parts of *Hypericum monogynum* were collected at the University of Peshawar campus during the flowering stage in July 2004 and the taxonomic identification was performed by Professor Abdul Rasheed. A voucher specimen (No. 29304-PUP) is deposited in the Herbarium of the Department of Botany, University of Peshawar.

Extraction and isolation

Air dried, powdered aerial parts (1 kg) were extracted by percolation with methanol at room temperature. The residue (180 g) obtained after solvent removal under reduced pressure was successively extracted with *n*-hexane and ethyl acetate to yield the HE-extract (40 g) and EA-extract (12 g) after evaporation of the solvents. Aliquot of the EA-extract (12 g) was chromatographed on silica gel column with chloroform, gradually increasing polarity by successive addition of methanol. The fraction eluted with chloroform/methanol = 7/1, after recrystallization from methanol/water gave *p*-chlorobenzoic acid (**1**, 60 mg), identified by the identity of its spectral data to those from the SDBS library.⁸ The fraction eluted with chloroform/methanol = 7/2, upon crystallization from methanol/water afforded a mixture of two flavonoids (FF, 1.5 g).

An aliquot of FF (122 mg) was chromatographed on polyamide SC_6 with $\text{MeOH}/\text{H}_2\text{O} = 1:1$ to afford astilbin (**3**, 41 mg) and quercitrin (**2**, 56 mg). The progress of the elution was monitored by TLC (RP-8 $\text{F}_{254\text{s}}$); the developing system was $\text{MeOH}/\text{H}_2\text{O} = 1:1$.

Repeated silica gel chromatography of the *n*-hexane extract residue (40 g) yielded β -sitosterol (20 mg), γ -sitosterol (17 mg), friedelin (24 mg) and β -amyrin (25 mg).

CONCLUSIONS

The plant constituents quercitrin and astilbin make a different flavonol profile of the *Hypericum monogynum* from Pakistan, compared with the *H. monogynum* from China, which contains quercitrin and its aglycone quercetin. Substituted phenoxyacetic and benzoic acids, such as *p*-chlorobenzoic acid, capable of displacement by an electron-rich plant substrate, could exhibit plant-growth activity. This is the first time *p*-chlorobenzoic acid has been found from plant sources.

Acknowledgement. The authors from Serbia acknowledge their gratitude to the Ministry of Science and Technological Development of the Republic of Serbia for financial support, Project No. 142053.

ИЗВОД

СЕКУНДАРНИ МЕТАБОЛИТИ БИЉНЕ ВРСТЕ *Hypericum monogynum* ИЗ ПАКИСТАНАМОНАММАД АРФАЊ¹, НАИЛА РАЗИЊ¹, ИВАНА АЉАНЧИЊ² И СЛОБОДАН МИЛОСАВЉЕВИЊ³¹*Institute of Chemical Science, Peshawar University, 25000 Peshawar, Pakistan,* ²*Институт за хемију, технологију и металургију, Универзитет у Београду, Беошова 12, 11000 Београд и* ³*Хемијски факултет, Универзитет у Београду, Студентски штрз 16, 11000 Београд*

4-Хлоробензоева киселина (**1**), кверцитрин (**2**), астилбин (**3**), као и β -ситостерол, γ -ситостерол, фриделин и β -амирин изоловани су из надземних делова биљне врсте *Hypericum monogynum*. По први пут једињење **1** је изоловано из природних извора, док флаванол **3** до сада није изолован из ове биљне врсте.

(Примљено 26. маја, ревидирано 15. октобра 2008)

REFERENCES

1. M. Oblozinsky, L. Bezakova, I. Holkova, M. Vanko, T. Kartnig, M. Psenak, *Biologia* **61** (2006) 331
2. V. Butterweck, M. Hegger, H. Winterhoff, *Planta Med.* **70** (2004) 1008
3. M. I. Nassar, A. M. Gamal-Eldeen, *Bull. Faculty Pharm.* **41** (2003) 107
4. Y. Lu, Z. Zhang, G. Shi, J. Meng, R. Tan, *Acta Bot. Sin.* **44** (2002) 743
5. *Hypericum monoginum* (and references therein), <http://www.pfaf.org/database/plants.php?Hypericum+monoginum> (December, 2008)
6. J. Wang, S. Peng, M. Wang, N. Chen, L. Ding, *Zhongguo Zhongyao Zazhi* **27** (2002) 120
7. B. Demirci, K. H. C. Baser, S. L. Crockett, I. A. Khan, *J. Essent. Oil Res.* **17** (2005) 659
8. Spectral Database for Organic Compounds, SDBS (from Japan), http://www.aist.go.jp/sdbs/cgi-bin/cre_index.cgi (December, 2008)
9. T. Fossen, A. Larsen, B. T. Kiremire, O. M. Andersen, *Phytochemistry* **51** (1999) 1133
10. K. Ohmori, K. Hatakeyama, H. Ohru, K. Suzuki, *Tetrahedron* **60** (2004) 1365
11. Scifinder® - Carbon 13 NMR Spectrum for 83-46-5
12. P. L. Chiu, G. W. Patterson, *Lipids* **16** (1981) 203
13. S. B. Mahato, A. P. Kundu, *Phytochemistry* **37** (1994) 1517
14. a) G. Jurgenliemk, A. Nahrstedt, *Pharmazie* **58** (2003) 200; b) G. Jurgenliemk, A. Nahrstedt, *Planta Med.* **68** (2002) 88
15. a) M. F. Muzitano, E. A. Cruz, A. P. de Almeida, S. A. G. Da Silva, C. R. Kaiser, C. Guette, B. Rossi-Bergmann, S. S. Costa, *Planta Med.* **72** (2006) 81; b) G. K. Jayaprakasha, M. Ohnishi-Kameyama, H. Ono, M. Yoshida, L. J. Rao, *J. Agric. Food Chem.* **54** (2006) 1672
16. a) L.-K. Han, H. Ninomiya, M. Taniguchi, K. Baba, Y. Kimura, H. Okuda, *J. Nat. Prod.* **61** (1998) 1006; b) L. G. Batista Pereira, F. Petacci, J. B. Fernandes, A. G. Correa, P. C. Vieira, M. da Silva, G. F. Fatima, O. Malaspina, *Pest Manage. Sci.* **58** (2002) 503; c) M. Kenji, K. Toshimitsu, T. Yukiyoshi, I. Takao, Z. Wen-Hua, K. Koichiro, S. Fumio, I. Kiharu, *Nippon Shokuhin Shinsozai Kenyukaiishi* **5** (2002) 48
17. a) R. M. Muir, C. Hansch, *Plant Physiol.* **26** (1951) 369; b) M. R. Muir, C. Hansch, *Plant Physiol.* **28** (1953) 218.



J. Serb. Chem. Soc. 74 (2) 133–139 (2009)
JSCS–3816

Journal of
the Serbian
Chemical Society

JSCS@tmf.bg.ac.rs • www.shd.org.rs/JSCS

UDC 639.61+665.12+577.115:615.281–188

Original scientific paper

Comparison of the antibacterial activity, volatiles and fatty acid composition of lipids of *Phycopsis* species collected at different locations from the Bay of Bengal (Orissa coast)

PRAVAT MANJARI MISHRA* and AYINAMPUDI SREE

Natural Product Department, Institute of Minerals & Materials Technology
(Formerly RRL), Bhubaneswar - 751013, Orissa, India

(Received 30 May, revised 7 August 2008)

Abstract: The fatty acid composition as well as the volatiles and an antibacterial screening of the total lipids isolated from marine sponge *Phycopsis* sp. collected at two different locations from the Bay of Bengal of the Orissa coast having different morphological features were studied. The content of linear saturated acids was 30.25 % in *Phycopsis* sp. 1, while their content reached 50.33 % in *Phycopsis* sp. 2. The amount of monobranched, saturated acids was 44.87 % in *Phycopsis* sp.1 and 38.83 % in *Phycopsis* sp. 2. There was more phytanic acid (7.92 %) in *Phycopsis* sp. 2 than in *Phycopsis* sp. 1 (4.06 %). The amount of 5,9-pentacosadienoic acid was found to be 5.54 % in *Phycopsis* sp. 1, while it was absent in *Phycopsis* sp. 2. Both species showed differences in their fatty acid composition and volatiles as well as in the antibacterial screening of their lipid extracts.

Keywords: sponges; *Phycopsis* sp.; fatty acids; volatiles; antibacterial.

INTRODUCTION

Over the past decade, marine sponges from the class Demospongiae have attracted growing interest because of their unique chemical composition and biological activity. A number of biologically active secondary metabolites have been found in sponges.¹ Some unusual fatty acids (FAs) of sponges also exhibit biological activity.² Many new FAs were identified in sponge lipids, such as unsaturated FAs with an unusual distribution of the double bonds,³ branched chain FAs⁴ and FAs with unusual substituents in the carbon chain, such as the cyclopropane group,⁵ methoxy group,⁶ acetoxy group,⁷ etc.

The bioactivity of the sponge *Phycopsis* sp. was already studied by Venkateswarlu *et al.* in 1995.⁸ A CH₂Cl₂–MeOH extract of this organism exhibited antibacterial activity against *E. coli* and *B. subtilis* and a prenylated aromatic com-

* Corresponding author. E-mail: pravatmanjari@yahoo.co.in
doi: 10.2298/JSC0902133M



pound, phycopsisenone, was isolated from this extract. This paper presents the fatty acid composition, volatiles and antibacterial screening of lipid extracts against different pathogens of the two *Phycopsis* species having different morphological features, which were collected from the same depth but at different locations from the Bay of Bengal.

EXPERIMENTAL

Sponge material

Sponge specimens *Phycopsis* sp. 1 and 2 (Class: Demospongiae Sollas, order: Halichondrida Vosmaer, Family: Axinellidae Ridley and Dendy) were collected from 25 m depth from the Bay of Bengal of the Orissa coast during February–March, 2006 from a newly found ridge lineation (sp. 1 – 18° 57.294' N, 84° 44.057' E; sp. 2 – 18° 57.717' N, 84° 44.410' E).^{9,10} The two samples were identified to genus level by Dr. P.A. Thomas, Ex-Emeritus Scientist (ICAR), Trivandrum, Kerala.

Extraction

Sponges were thoroughly washed and air-dried. Ten grams of each species was homogenised and successively extracted three times with chloroform–methanol (2:1, v/v) to isolate the lipids.¹¹ The crude lipid extracts were purified by a “folch wash”¹² to remove non-lipid contaminants. The chloroform phase was separated from the combined extract, dried over anhydrous sodium sulphate and concentrated under a nitrogen atmosphere. The yield of lipids was 4.0 % of the dry weight of the sponges.

Preparation of fatty acid methyl esters

The fatty acids so obtained were converted to the corresponding methyl esters. Fatty acids (10 mg) were dissolved in 4 ml of 5 % hydrochloric acid in methanol and 0.5 ml benzene and then the mixture was refluxed in a silicone bath at 80–100 °C for 2 h. After cooling, the methyl esters were extracted with petroleum ether, simultaneously neutralized and dried over a sodium sulphate–sodium bicarbonate mixture. The solvent was evaporated to dryness under reduced pressure at 40 °C in a water bath. These fatty acid methyl esters (FAME) were then analysed by GC/MS for identification.

Isolation and analysis of the volatile compounds

Part of the crude lipophilic extract (100 mg) was subjected to a 4-h distillation–extraction in a Lickens–Nickerson apparatus.¹³ The volatiles were extracted from the distillate with diethyl ether (yield: 3 mg) and investigated using a Shimadzu QP-5000 GC-MS with a 25 m × 0.25 mm, 0.25 µm film thickness, WCOT column coated with 5 % diphenyl siloxane, supplied by J & W (DB-5). Helium was used as the carrier gas at a flow rate of 1.2 ml/min, at a column pressure of 42 kPa. The column temperature was programmed from 40 to 280 °C at a rate of 4 °C/min. The ionization voltage (EI) was 70 eV.

Antibiotic activity testing of lipid extracts of the Phycopsis species

The antibacterial assay of the crude lipid extracts of *Phycopsis* sp. 1 and 2 (200 µg/6 mm disc) were performed against five fish pathogens (*Edwardsiella tarda*, *Staphylococcus aureus*, *Micrococcus* sp., *Pseudomonas aeruginosa* and *Escherichia coli*) and two human pathogens (*S. aureus* and *Salmonella typhi*), including three MDR (multi drug resistant) strains (*Staphylococcus pyogenes*, *Acinetobacter* sp. and *S. typhi*), by the disc-assay method.¹⁴

The test bacterial fish pathogen cultures were obtained from the stock cultures maintained in the Pathology Laboratory of Central Institute of Fresh Water Aquaculture, ICAR, Bhubaneswar.

Fatty acid methyl esters, FAME, analysis

FAME analyses were performed on a Shimadzu QP-5000 GCMS equipped with a mass selective detector and a 25 m×0.25 mm, 0.25 µm film thickness, WCOT column coated with 5 % diphenyl siloxane, supplied by J & W (DB-5). Helium was used as the carrier gas at a flow rate of 1.2 ml/min, at a column pressure of 42 KPa. The column temperature was programmed for fatty acid methyl esters (FAMES) from 120–300 °C at a heating rate of 2 °C/min and 300 °C for 10 min, with a total run time of 100 min. An ionization voltage (EI) of 70 eV was used. Peak identification was performed by comparison of their mass spectra with those available in the Nist and Wiley libraries.

RESULTS AND DISCUSSION

Both *Phycopsis* species 1 and 2, collected at two different locations from a depth of 25 m from the Bay of Bengal of the Orissa coast, had different morphological features. *Phycopsis* sp. 1 was light orange in colour and had a finger-like structure (Fig. 1), while *Phycopsis* sp. 2 was light yellowish orange in colour with a rough body and soft structure (Fig. 2). The aim was to determine the difference in the fatty acid composition of the total lipids of two species of the same genus but having a different structural pattern. *Phycopsis* sp. 1 contained a greater number of fatty acids in comparison to *Phycopsis* sp. 2 (see Table I).



Fig. 1. *Phycopsis* sp. 1.



Fig. 2. *Phycopsis* sp. 2.

The whole series of linear saturated fatty acids from C14 up to C32 were revealed in the lipid composition of the sponges. The content of linear saturated fatty acid was 30.25 % in *Phycopsis* sp. 1, while the content was 50.33 % in *Phycopsis* sp. 2. All acids from C14:0 to C23:0 were found in *Phycopsis* sp. 1, except C19 and C22:0, among which C16:0 and C18:0 were dominant (11.76 and 9.29 %, respectively), while in *Phycopsis* sp. 2, except for C17:0, C19:0 and C22:0, all acids were present from C14:0–C23:0, among which C16:0, C18:0 dominated (8.95 and 8.88 %, respectively). The content of C21:0 was only 3.89 % in *Phycopsis* sp. 1, while in *Phycopsis* sp. 2, it was present in a reasonable amount (7.63

%). The total amount of tricosanoic acid was only 0.53 % in *Phycopsis* sp. 1, while its amount in *Phycopsis* sp. 2 was 6.02 %.

TABLE I. GC/MS analysis of the FAME of the total lipid of *Phycopsis* sp. collected at two different locations

Acid	Retention time min	Acid content, %	
		<i>Phycopsis</i> sp. 1	<i>Phycopsis</i> sp. 2
Tridecanoic acid, 3-methyl (C13:0, br ^a)	4.21	2.24	–
Nonanoic acid (C9:0)	5.52	–	4.18
Tetradecanoic acid (C14:0)	7.75	2.35	2.64
Pentadecanoic acid (C15:0)	8.73	7.64	9.39
Tetradecanoic acid, 12-methyl (C14:0, br)	8.85	2.81	–
9-Hexadecenoic acid (C16:1)	10.55	1.14	–
Hexadecanoic acid (C16:0)	10.89	11.76	8.95
2-Hexylcyclopropaneoctanoic acid	11.49	5.34	6.68
14-Methylhexadecanoic acid (C16:0, br)	11.56	7.92	–
Heptadecanoic acid (C17:0)	11.87	2.58	–
3,7,11,15-Tetramethylhexadecanoic acid	13.45	4.06	7.92
15-Octadecenoic acid (C18:1)	13.62	–	2.86
10-Octadecenoic acid (C18:1)	13.63	3.77	–
Octadecanoic acid (C18:0)	13.94	9.92	8.88
11-Methyloctadecanoic acid	14.52	–	24.96
17-Methyloctadecanoic acid	14.55	25.03	–
2-Octylcyclopropaneoctanoic acid	15.20	1.53	–
Eicosanoic acid (C20:0)	16.79	1.90	2.64
16-Methylheptadecanoic acid	17.65	–	7.19
Heneicosanoic acid (C21:0)	17.79	3.89	7.63
Tricosanoic acid (C23:0)	20.26	0.53	6.02
5,9-Pentacosadienoic acid (C25:2)	22.21	5.54	–

^aBranched

The total content of monobranched, saturated acids was 44.87 % of total FA content in *Phycopsis* sp. 1, while its amount was less in *Phycopsis* sp. 2 (38.83 %).

17-Methyloctadecanoic acid represented 25.03 % of the total monobranched FAs in *Phycopsis* sp. 1, while in *Phycopsis* sp. 2 11-methyloctadecanoic acid was dominant in the total monobranched FAs (24.96 %). 14-Methylhexadecanoic acid was also present in *Phycopsis* sp. 1 in a significant amount (7.92 %), while in *Phycopsis* sp. 2, 16-methylheptadecanoic acid was present in a significant amount (7.19 %). The amount of 2-hexylcyclopropaneoctanoic acid was found to be 5.34 % in *Phycopsis* sp. 1, while in *Phycopsis* sp. 2 it was 6.68 %. 2-Octylcyclopropaneoctanoic acid, was found in *Phycopsis* sp. 1, while it was absent in *Phycopsis* sp. 2.

The polymethyl branched saturated FAs of the sponges were represented by the usual isoprenoid FAs, 4,8,12-trimethyltridecanoic acid, phytanic acid and pristanic acids, their contents varying from 0.5 up to 20 % of the total FAs. Only

one isoprenoid fatty acid, *i.e.*, phytanic acid, was found in both species (4.06 and 7.92 % in species 1 and 2, respectively).

Monoenes are reported to vary from 2 to 50 % of the FA total content in various sponge species.¹⁵ However, only two monoenes were found in *Phycopsis* sp. 1 and only one in *Phycopsis* sp. 2. Among the six isomers of the C16:1 acid, C16:1 Δ 9 prevailed in most of the species and its relative content was about 3–5 % on average.¹⁵ In *Phycopsis* sp. 1, the C16:1 Δ 9 content was 1.14 % but it was not found in *Phycopsis* sp. 2. The content of C18:1 Δ 10 was found to be 3.77 % in *Phycopsis* sp. 1, but it was also absent in *Phycopsis* sp. 2. In *Phycopsis* sp. 2 only one monoenic acid was found and that was C18:1 Δ 15 (2.86 % of the total FA content), but it was absent in *Phycopsis* sp. 1.

In some species of sponges, polyenic FAs are represented exclusively by dienes. Thus, the ratio of dienes can reach 6–12 % of the FA total, *e.g.*, in the sponges *Agelas dispar*, *Anthosigmella varians* and *Chondrilla nucula*.¹⁶ The amount of 5,9-pentacosadienoic acid was found to be 5.54 % in *Phycopsis* sp. 1 but it was absent in *Phycopsis* sp. 2.

Volatile compounds

Volatile compounds often possess valuable biological activities. They serve as allelochemicals defending the organism from bacteria, fungi and viruses. Analogous to other investigated sponges,^{17,18} the volatiles in both *Phycopsis* sp. 1 and 2 appeared to be relatively simple (see Table II). *Phycopsis* sp. 2 contained no saturated *n*-hydrocarbons, while the amount of saturated *n*-hydrocarbons was 16.55 % in *Phycopsis* sp. 1. A number of saturated aliphatic aldehydes were found in *Phycopsis* sp. 2, whereas no such aldehydes were found in *Phycopsis* sp. 1. Significant concentrations of these compounds are an indication for the participation of bacteria (coming from the diet or associated with the tissues) in their formation.¹⁸ 1,2-Benzenedicarboxylic acid, dioctyl ester constituted 89.49 % of the total volatiles content of *Phycopsis* sp. 2, which was absent in *Phycopsis* sp. 1. Only one ketone, *i.e.*, (*E*)-hept-3-en-2-one, was found in *Phycopsis* sp. 2, which was absent in *Phycopsis* sp. 1. Dodecan-1-ol was the only alcohol found in *Phycopsis* sp. 1, whereas *trans*-2-decenol, an unsaturated alcohol, was found in *Phycopsis* sp. 2. The volatiles in both the species collected at two different locations were found to differ significantly from each other.

Antibacterial activity

Antibacterial screening of the lipid extract of both species *Phycopsis* sp. 1 and *Phycopsis* sp. 2 were performed against different pathogens. The lipid extract of *Phycopsis* sp. 1 exhibited trace activity against only *Escherichia coli* (fish pathogen), while that of *Phycopsis* sp. 2 showed trace activity against four pathogens, *i.e.*, *Staphylococcus aureus* (human pathogen), *S. aureus* (fish pathogen), *Micrococcus* sp. and *E. coli* (Fish pathogen).

TABLE II. Composition of the volatile compounds in *Phycopsis* sp. collected at two different locations

Volatiles	Content, %	
	<i>Phycopsis</i> sp. 1	<i>Phycopsis</i> sp. 2
Pentanal	–	0.28
Hexanal	2.2	0.72
(<i>E</i>)-Hept-3-en-2-one	–	5.31
Heptanal	–	1.48
Undecane	11.24	–
Undecanal	1.98	–
Dodecane	5.31	–
Dodec-1-ene	16.08	1.25
<i>trans</i> -2-Decenol	1.24	–
Dodecan-1-ol	29.39	–
Non-2-enal	1.53	–
Nonanal	–	2.91
1,2-Dichlorohexane	7.43	–
1,2- Benzenedicarboxylic acid, dioctyl ester	–	89.49
Butane, 1-(2,2-dichloro-3-ethylcyclopropyl)	–	3.79
Dihydrocitronellol	18.62	–

CONCLUSIONS

From the above studies, it can be concluded that the two specimens of the *Phycopsis* genus, collected from same depth but at different locations and having different morphological features, differ in their volatiles and composition of fatty acids, as well as in the antibacterial activity of their lipid extracts.

Acknowledgements. The authors thank Director, IMMT, Bhubaneswar for the facilities and Dr. P.A. Thomas, Ex-Emeritus Scientist (ICAR), Trivandrum, Kerala for identification of the sponges.

ИЗВОД

ПОРЕЂЕЊЕ АНТИБАКТЕРИЈСКЕ АКТИВНОСТИ И САДРЖАЈА ИСПАРЉИВИХ
МАТЕРИЈА И МАСНИХ КИСЕЛИНА У МАСТИМА ВРСТА *Phycopsis*
САКУПЉЕНИХ НА РАЗЛИЧИТИМ ЛОКАЦИЈАМА БЕНГАЛСКОГ ЗАЛИВА
(ОБАЛА ДРЖАВЕ ОРИСА, ИНДИЈА)

PRAVAT MANJARI MISHRA и А. SREE

*Natural Product Department, Institute of Minerals & Materials Technology (Formerly RRL),
Bhubaneswar-751013, Orissa, India*

Испитиван је садржај масних киселина и испарљивих материја, као и антибактеријска активност укупних масти изолованих из морских сунђера *Phycopsis* sp. различитих морфолошких карактеристика, сакупљених на две различите локације у Бенгалском заливу, обала државе Ориса, Индија. Садржај линеарних засићених киселина у *Phycopsis* sp. 1 износио је 30,25 %, док њихов садржај у *Phycopsis* sp. 2 достиже 50,33 %. Садржај моноразгранатих засићених киселина у *Phycopsis* sp. 1 и sp. 2 износио је 44,87%, односно 38,83 %. Садржај

фитанске киселине био је већи у *Phycopsis* sp. 2 (7,92 %) него у *Phycopsis* sp. 1 (4,06 %). Количина 5,9-пентакозадиенске киселине износила је 5,54 % у *Phycopsis* sp. 1, док у *Phycopsis* sp. 2 ова киселина није нађена. Ове врсте разликују је по садржају масних киселина и испарљивих материја, као и по антибактеријској активности липидних екстраката.

(Примљено 30. маја, ревидирано 7. августа 2008)

REFERENCES

1. J. Kobayashi, M. Ishibashi, *Chem. Rev.* **93** (1993) 1753
2. P. Ciminiello, E. Fattorusso, S. Magno, A. Mangoni, A. Ialenti, M. Dirosa, *Experientia* **47** (1991) 739
3. T. Rezanka, V. M. Dembitsky, *J. Nat. Prod.* **56** (1993) 617
4. E. Ayanoglu, R. Walkup, D. Sica, C. Djerassi, *Lipids* **17** (1982) 617
5. J. Lankelma, E. Ayanoglu, C. Djerassi, *Lipids* **18** (1983) 853
6. E. Ayanoglu, A. Aboubichara, C. Djerassi, J. M. Kornprobst, S. Popov, *Lipids* **18** (1983) 830
7. E. Ayanoglu, C. Djerassi, J. M. Kornprobst, K. Kurtz, *Lipids* **20** (1985) 141
8. Y. Venkateswarlu, M. A. Farooq Biabin, J. V. Rao, *J. Nat. Prod.* **58** (1995) 269
9. M. Bapuji, A. Sree, S. Mishra, A. Vimala, S. K. Sahu, S. Choudhury, P. A. Thomas, *Curr. Sci.* **77** (1999) 220
10. K. Mohan Rao, K. S. R. Murthy, N. P. C. Reddy, A. S. Subrahmanyam, S. Lakshinayyan, M. K. Prem Kumar, K. V. L. N. Sarma, Y. S. N. Raju, A. Sree, M. Bapuji, *Curr. Sci.* **81** (2001) 828
11. W. W. Christie, *Lipid analysis*, 2nd Edition, Pergamon Press, Oxford, 1982, p. 22
12. J. Folch, M. Lees, G. H. S. Stanely, *J. Biol. Chem.* **226** (1957) 497
13. H. Hendriks, J. Geerts, Th. Malingre, *Pharm. Weekblad Sci.* **116** (1981) 1316
14. J. F. Acar, in *The disc susceptibility test: Antibiotic in Laboratory Medicine*, V. Lorian, Ed., Williams and Wilkins, London, 1980, p. 24
15. S. A. Rod'kina, *Russ. J. Mar. Biol.* **31** (2005) S49
16. N. M. Carballeira, L. Maldonado, B. Porras, *Lipids* **22** (1987) 767
17. S. De Rosa, C. Iodice, J. Nechev, K. Stefanov, S. Popov, *J. Serb. Chem. Soc.* **68** (2003) 249
18. S. De Rosa, S. De Caro, G. Tommonaro, K. Slantchev, K. Stefanov, S. Popov, *Mar. Biol.* **140** (2002) 465.



J. Serb. Chem. Soc. 74 (2) 141–154 (2009)
JSCS–3817

Synthesis, coordination and biological aspects of organotin(IV) derivatives of 4-[(2,4-dinitrophenyl)amino]-4-oxo-2-butenic acid and 2-[(2,4-dinitrophenyl)amino]carbonylbenzoic acid

KHADIJA SHAHID¹, SAIRA SHAHZADI² and SAQIB ALI^{1*}

¹Department of Chemistry, Quaid-i-Azam University, Islamabad – 45320 and

²Department of Chemistry, GC University, Faisalabad, Pakistan

(Received 29 February, revised 13 June 2008)

Abstract: New series of organotin(IV) complexes of aniline derivatives, R_2SnL_2 and R_3SnL [where $R = Me, n-Bu, Ph, n-Oct$] have been synthesized by the reaction of HL^1 and HL^2 with respective organotin halides or oxides. Experimental details for the preparation and characterization (including elemental analysis, IR and multinuclear NMR (1H -, ^{13}C - and ^{119}Sn -) spectra in $CDCl_3$ and EI mass spectra of both series are provided. The binding sites of the ligands were identified by means of FTIR spectroscopic measurements. It was found that in all cases the organotin(IV) moiety reacts with the oxygen of COO^- group to form new complexes. In the diorganotin complexes, the COO^- group is coordinated to the organotin(IV) centres in a bidentate manner in the solid state. The ^{119}Sn NMR data and the $^nJ(^{13}C-^{119/117}Sn)$ coupling constant support the tetrahedral coordination geometry of the organotin complexes in non-coordinating solvents. Biological activities (antibacterial, antifungal, cytotoxicity, antileishmanial and insecticidal) of these compounds are also reported.

Keywords: organotin(IV) carboxylates; IR; multinuclear NMR (1H , ^{13}C and ^{119}Sn); mass spectrometry; biological activity.

INTRODUCTION

The chemistry of organotin(IV) complexes has developed considerably during the last 30 years, highlighting the syntheses of a number of complexes with interesting properties.^{1–3} Organotin carboxylates are widely used owing to their potential biocidal activity⁴ and cytotoxicity,⁵ as well as to their industrial and agricultural applications.^{6–10} In general, the biocidal activity of organotin complexes is greatly influenced by the molecular structures and coordination number of the tin atom.¹¹

* Corresponding author. E-mail: drsa54@yahoo.com

doi: 10.2298/JSC0902141S

The environmental and biological chemistry of organotin(IV) carboxylates have been the subject of interest for some time, due to their increasingly widespread use in industry and agriculture.^{12–16} Our current interest focuses on the synthesis, characterization and biological studies of different aniline derivatives of carboxylic acids.

EXPERIMENTAL

Physical measurements

Melting points were determined in capillary tubes using a MP-D Mitamura Riken Kogyo (Japan) electrothermal melting point apparatus and are uncorrected. Infrared absorption spectra (4000–400 cm^{-1}) were recorded as KBr pellets on a Bio-rad FTIR spectrophotometer.

^1H -, ^{13}C - and ^{119}Sn -NMR spectra were recorded on a Bruker AM 250 spectrometer (Germany), using CDCl_3 as an internal reference ($\delta\ ^1\text{H}(\text{CDCl}_3) = 7.25$ and $\delta\ ^{13}\text{C}(\text{CDCl}_3) = 77.0$). Coupling constants (in H_2) are given in brackets. ^{119}Sn -NMR spectra were obtained with Me_4Sn as the external reference ($\delta(\text{Sn}) = 37.290665$). The numbering schemes for the organotin(IV) derivatives of HL^1 and HL^2 are given in Schemes 1 and 2, respectively.

Mass spectral data were measured on a MAT 8500 Finnigan 70 eV mass spectrometer (Germany).

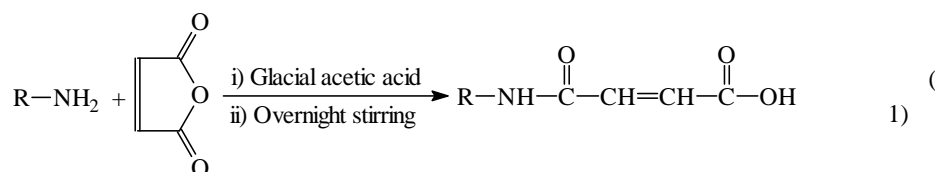
Materials and chemicals

Organotin compounds are moisture and air sensitive; hence, the reactions were performed under an inert atmosphere. All the glass apparatus with standard quick fit joints used throughout the work were cleaned and dried at 120 $^\circ\text{C}$. Di- and tri-organotin(IV) salts were purchased from Aldrich. All other reagents were of the purest grade available. Solvents were purified as in previously published methods.¹⁷ The anhydrides and 2,4-dinitroaniline were commercial products and used without further purification.

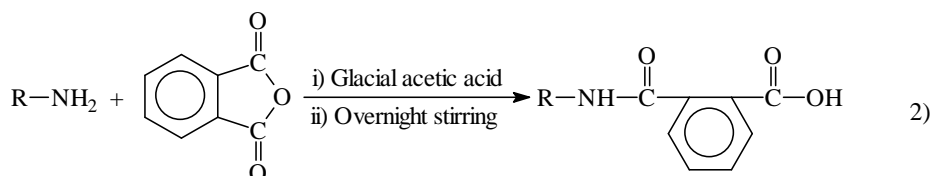
General procedure for the synthesis of the ligands (HL^1 , HL^2)

A solution of anhydride (1 mmol) in acetic acid (300 ml) was added to a solution of 2,4-dinitroaniline (1 mmol) in acetic acid (150 ml) and the mixture was stirred at room temperature overnight. The coloured precipitates formed were filtered off, washed with cold distilled H_2O (200 ml) and air-dried. The general chemical reaction is given by Eqs. (1) and (2).

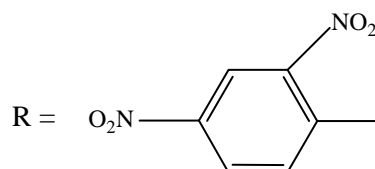
For HL^1 :



For HL^2 :



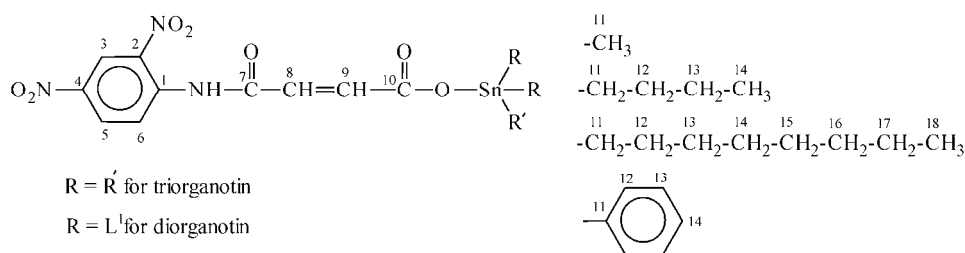
where



General procedure for the synthesis of the di/tri-organotin(IV) complexes

The ligand (5 mmol) was suspended in dry toluene (100 ml) and treated with triethylamine (0.59 ml, 5 mmol). The mixture was refluxed for 2–4 h. To a reaction mixture, diorganotin dichloride or triorganotin chloride (2.5 mmol/5 mmol) was added as a solid to the reaction flask under constant stirring and then refluxed for 8–10 h. The reaction mixture containing Et_3NHCl was filtered off such that the filtrate contained the organotin(IV) derivative. The solvent was removed under reduced pressure using a rotary evaporation (Eqs. (3) and (4)). However, for $\text{Oct}_2\text{Sn}(\text{L}^1/\text{L}^2)_2$, 5 mmol of the ligand HL^1/HL^2 was suspended in dry toluene (100 ml), solid Oct_2SnO (2.5 mmol) was added under constant stirring and refluxed for 8–10 h. The formed water was removed *via* a Dean-Stark trap. After cooling to room temperature, the solvent was removed under reduced pressure using a rotary evaporator (Eq. (5)).

The general chemical reactions for the synthesis of the di/triorganotin compounds are given by Eqs. (3)–(5).



Scheme 1. NMR numbering scheme for the organotin(IV) derivatives of 4-[(2,4-dinitrophenyl)amino]-4-oxo-2-butenoic acid (HL^1).

Biological activity

Antibacterial activities. The antibacterial activities were determined using the agar well diffusion method.¹⁸ Wells (diameter, 25 mm) were made in the media with a sterile borer and an eight-hour-old bacterial inoculum containing *ca.* 10^4 – 10^6 colony forming units (CFU)/mL was spread on the surface of the nutrient agar using a sterile cotton swab. The recommended concentration of the test sample (2 mg/mL in DMSO) was introduced into the respective wells. Other wells containing DMSO and the reference antibacterial drug served as negative and positive controls, respectively. The plates were incubated immediately at 37 °C for 20 h. The activity was determined by measuring the diameter (in mm) of the inhibition zone

showing complete inhibition. Growth inhibition was calculated with reference to the positive control.

LD₅₀ data of the compounds were determined by the brine-shrimp assay method.¹⁸

Insecticidal activity. The insects were exposed to the test compounds by the contact method¹⁸ using filter paper. Different concentrations of every compound (1 ml) were applied by micropipette to 90 mm diameter filter papers, which were then placed in petri dishes. Subsequently, four adult insects of the same size and age of each batch were transferred to the petri dishes. A control batch was treated with solvent for the determination of the environmental effects. Another batch was supplemented with reference insecticides, *i.e.*, Coopex and Decis (synthetic pyrethroids). All batches were kept without food throughout the 24 h exposure period, after which the mortality counts were determined.

Antileishmanial activity. Leishmania promastigotes were grown in bulk early in a liquid medium RPMI-1640 supplemented with 10 % foetal calf serum. At the log phase, the parasites were centrifuged at 2000 rpm for 10 min and the old medium was discarded. The parasites were diluted with fresh culture medium to a final density of 106 cells ml⁻¹. 100 µl of the culture was added in all the wells, except the first column, which received 180 µl. The last two rows of the microtiter plate were control containing varying concentrations of standard antileishmanial compounds, *e.g.*, amphotericin B or pentmidine.

The samples were prepared by dissolving 1.0 mg of the experimental compounds/crude extract (test sample) in 50 µl of DMSO and diluted up to 1.0 ml with complete medium containing antibiotics.

The method of addition and serial dilution of the samples was applied. Thus, 20 µl of a solubilised compound was added in to the first well (duplicate or triplicate) and mixed well with the micropipette. 100 µl of sample was removed and added into the next well, mixed well, 100 µl removed and added into the next well until the 8th well was reached. The remaining 100 µl was discarded. In this manner, the first well received a final concentration of 100 µg ml⁻¹, and the last 0.78 µg ml⁻¹ of the compound/crude extract to be tested. The plate was incubated in the dark at 25 °C for 3–5 days (preferably on an orbital shaker).

After 5 days exposure, the drug activity was assessed microscopically using an improved Neubauer chamber (hemocytometer). Thus, using a micropipette, 10 µl of the culture was removed and transferred to both chambers of the hemocytometer. Starting with chamber “o” of the hemocytometer, the cells were counted in the 1 mm centre square and the four 1 mm corner square at a magnification of 40×. The number of cells/ml was determined using the following formula: cells per ml = the average count per square × 10⁴, *e.g.*, if the average counts per large square was 45 cells, then there were 4.5 × 10⁵ cells/ml.

The average number of parasites were counted in several negative control wells.¹⁹ The parasites exposed to varying concentration of the test compounds were counted and the % mortality was calculated by the following formula: % survival = (no. of parasites test) × 100 / (no. of parasites negative control).

RESULTS AND DISCUSSION

The synthesized complexes were obtained pure in good yields and were air stable. They were characterized by elemental analysis, IR, multinuclear NMR spectroscopy and mass spectrometry and screened to check their biological activity.

Analytical and spectral characterization

Ligand (HL¹). Yield: 85 %; m.p. 127 °C. Anal. Calcd. for C₁₀H₇N₃O₇ (M.W. 281): C, 42.70; H, 2.48; N, 14.94 %. Found: C, 42.74; H, 2.50; N, 14.51 %. IR (KBr, cm⁻¹): 2850 (–OH), 3336 (–NH), 1769 (C=O), 1530 (COO)_{asym}, 1314 (COO)_{sym}, 216 (Δν). ¹H-NMR (CDCl₃, δ, ppm): 9.15 (*d*, [2.7] (N₂O₄–C₆H₃), 4.35 (*s*, –NH), 8.24 (*d*, [2.6]), 8.27 (*d*, [2.6], –CH=CH), 9.10 (*s*, –OH). ¹³C-NMR (CDCl₃, δ, ppm): 142.9 (C₁), 132.4 (C₂), 118.8 (C₃), 129.8 (C₄), 123.8 (C₅), 128.6 (C₆), 163.2 (C₇), 152.6 (C₈), 160.2 (C₉), 172.0 (C₁₀). EIMS (*m/z*, (relative abundance, %)): 183 (100) [C₆H₅N₃O₄]⁺, 99 (20) [C₄H₃O₃]⁺, 72 (100) [C₃H₄O₂]⁺, 55 (25) [C₂HNO]⁺, 45 (62) [CHO₂]⁺.

Me₂Sn(L¹)₂ (1). Yield: 75 %; m.p. 119 °C. Anal. Calcd. for C₂₂H₁₈N₆O₁₄Sn (M.W. 709): C, 37.23; H, 2.53; N, 11.84 %. Found: C, 37.27; H, 2.49; N, 11.80 %. IR (KBr, cm⁻¹): 3334 (–NH), 1765 (C=O), 1578 (COO)_{asym}, 1452 (COO)_{sym}, 126 (Δν), 526 (Sn–C), 408 (Sn–O). ¹H-NMR (CDCl₃, δ, ppm): 9.14 (*d*, [2.4], N₂O₄–C₆H₃), 4.35 (*s*, –NH), 8.21 (*d*, [2.8]), 8.24 (*d*, [2.8], –CH=CH), 0.91 (*s* (Sn–CH₃)). ¹³C-NMR (CDCl₃, δ, ppm): 142.0 (C₁), 131.1 (C₂), 119.0 (C₃), 129.4 (C₄), 123.9 (C₅), 128.7 (C₆), 162.2 (C₇), 152.4 (C₈), 161.5 (C₉), 176.1 (C₁₀), 6.4 [535] (C₁₁). EIMS (*m/z*, (relative abundance, %)): 709 (55) [R₂Sn(OOCR')₂]⁺ or [M]⁺, 696 (45) [RSn(OOCR')₂]⁺, 183 (82) [C₆H₅N₃O₄]⁺, 149 (45) [R₂Sn]⁺, 134 (55) [RSn]⁺, 123 (70) [C₆H₅NO₂]⁺, 120 (15) [Sn]⁺, 91 (100) [C₆H₅N]⁺, 57 (80) [C₂H₂NO]⁺.

Bu₂Sn(L¹)₂ (2). Yield: 72 %; m.p. 142 °C. Anal. Calcd. for C₂₈H₃₂N₆O₁₄Sn (M.W. 795): C, 42.26; H, 4.02; N, 10.56 %. Found: C, 42.22; H, 4.06; N, 10.60 %. IR (KBr, cm⁻¹): 3341 (–NH), 1762 (C=O), 1565 (COO)_{asym}, 1435 (COO)_{sym}, 130 (Δν), 538 (Sn–C), 420 (Sn–O). ¹H-NMR (CDCl₃, δ, ppm): 9.08 (*d*, [2.5], N₂O₄–C₆H₃), 4.35 (*s*, –NH), 8.18 (*d*, [2.6]), 8.48 (*d*, [2.6], –CH=CH), 0.92 (*t*) 1.26–1.36 (*m*), 1.39 (*t*, Sn–C₄H₉). ¹³C-NMR (CDCl₃, δ, ppm): 142.6 (C₁), 131.2 (C₂), 119.4 (C₃), 129.5 (C₄), 123.8 (C₅), 128.2 (C₆), 169.5 (C₇), 152.1 (C₈), 161.6 (C₉), 175.0 (C₁₀), 13.5 (C₁₁), 26.3 (C₁₂), 26.9 (C₁₃), 29.6 (C₁₄). ¹¹⁹Sn-NMR (δ, ppm): –138.5. EIMS (*m/z*, (relative abundance, %)): 711 (55) [R₂Sn(OOCR')₂]⁺, 696 (45) [RSn(OOCR')₂]⁺, 149 (45) [R₂Sn]⁺, 134 (55) [RSn]⁺, 120 (15) [Sn]⁺, 86 (100) [C₄H₆O₂]⁺, 57 (90) [C₄H₉]⁺.

Oct₂Sn(L¹)₂ (3). Yield: 68 %; m.p. 185 °C. Anal. Calcd. for C₃₆H₄₈N₆O₁₄Sn (M.W. 907): C, 47.62; H, 5.29; N, 9.26 %. Found: C, 47.66; H, 5.34; N, 9.30 %. IR (KBr, cm⁻¹): 3342 (–NH), 1763 (C=O), 1591 (COO)_{asym}, 1442 (COO)_{sym}, 149 (Δν), 536 (Sn–C), 422 (Sn–O). ¹H-NMR (CDCl₃, δ, ppm): 9.11 (*d*, [2.6], N₂O₄–C₆H₃), 4.35 (*s*, –NH), 8.19 (*d*, [2.6]), 8.52 (*d*, [2.6], –CH=CH), 0.89 (*t*), 1.75–1.80 (*m*, Sn–C₈H₁₃). ¹³C-NMR (CDCl₃, δ, ppm): 142.7 (C₁), 131.1 (C₂), 119.0 (C₃), 129.7 (C₄), 123.5 (C₅), 128.4 (C₆), 165.6 (C₇), 152.5 (C₈), 161.7 (C₉), 177.9 (C₁₀), 14.0 (C₁₁), 24.8 (C₁₂), 26.3 (C₁₃), 27.0 (C₁₄), 29.1 (C₁₅), 29.6 (C₁₆), 31.8 (C₁₇), 37.0 (C₁₈). ¹¹⁹Sn-NMR (δ, ppm): –127.4. EIMS (*m/z*, (relative abundance,

)): 907 (45) $[\text{R}_2\text{Sn}(\text{OOCR}')_2]^+$, 794 (35) $[\text{R}_2\text{Sn}(\text{OOCR}')_2]^+$, 345 (40) $[\text{R}_2\text{Sn}]^+$, 232 (25) $[\text{RSn}]^+$, 183 (78) $[\text{C}_6\text{H}_5\text{N}_3\text{O}_4]^+$, 120 (12) $[\text{Sn}]^+$, 86 (60) $[\text{C}_4\text{H}_6\text{O}_2]^+$, 57 (100) $[\text{C}_2\text{H}_2\text{NO}]^+$, 43 (70) $[\text{C}_2\text{H}_3\text{O}]^+$.

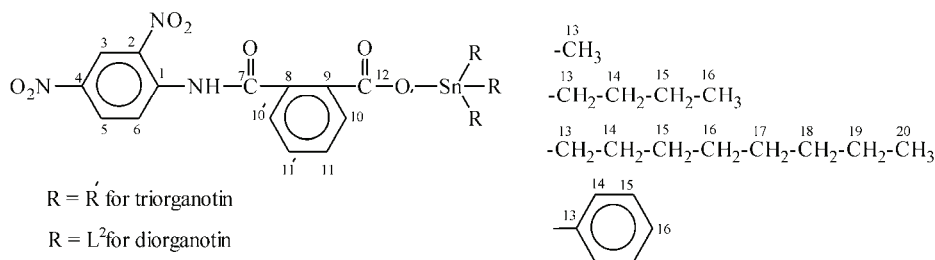
Me₃SnL^I (**4**). Yield: 78 %; m.p. 101 °C. Anal. Calcd. for $\text{C}_{13}\text{H}_{16}\text{N}_3\text{O}_7\text{Sn}$ (M.W. 445): C, 35.05; H, 3.59; N, 9.43 %. Found: C, 35.01; H, 3.63; N, 9.39 %. IR (KBr, cm^{-1}): 3332 (–NH), 1774 (C=O), 1589 (COO)_{asym}, 1462 (COO)_{sym}, 127 ($\Delta\nu$), 532 (Sn–C), 418 (Sn–O). ¹H-NMR (CDCl_3 , δ , ppm): 9.12 (*d*, [2.6], $\text{N}_2\text{O}_4\text{–C}_6\text{H}_3$), 4.35 (*s*, –NH), 8.18 (*d*, [2.5], 8.94 (*d*, [2.5], –CH=CH), 0.65 (*s*, [57, 60], (Sn–CH₃)). ¹³C-NMR (CDCl_3 , δ , ppm): 148.6 (C₁), 131.8 (C₂), 119.1 (C₃), 129.7 (C₄), 123.7 (C₅), 128.9 (C₆), 169.5 (C₇), 152.6 (C₈), 161.4 (C₉), 178.2 (C₁₀), –1.4 [382,394] (C₁₁). ¹¹⁹Sn-NMR (δ , ppm): 144.7. EIMS (*m/z*, (relative abundance, %)): 445 (50) $[\text{R}_3\text{SnOOCR}']^+$, 430 (40) $[\text{R}_2\text{SnOOCR}']^+$, 415 (60) $[\text{RSnOOCR}']^+$, 183 (75) $[\text{C}_6\text{H}_5\text{N}_3\text{O}_4]^+$, 164 (35) $[\text{R}_3\text{Sn}]^+$, 149 (38) $[\text{R}_2\text{Sn}]^+$, 120 (10) $[\text{Sn}]^+$, 154 (80) $[\text{C}_8\text{H}_{10}\text{O}_3]^+$, 57 (100) $[\text{C}_2\text{H}_2\text{NO}]^+$, 43 (76) $[\text{C}_2\text{H}_3\text{O}]^+$.

Bu₃SnL^I (**5**). Yield: 70 %; m.p. = 165 °C. Anal. Calcd. for $\text{C}_{22}\text{H}_{34}\text{N}_3\text{O}_7\text{Sn}$ (M.W. 571): C, 46.23; H, 5.95; N, 7.35 %. Found: C, 46.27; H, 5.90; N, 7.39 %. IR (KBr, cm^{-1}): 3330 (–NH), 1760 (C=O), 1545 (COO)_{asym}, 1416 (COO)_{sym}, 129 ($\Delta\nu$), 540 (Sn–C), 426 (Sn–O). ¹H-NMR (CDCl_3 , δ , ppm): 9.11 (*d*, [2.5], $\text{N}_2\text{O}_4\text{–C}_6\text{H}_3$), 4.35 (*s*, –NH), 8.19 (*d*, [2.6]), 8.46 (*d*, [2.6], –CH=CH), 0.93 (*t*), 1.27–1.36 (*m*), 1.63 (*t*, Sn–C₄H₉). ¹³C-NMR (CDCl_3 , δ , ppm): 142.2 (C₁), 132.3 (C₂), 119.2 (C₃), 129.7 (C₄), 123.9 (C₅), 128.3 (C₆), 169.3 (C₇), 152.3 (C₈), 161.2 (C₉), 175.6 (C₁₀), 17.4 [325, 341] (C₁₁), 26.8 [22.4] (C₁₂), 27.8 [62.6, 65.2] (C₁₃), 29.6 (C₁₄). ¹¹⁹Sn-NMR (δ , ppm): 152.2. EIMS (*m/z*, (relative abundance, %)): 571 (20) $[\text{R}_3\text{SnOOCR}']^+$, 514 (40) $[\text{R}_2\text{SnOOCR}']^+$, 290 (35) $[\text{R}_3\text{Sn}]^+$, 233 (45) $[\text{R}_2\text{Sn}]^+$, 183 (75) $[\text{C}_6\text{H}_5\text{N}_3\text{O}_4]^+$, 120 (25) $[\text{Sn}]^+$, 86 (55) $[\text{C}_4\text{H}_6\text{O}_2]^+$, 57 (100) $[\text{C}_2\text{H}_2\text{NO}]^+$, 43 (76) $[\text{C}_2\text{H}_3\text{O}]^+$.

Ph₃SnL^I (**6**). Yield: 72 %; m.p. 95 °C. Anal. Calcd. for $\text{C}_{28}\text{H}_{22}\text{N}_3\text{O}_7\text{Sn}$ (M.W. 779): C, 43.13; H, 2.82; N, 5.39. Found: C, 43.17; H, 2.78; N, 5.34. IR (KBr, cm^{-1}): 3339 (–NH), 1772 (C=O), 1555 (COO)_{asym}, 1420 (COO)_{sym}, 135 ($\Delta\nu$), 411 (Sn–O). ¹H-NMR (CDCl_3 , δ , ppm): 9.12 (*d*, [2.6], $\text{N}_2\text{O}_4\text{–C}_6\text{H}_3$), 4.35 (*s*, –NH), 8.15 (*d*, [2.5]), 8.38 (*d*, [2.6], –CH=CH), 7.48–7.75 (*m*, Sn–C₆H₅); ¹³C-NMR (CDCl_3 , δ , ppm): 142.2 (C₁), 130.3 (C₂), 119.1 (C₃), 129.5 (C₄), 124.0 (C₅), 128.5 (C₆), 169.5 (C₇), 152.4 (C₈), 161.3 (C₉), 176.4 (C₁₀), 137.4 (C₁₁), 136.1 (C₁₂), 129.0 (C₁₃), 128.7 (C₁₄). ¹¹⁹Sn-NMR (δ , ppm): –52.4. EIMS (*m/z*, (relative abundance, %)): 631 (30) $[\text{R}_3\text{SnOOCR}']^+$, 554 (20) $[\text{R}_2\text{SnOOCR}']^+$, 350 (45) $[\text{R}_3\text{Sn}]^+$, 273 (50) $[\text{R}_2\text{Sn}]^+$, 196 (45) $[\text{RSn}]^+$, 120 (15) $[\text{Sn}]^+$, 154 (80) $[\text{C}_8\text{H}_{10}\text{O}_3]^+$, 57 (100) $[\text{C}_2\text{H}_3\text{NO}]^+$.

Ligand (HL²). Yield: 84 %; m.p. 138 °C. Anal. Calcd. for $\text{C}_{14}\text{H}_9\text{N}_3\text{O}_7$ (M.W. 331): C, 50.75; H, 2.71; N, 12.68 %. Found: C, 51.71; H, 2.67; N, 12.64 %. IR (KBr, cm^{-1}): 3189 (–OH), 3325 (–NH), 1790 (C=O), 1584 (COO)_{asym}, 1328 (COO)_{sym}, 256 ($\Delta\nu$). ¹H-NMR (CDCl_3 , δ , ppm): 7.94 (*m*, $\text{N}_2\text{O}_4\text{–C}_6\text{H}_3$), 4.12 (*s*, –NH), 8.04 (*m*, –CO–C₆H₄–CO), 8.26 (*s*, –OH). ¹³C-NMR (CDCl_3 , δ ,

ppm): 162.7 (C₁), 118.9 (C₂), 129.9 (C₃), 123.9 (C₄), 128.5 (C₅), 131.3 (C₆), 142.0 (C₇), 129.1 (C₈), 152.5 (C₉), 136.0 (C_{10,10'}), 129.7 (C_{11,11'}), 170.5 (C₁₂). EIMS (*m/z*, (relative abundance, %)): 183 (100) [C₆H₃N₃O₄]⁺, 153 (24) [C₆H₅NO₄]⁺, 107 (16) [C₇H₇O]⁺, 91 (25) [C₆H₅N]⁺.



Scheme 2. NMR numbering scheme for organotin(IV) derivatives of 2-[(2,4-dinitrophenyl)amino]benzoic acid (HL²).

*Me*₂Sn(L²)₂ (**7**). Yield: 65 %; m.p. 148 °C. Anal. Calcd. for C₃₀H₂₄N₆O₁₄Sn (M.W. 811): C, 44.38; H, 2.95; N, 10.35 %. Found: C, 44.42; H, 2.91; N, 10.31 %. IR (KBr, cm⁻¹): 3318 (–NH), 1791 (C=O), 1581 (COO)_{asym}, 1422 (COO)_{sym}, 159 (Δν), 522 (Sn–C), 416 (Sn–O). ¹H-NMR (CDCl₃, δ, ppm): 7.74 (*m*, N₂O₄–C₆H₃), 4.11 (*s*, –NH), 8.33 (*m*, –CO–C₆H₄–CO), 1.26 (*s*, Sn–CH₃). ¹³C-NMR (CDCl₃, δ, ppm): 142.5 (C₁), 119.7 (C₂), 129.2 (C₃), 123.7 (C₄), 128.4 (C₅), 131.5 (C₆), 165.0 (C₇), 128.4 (C₈), 152.6 (C₉), 137.3 (C_{10,10'}), 127.2 (C_{11,11'}), 172.7 (C₁₂), 8.4 [532] (C₁₃). ¹¹⁹Sn-NMR (δ, ppm): –185.6. EIMS (*m/z*, (relative abundance, %)): 167 (52) [C₆H₃N₂O₉]⁺, 149 (6) [SnR₂]⁺, 121 (8) [SnH]⁺, 91 (84) [C₆H₅N]⁺, 86 (90) [C₄H₆O₂]⁺, 84 (100) [C₄H₄O₂]⁺, 77 (8) [C₆H₅]⁺.

*Bu*₂Sn(L²)₂ (**8**). Yield: 79 %; m.p. 179 °C. Anal. Calcd. for C₃₆H₃₆N₆O₁₄Sn (M.W. 895): C, 48.26; H, 4.02; N, 9.38 %. Found: C, 48.22; H, 4.06; N, 9.42. IR (KBr, cm⁻¹): 3323 (–NH), 1783 (C=O), 1578 (COO)_{asym}, 1430 (COO)_{sym}, 148 (Δν), 528 (Sn–C), 412 (Sn–O). ¹H-NMR (CDCl₃, δ, ppm): 7.91 (*m*, N₂O₄–C₆H₃), 4.10 (*s*, –NH), 8.03 (*m*, –CO–C₆H₄–CO), 1.35 – 1.38 (*m*), 1.93 (*t*, Sn–C₄H₉); ¹³C-NMR (CDCl₃, δ, ppm): 142.6 (C₁), 121.3 (C₂), 129.5 (C₃), 123.9 (C₄), 128.2 (C₅), 131.1 (C₆), 167.2 (C₇), 128.2 (C₈), 152.4 (C₉), 136.2 (C_{10,10'}), 124.5 (C_{11,11'}), 176.2 (C₁₂), 14.0 (C₁₃), 22.6 (C₁₄), 29.3 (C₁₅), 31.8 (C₁₆). ¹¹⁹Sn-NMR (δ, ppm): –137.5. EIMS (*m/z*, (relative abundance, %)): 267 (100) [C₆H₃N₂O₉]⁺, 233 (8) [SnR₂]⁺, 176 (9) [SnR]⁺, 77 (67) [C₆H₅]⁺, 57 (84) [C₄H₉]⁺.

*Oct*₂Sn(L²)₂ (**9**). Yield: 66 %; m.p. 135 °C. Anal. Calcd. for C₄₄H₅₂N₆O₁₄Sn (M.W. 1007): C, 52.43; H, 5.16; N, 8.34 %. Found: C, 52.47; H, 5.12; N, 8.38 %. IR (KBr, cm⁻¹): 3320 (–NH), 1793 (C=O), 1569 (COO)_{asym}, 1428 (COO)_{sym}, 141 (Δν), 530 (Sn–C), 418 (Sn–O). ¹H-NMR (CDCl₃, δ, ppm): 7.93 (*m*, N₂O₄–C₆H₃), 4.12 (*s*, –NH), 8.02 (*m*, –CO–C₆H₄–CO), 0.90, 1.17 – 1.28 (*m*), 1.72–1.78 (*m*, Sn–C₈H₁₃). ¹³C-NMR (CDCl₃, δ, ppm): 142.2 (C₁), 118.9 (C₂), 129.1 (C₃), 123.7 (C₄), 128.4 (C₅), 131.4 (C₆), 167.4 (C₇), 128.4 (C₈), 152.9 (C₉), 136.5

(C_{10,10'}), 124.6 (C_{11,11'}), 177.4 (C₁₂), 14.1 (C₁₃), 22.6 (C₁₄), 25.8 (C₁₅), 26.2 (C₁₆), 29.3 (C₁₇), 29.3 (C₁₈), 31.8 (C₁₉), 33.4 [101] (C₂₀). ¹¹⁹Sn-NMR (δ , ppm): -139.2. EIMS (m/z , (relative abundance, %)): 345 (4) [SnR₂]⁺, 232 (3) [SnR]⁺, 167 (67) [C₆H₃N₂O₄]⁺, 91 (18) [C₆H₅N]⁺, 85 (56) [C₄H₅O₂]⁺, 57 (100) [C₄H₉]⁺.

Me₃SnL² (I0). Yield; 72 %; m.p. 101 °C. Anal. Calcd. for C₁₇H₁₈N₃O₇Sn (M.W. 495): C, 41.21; H, 3.63; N, 8.48 %. Found: C, 41.25; H, 3.67; N, 8.52 %. IR (KBr, cm⁻¹): 3326 (-NH), 1780 (C=O), 1593 (COO)_{asym}, 1415 (COO)_{sym}, 178 ($\Delta\nu$), 542 (Sn-C), 422 (Sn-O). ¹H-NMR (CDCl₃, δ , ppm): 7.92 (*m*, N₂O₄-C₆H₃), 4.11 (*s*, -NH), 8.66 (*m*, -CO-C₆H₄-CO), 0.88 (*s*, [57], Sn-CH₃). ¹³C-NMR (CDCl₃, δ , ppm): 142.6 (C₁), 119.6 (C₂), 129.4 (C₃), 123.6 (C₄), 128.0 (C₅), 131.5 (C₆), 165.2 (C₇), 128.0 (C₈), 152.4 (C₉), 136.2 (C_{10,10'}), 125.2 (C_{11,11'}), 171.4 (C₁₂), -1.6 [383,395] (C₁₃). ¹¹⁹Sn-NMR (δ , ppm): 111.6. EIMS (m/z , (relative abundance, %)): 166 (22) [C₆H₂N₂O₄]⁺, 164 (16) [SnR₃]⁺, 149 (28) [SnR₂]⁺, 134 (6) [SnR]⁺, 120 (7) [Sn]⁺, 91 (11) [C₆H₅N]⁺, 77 (37) [C₆H₅]⁺, 57 (100) [C₄H₉]⁺.

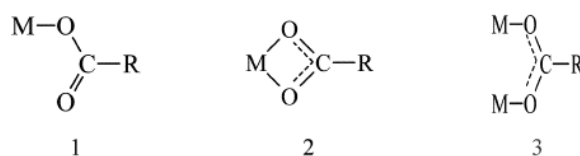
Ph₃SnL² (II). Yield: 55 %; m.p. 163 °C; Anal. Calcd. for C₃₂H₂₄N₃O₇Sn (M.W. 681): C, 56.38; H, 3.52; N, 6.16 %. Found: C, 56.34; H, 3.48; N, 6.20 %. IR (KBr, cm⁻¹): 3324 (-NH), 1788 (C=O), 1572 (COO)_{asym}, 1410 (COO)_{sym}, 162 ($\Delta\nu$), 425 (Sn-O). ¹H-NMR (CDCl₃, δ , ppm): 7.95 (*m*, N₂O₄-C₆H₃), 4.13 (*s*, -NH), 8.65 (*m*, -CO-C₆H₄-CO), 7.28-7.59 (*m*, Sn-C₆H₅). ¹³C-NMR (CDCl₃, δ [^{117/119}Sn-¹³C], ppm): 142.1 (C₁), 118.2 (C₂), 129.5 (C₃), 123.7 (C₄), 128.4 (C₅), 131.2 (C₆), 168.8 (C₇), 128.4 (C₈), 152.7 (C₉), 136.4 (C_{10,10'}), 125.5 (C_{11,11'}), 182.1 (C₁₂), 136.2 [46, 48] (C₁₃), 135.8 (C₁₄), 128.0 [62, 65] (C₁₅), 127.5 [13] (C₁₆). ¹¹⁹Sn-NMR (δ , ppm): -109.75.; EIMS (m/z , (relative abundance, %)): 350 (4) [SnR₃]⁺, 315 (10) [C₁₄H₈N₃O₆]⁺, 309 (95) [C₂₀H₂₅O₃]⁺, 273 (5) [SnR₂]⁺, 196 (7) [SnPh]⁺, 154 (100) [C₈H₁₀O₃]⁺, 120 (10) [Sn]⁺, 77 (20) [C₆H₅]⁺.

Infrared spectra

The FTIR data are consistent with the formation of compounds with the composition R₂SnL₂ and R₃SnL. The carboxylate groups of the ligand coordinate to the metal ion in different modes as shown in Scheme 3.²⁰ The disappearance of a broad band in the spectra of the complexes in the region 3200–2800 cm⁻¹, which was present in the free ligands, suggests deprotonation of the free COOH group upon complexation. The bonding of the tin(IV) to the ligand was confirmed by the presence of Sn–O bands in the range of 426–408 cm⁻¹.²¹ Sn–C absorption bands in the region of 542–520 cm⁻¹ were observed in all complexes.

Based on the difference between $\nu(\text{COO})_{\text{sym}}$ and $\nu(\text{COO})_{\text{asym}}$ and the corresponding band position, it is proposed that the carboxylate group acts as bidentate in all these complexes in the solid state.²² According to Lebl *et al.*,²³ the

values $\Delta\nu$ ($\Delta\nu = \nu(\text{COO})_{\text{asym}} - \nu(\text{COO})_{\text{sym}}$) can be divided into three groups: (a) when $\Delta\nu(\text{COO}) > 350$, the compounds contain, with a high probability, a monodentate carboxylate group. However, other very weak intra- and intermolecular interactions cannot be excluded; (b) when $\Delta\nu(\text{COO}) < 200$, the carboxylate groups of these compounds can be considered to be practically bidentate; (c) compounds where $\Delta\nu(\text{COO})$ is between 350 and 200 are considered as intermediate between monodentate and bidentate, which is called anisobidentate. It has also been suggested that the $\Delta\nu(\text{COO})$ value in the chelating mode is less than $\Delta\nu(\text{COO})$ in the bridging mode.²⁰ Some characteristic vibrational frequencies of different groups fall within the range $\nu(\text{C}=\text{O})$ 1793–1762 cm^{-1} and $\nu(\text{N}-\text{H})$ 3342–3320 cm^{-1} .



Scheme 3. Possible coordination modes of the carboxylate group to the metal.

¹H-NMR spectra

The ¹H-NMR spectra for the investigated compounds were recorded in deuterated chloroform at room temperature. Different protons were assigned based on their multiplicity and intensity patterns. The integration of the spectra was in accordance with the number of protons proposed for each molecular fragment. The ¹H-NMR spectra of the complexes exhibited useful features.

In the studied complexes, the COOH resonance of the ligands was absent, which suggests the replacement of the carboxylic proton by the organotin(IV) moiety. Charge donation from the COO⁻ donor to the tin atom decreased the electron density and resulted in a deshielding of the ligand protons. Singlets and multiplets were observed in the case of the methyl and phenyl groups, respectively. Simultaneously, the signals of the aromatic protons were shifted downfield because of the ring current effect. The aromatic protons of the phenyl group and the benzoate group were assigned with difficulty due to the narrow range on the NMR scale, hence the phenyl group gave a multiplet due to a complex pattern. The alkyl groups bonded to tin were assigned in their characteristic range. The ⁿJ(¹¹⁹Sn, ¹H) for the dimethyl and trimethyltin(IV) derivatives had approximately the same value, confirming a tetrahedral environment in solution, *i.e.*, the carboxylate groups act as monodentate in solution. The ⁿJ(¹H, ¹H) values for the different compounds suggest that the protons of the ethylene group (HC=HC) were in the *cis*-position.²⁴ In all diorganotin(IV) and triorganotin(IV) derivatives, the -NH resonance was observed as a broad or a sharp weak signal. The aromatic proton resonances were assigned by comparing the experimental chemical shifts with those calculated by the incremental method.²⁵ In triorganotin carboxylates,

the $^2J(^{119}\text{Sn}, ^1\text{H})$ values for the triorganotin compounds suggest tetrahedral geometry (Fig. 1(a)) of the tin atom.

Unlike the triorganotin carboxylates in solution, the geometry of diorganotin dicarboxylates cannot be defined with certainty because of dynamic processes involving different modes of coordination of the carboxylate oxygens to the tin atom.²⁶ However, in the solid state, the tin atom is mostly hexa-coordinated in such systems (Fig.1(b)).²⁷

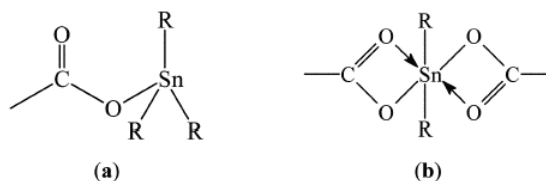


Fig. 1. Suggested structures of the complexes.

^{13}C -NMR spectra

The ^{13}C -NMR spectra of the organotin(IV) derivatives are consistent with the following observations:

According to ^{13}C -NMR data, the involvement of the carboxylate group in the bonding to Sn was confirmed by the resonance of the carboxylic carbon in all the compounds, which exhibited a lower shift after coordination as compared with the ligands, suggesting the coordination of the ligand through a carboxylic oxygen to the organotin(IV) moiety. The remaining carbons did not shift significantly after complexation.

The carbon of the phenyl and alkyl groups attached to tin were observed at almost similar positions as calculated by the incremental method²⁴ and reported in the literature.^{28–32} Two resonances were observed in the expected range for the carboxyl and amide groups.

The tributyltin and trimethyltin complexes of the present investigation exhibit $^1J(^{13}\text{C}, ^{117/119}\text{Sn})$ coupling satellites in the range 325–363 Hz in CDCl_3 solution, suggesting that the tin atom is four-coordinated in solution.^{33–36}

^{119}Sn -NMR spectra

The ^{119}Sn chemical shifts of the organotin compounds covered a range $\delta \pm 600$. As the electron releasing power of the alkyl group bonded to tin increases, the tin atom becomes progressively more shielded and the $\delta(^{119}\text{Sn})$ value moves to a higher field.³⁷ It was reported earlier that ^{119}Sn -NMR is also a powerful technique and the value of $\delta(^{119}\text{Sn})$ is directly linked to the coordination number of the central tin atom.³⁸

In all the complexes, the ^{119}Sn spectra show only a sharp singlet, indicating the formation of single species. In general, the ^{119}Sn chemical shifts move to lower frequency with increasing coordination number, although the shift ranges

are somewhat dependent on the nature of the substituents at the tin atom. In all the complexes, the ^{119}Sn chemical shift values for the triorganotin complexes agree well with a tetrahedral environment around the tin atom in non-coordinated solvents, whereas those of the diorganotin complexes indicate penta coordination, *i.e.*, the tendency towards increased coordination number decreases as the number of R groups increases. However, in solution, such structures appear four-coordinate, the additional coordination from the carbonyl oxygen to tin being lost.³⁹

Mass spectrometry

Mass spectra for the investigated compounds were recorded at 70 eV for all di- and tri-organotin(IV) derivatives. Molecular ion peaks of very low intensity are observed in few complexes.⁴⁰ In the di- and tri-organotin(IV) derivatives, a rather similar pattern of fragmentation was observed. In both cases, primary fragmentation was due to the successive loss of R groups followed by the elimination of CO_2 from the ligand and then the remaining part of the ligand, which leaves Sn^+ or SnH^+ as the end product. The second route of fragmentation was the loss of CO_2 and other neutral species, which ultimately gives $[\text{C}_6\text{H}_5]^+$ in the first step. Another possible route is the disintegration of the ligand and stepwise elimination of R groups to Sn^+ or SnH^+ as the residue.

Biological activity

The results of the antibacterial activities are given in Table I. The screening tests show that the phenyltin carboxylates were the most potent candidates against the tested bacteria. The activity of the other derivatives varies according to their R groups.

TABLE I. Antibacterial activity data for $\text{R}_2\text{Sn}(\text{L}^1)_2/\text{R}_2\text{Sn}(\text{L}^2)_2$ and $\text{R}_3\text{SnL}^1/\text{R}_3\text{SnL}^2$

Bacterium	Zone of inhibition, mm										
	Compound number										
	1	2	3	4	5	6	7	8	9	10	11
<i>Escherichia coli</i>	10	–	10	14	14	20	–	–	16	–	10
<i>Bacillus subtilis</i>	10	–	12	–	14	10	–	–	27	–	10
<i>Shigella flexenari</i>	10	–	14	14	–	–	–	–	18	–	–
<i>Staphylococcus aureus</i>	–	–	14	20	–	–	–	–	14	–	–
<i>Pseudomonas aeruginosa</i>	–	–	–	–	14	16	–	–	18	–	16
<i>Salmonella typhi</i>	10	–	14	10	–	–	–	–	20	–	18

The LD_{50} data are summarized in Table II. A previous report⁴¹ showed that the nature of the organic group is responsible for the toxicity of organotin compounds. Compound **5** did not show any toxicity at all.

The insecticidal activity data of the compounds are given in Table III. The trimethyltin(IV) carboxylate of HL^2 was inactive against the tested insects, while the other organotin(IV) carboxylates exhibited activity. This can be explained as

follows: as the length or number of the R group increases, the activity also increases.

TABLE II. Cytotoxicity data for $R_2Sn(L^1)_2/R_2Sn(L^2)_2$ and R_3SnL^1/R_3SnL^2 (standard drug: etoposide, $LD_{50} = 7.4625 \mu\text{g/ml}$)

Compound	1	2	3	4	5	6	7	8	9	10	11
$LD_{50}/\mu\text{g ml}^{-1}$	8.64	9.14	8.00	7.99	–	5.18	16.89	16.89	13.92	14.29	18.19

TABLE III. Insecticidal data for $R_2Sn(L^1)_2/R_2Sn(L^2)_2$ and R_3SnL^1/R_3SnL^2 . Concentration of samples: 1571.2 $\mu\text{g/ml}$. Standard drug: Permethrin (235.7 $\mu\text{g/ml}$)

Compound	1	2	3	4	5	6	7	8	9	10	11
$IC_{50}/\mu\text{g/ml}$	62.12	–	65.71	64.50	64.80	–	60	65	67.8	65.5	65

Leishmaniasis is a class of diseases caused by protozoan haemoflagellates of the genus *Leishmania*. The disease is transmitted by female sandflies (*Phlebotomus* or *Lutzomyia*) that feed on the blood of an animal or human host. The disease occurs in most tropical and sub-tropical areas of the world. The anti-leishmanial activity data of the complexes are given in Table IV. All the compounds showed antileishmanial activity with a few exceptions.

TABLE IV. Antileishmanial activity data for $R_2Sn(L^1)_2/R_2Sn(L^2)_2$ and R_3SnL^1/R_3SnL^2 . Test Organism-Leishmanial major (DESTO). Standard drug: Amphotericin B (0.19 $\mu\text{g/ml}$)

Insect	Compound										
	1	2	3	4	5	6	7	8	9	10	11
<i>Tribolium castaneum</i>	25	25	25	25	25	25	40	20	25	–	20
<i>Sitophilus oryzae</i>	25	25	25	25	25	25	–	–	25	–	20
<i>Rhyzoperthadominia</i>	50	50	20	25	–	25	25	–	25	–	–
<i>Callosbruchus analis</i>	25	25	25	25	25	22	25	–	60	–	40

CONCLUSIONS

The synthesis of R_2SnL_2 and R_3SnL resulted in compounds with a 1:1 or 1:2 metal-to-ligand ratio in good yield. The FTIR data evidenced the formation of well-defined complexes by the appearance of the Sn–O band. The NMR data were analyzed and almost all their signals were assigned. The di- and tri-organotin complexes were proposed to have penta- and tetra-coordinated geometry around tin atom in solution, confirmed by the ^{13}C , $^{117/119}\text{Sn}$ satellites, as well as ^1H - and ^{119}Sn -NMR data. The results demonstrated that the effect of different alkyl groups was minor. The screening results show that the reported complexes 1–11 exhibited good biological activity with a few exceptions.

Acknowledgement. S. A. is grateful to Pakistan Science Foundation for the grant No. PSF/R & D/C-QU/Chem (270).

ИЗВОД

СИНТЕЗА, КООРДИНАЦИЈА И БИОЛОШКИ АСПЕКТИ ОРГАНОКАЛАЈ(IV) ДЕРИВАТА
4-[(2,4-ДИНИТРОФЕНИЛ)АМИНО]-4-ОКСО-2-БУТЕНСКЕ АКРИЛНЕ КИСЕЛИНЕ И
2-[(2,4-ДИНИТРОФЕНИЛ)АМИНО]КАРБОНИЛ} БЕНЗОЕВЕ КИСЕЛИНЕКНАДЈА ШАНИД¹, SAIRA SHANZADI² и SAQIB ALI¹¹Department of Chemistry, Quaid-i-Azam University, Islamabad – 45320 и ²Department of Chemistry,
GC University, Faisalabad, Pakistan

Синтетисана је нова серија оргонокалај(IV) комплекса анилинских деривата, R₂SnL₂ и R₃SnL [где је R = Me, *n*-Bu, Ph, *n*-Oct], реакцијом HL¹ и HL² са одговарајућим оргонокалајним халогенидима или оксидима. Дати су експериментални детаљи за добијање и карактеризацију (укључујући елементалну анализу, IR и мултинуклеарну NMR (¹H, ¹³C и ¹¹⁹Sn спектри у CDCl₃) и EI масене спектре) обе серије. Везујућа места лиганата су идентификована помоћу FTIR спектроскопских мерења, и нађено је да у свим случајевима оргонокалајни(IV) део реагује са кисеоником COO⁻ групе градећи нове комплексе. У диоргонокалајним комплексима у чврстом стању COO⁻ група је координована за оргонокалај(IV) центре као бидентат. ¹¹⁹Sn-NMR подаци и ⁿJ(¹³C–^{119/117}Sn) константа купловања у складу су са тетраедарском координационом геометријом оргонокалајних комплекса у растварачима који немају координациона својства. Такође је објављена биолошка активност ових једињења (антибактеријска, антифунгална, инсектицидна, цитотоксичност и против протозоа из рода *Leishmania*).

(Примљено 29. фебруара, ревидирано 13. јуна 2008)

REFERENCES

1. M. J. Clarke, F. Zhu, D. R. Frasca, *Chem. Rev.* **99** (1999) 2511
2. J. Beckmann, K. Jurkschat, *Coord. Chem. Rev.* **215** (2001) 267
3. L. Pellerito, L. Nagy, *Chem. Rev.* **224** (2002) 111
4. K. C. Molloy, T. G. Purcell, E. Hahn, H. Schumann, J. J. Zuckerman, *Organometallics* **5** (1986) 85
5. M. Gielen, *Appl. Organomet. Chem.* **16** (2002) 481
6. J. A. Zubita, J. J. Zuckerman, *Inorg. Chem.* **24** (1987) 251
7. G. K. Sandhu, R. Gupta, S. S. Sandhu, R. V. Parish, *Polyhedron* **4** (1985) 81
8. G. K. Sandhu, R. Gupta, S. S. Sandhu, R. V. Parish, K. Brown, *J. Organomet. Chem.* **279** (1985) 372
9. T. P. Lockhart, F. Davidson, *Organometallics* **6** (1987) 2471
10. I. W. Nowell, J. S. Brooks, G. Beech, R. Hill, *J. Organomet. Chem.* **244** (1983) 119
11. Q. L. Xie, X. H. Xu, H. G. Wang, X. K. Yao, R. J. Wang, Z. G. Zhang, J. M. Hu, *Acad. Chim. Sinica* **49** (1991) 1085
12. H. D. Yin, C. H. Wang, Y. Wang, C. L. Ma, J. X. Sao, J. H. Zhang, *Acta Chim. Sinica* **60** (2002) 143
13. S. P. Narula, S. Kaur, R. Shankar, S. K. Bharadwaj, R. K. Chadha, *J. Organomet. Chem.* **506** (1996) 181
14. S. B. B. Tushar, S. S. Keisham, H. Michal, J. Robert, L. Anthony, Q. S. Xue, Z. Alejandra, G. Eng, *Appl. Organomet. Chem.* **19** (2005) 935
15. H. D. Yin, G. Li, Z. J. Gao, H. L. Xu, *J. Organomet. Chem.* **691** (2006) 1235
16. S. B. B. Tushar, M. Cheerfulman, W. Rudolph, B. Monique, H. Michal, J. Robert, L. Anthony, *J. Organomet. Chem.* **690** (2005) 3080

17. W. F. F. Armarego, C. L. L. Cahi, *Purification of Laboratory Chemicals*; 5th Ed., Butterworth, Oxford, 2003
18. A. Rahman, M. I. Choudhary, W. J. Thomsen, *Bioassay Techniques for Drug Development*, Harwood Academic Publishers, Amsterdam, The Netherlands, 2001
19. A. Fournet, A. B. Anqelo, V. Munoz, *J. Ethnopharmacol.* **41** (1994) 19
20. G. B. Deacon, R. J. Phillips, *Coord. Chem. Rev.* **33** (1980) 227
21. Q. L. Xie, Z. Q. Yang, Z. X. Zhang, D. K. Zhang, *Appl. Organomet. Chem.* **6** (1992) 193
22. Q. L. Xie, Z. Q. Yang, L. Jiang, *Main Group Met. Chem.* **19** (1996) 509
23. T. Lebl, J. Holecek, A. Lycka, *Sci. Pap. Univ. Pardubice Ser. A2* (1996) 5
24. J. K. M. Sanders, B. K. Hunte, *Modern NMR Spectroscopy*, 2nd Ed., Oxford University Press, Oxford, UK, 1993
25. H. O. Kalinowski, S. Berger, S. Brown, *¹³C-NMR Spectroskopie*, Thieme Verlag, Stuttgart, Germany, 1984
26. M. Danish, S. Ali, M. Mazhar, A. Badshah, E. R. T. Tiekink, *Main Group Met. Chem.* **18** (1995) 697
27. M. Parvez, S. Ali, T. M. Masood, M. Mazhar, M. Danish, *Acta Crystallog., C* **53** (1997) 1211
28. M. T. Masood, S. Ali, M. Danish, M. Mazhar, *Synth. React. Inorg. Met.-Org. Chem.* **32** (2002) 9
29. S. Ahmed, S. Ali, F. Ahmed, M. H. Bhatti, A. Badshah, M. Mazhar, K. M. Khan, *Synth. React. Inorg. Met.-Org. Chem.* **32** (2002) 1521
30. F. Marchetti, M. Pelli, C. Pettinari, R. Pettinari, E. Rivarola, C. Santini, B. W. Skeltom, A. H. White, *Appl. Organomet. Chem.* **690** (2005) 1878
31. S. Ali, M. N. Khokhar, M. H. Bhatti, M. Mazhar, M. T. Masood, K. Shahid, A. Badshah, *Synth. React. Inorg. Met.-Org. Chem.* **32** (2002) 1373
32. F. Ahmad, S. Ali, M. Parvez, A. Munir, M. Mazhar, K. M. Khan, T. A. Shah, *Heteroatom Chem.* **13** (2002) 638
33. J. Holecek, M. Nadvornik, K. Handlir, A. Lycka, *J. Organomet. Chem.* **241** (1983) 177
34. M. Nadvornik, J. Holecek, K. Handlir, A. Lycka, *J. Organomet. Chem.* **275** (1984) 43
35. A. Lycka, J. Holecek, M. Nadvornik, K. Handlir, *J. Organomet. Chem.* **280** (1985) 323
36. J. Holecek, K. Handlir, M. Nadvornik, A. Lycka, *J. Organomet. Chem.* **258** (1983) 147
37. J. Holecek, A. Lycka, *Inorg. Chim. Acta* **118** (1986) L15
38. A. G. Davies, P. J. Smith, *COMC-I* **2** (1982) 519
39. V. Pejchal, J. Holecek, M. Nadvornik, A. Lycka, *Collect. Czech. Chem. Commun.* **60** (1995) 1492
40. R. Willem, A. Bouhdid, B. Mahieu, L. Ghys, M. Biesemans, E. R. T. Tiekink, D. de Vos, M. Gielen, *J. Organomet. Chem.* **531** (1997) 151
41. M. R. Krigman, A. P. Silverman, *Neurotoxicology* **5** (1984) 129.



J. Serb. Chem. Soc. 74 (2) 155–158 (2009)
JSCS–3818

SHORT COMMUNICATION

**Stability order of isomeric benzenoid hydrocarbons
and Kekulé structure count**

SLAVKO RADENKOVIĆ[#] and IVAN GUTMAN^{*#}

Faculty of Science, University of Kragujevac, P. O. Box 60, 34000 Kragujevac, Serbia

(Received 10 September 2008)

Abstract: The commonly accepted opinion that the thermodynamic stability of isomeric benzenoid hydrocarbons (assessed by their total π -electron energy and various resonance energies) increases with increasing number of Kekulé structures is shown to be violated in numerous cases. The smallest examples of such anomalous behavior are two hexacyclic pericondensed benzenoids of formula $C_{24}H_{14}$ and several pairs of heptacyclic catacondensed benzenoids of formula $C_{30}H_{18}$.

Keywords: total π -electron energy; Kekulé structures; benzenoid hydrocarbons.

INTRODUCTION

One of the basic postulates of resonance theory¹ is that the thermodynamic stability of isomeric conjugated molecules increases with the number K of Kekulé structural formulas. In the early days of quantum chemistry,^{2–4} it was discovered that concepts from resonance theory occur also within the molecular orbital theory of benzenoid hydrocarbons. Knowing this, it was then natural to anticipate that the (molecular orbital) total π -electron energy (E) and the various (molecular-orbital-based) resonance energies of benzenoid hydrocarbons are all somehow proportional to K . The first approximation in which E was related with K was put forward⁵ already in the 1940s, and was eventually followed by a large number of other researches in the same direction. Of these are especially relevant those of Hall (claiming that the relation between E and K is linear),^{6,7} of Cio-slawski (claiming that the parameter influencing E is $K^{2/n}$, where n is the number of carbon atoms)^{8–12} and of some other authors^{13–15} (according to whom E depends on K in a logarithmic manner). After painstaking studies,^{16–21} the linear Hall rule has prevailed, although later work^{22–26} required its significant modification. Details of the examination of the (E/K) dependence in benzenoid sys-

* Corresponding author. E-mail: gutman@kg.ac.yu

Serbian Chemical Society member.

doi: 10.2298/JSC0902155R

tems are found in the reviews^{27,28} and references quoted therein. For some recent related investigations along these lines see the papers.^{29–34}

All the earlier numerical studies on the (E/K) dependence^{18,20,22–26,29–31,33} were performed on large sets of benzenoid isomers, and the conclusions drawn were based on statistical inferences. It is remarkable that until now nobody checked if the simple relation:

$$K(A) > K(B) \Rightarrow E(A) > E(B) \quad (1)$$

holds for all pairs A,B of benzenoid isomers. In this study, this checking was performed and it was found that Condition (1) is violated in a large number of cases.

It should be noted that the Requirement (1) is weaker than any of the assumed and previously considered approximate analytical relations between E and K . Thus, if (1) is violated, then each of these relations between E and K is violated. A violation of (1) was reported³⁵ already in the 1970s, but for acyclic systems (for which the Kekulé structure count is either 1 or 0).

VIOLATIONS FROM CONDITION (1)

The present systematic numerical testing revealed that Condition (1) is, indeed, satisfied by all catacondensed benzenoid hydrocarbons with six and fewer hexagons and by all pericondensed benzenoids with five and fewer hexagons. This fact, combined with the *a priori* expectations originating from the resonance theory, was probably the reason for overlooking the violations from (1) until now. Anyway, the two smallest benzenoid hydrocarbons violating Condition (1) are benzo[*b*]perylene and dibenzo[*de,qr*]naphthacene, depicted in Fig. 1. This is the only such pair with six hexagons that was found.

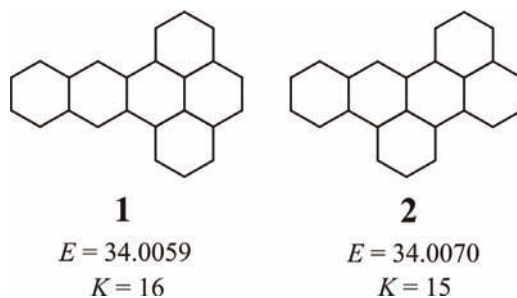


Fig. 1. Dibenzo[*de,qr*]naphthacene (**1**) and benzo[*b*]perylene (**2**), both with the formula $C_{24}H_{14}$, are the smallest pair of benzenoid isomers for which Condition (1) is violated; E = HMO total π -electron energy;^{27,28} K = Kekulé structure count. The energy difference of **1** and **2** of *ca.* 0.001 β -units implies that their heats of formation should differ by 0.15 kJ/mol; for details see in the book.³⁶

Among the heptacyclic benzenoids, violations from Condition (1) are quite numerous. In the set of heptacyclic catacondensed benzenoids, $C_{30}H_{18}$, already 69 pairs that violate (1) were found. There are a total of 118 such benzenoid hyd-

rocarbons, forming 6903 pairs. Thus, roughly 1 % of these violate Condition (1). A characteristic example is shown in Fig. 2.

Among the 62 heptacyclic Kekuléan pericondensed benzenoids of formula $C_{28}H_{16}$, 30 pairs were found that violate Condition (1), which is around 1.5 % of the total number of pairs (= 1891). Among the 9 heptacyclic Kekuléan pericondensed benzenoids of formula $C_{26}H_{14}$, there is not a single violation from Condition (1). Details can be obtained from the authors, upon request.

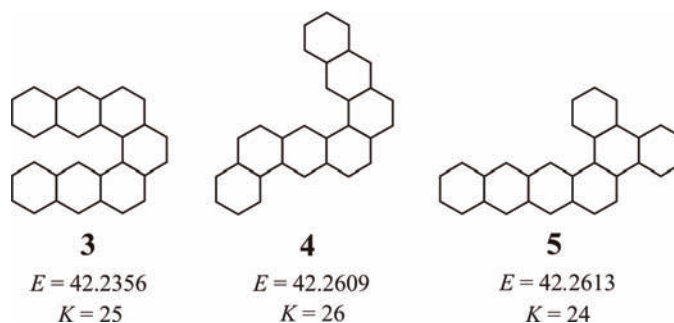


Fig. 2. Three catacondensed benzenoid systems that violate Condition (1): benzo[2,1-*a*:3,4-*a'*]-dianthracene (**3**), anthra[1,2-*a*]benz[*h*]anthracene (**4**), and phenanthro[9,10-*a*]naphthacene (**5**), all with the formula $C_{30}H_{18}$; E and K are the same as in Fig. 1. Note that the difference between the heats of formation of **3** and **5** was estimated³⁶ to be 3.5 kJ/mol. In fact, because of the non-planarity of **3** and steric strain, the stability difference between **3** and **5** should be even greater (in favor of **5**).

CONCLUDING REMARKS

The often repeated claim that “the greater is the Kekulé structure count, the greater is the (thermodynamic) stability of a benzenoid hydrocarbon” is simply not true. What is true is that within sets of isomeric benzenoid hydrocarbons there is a (statistically significant) trend that the thermodynamic stability increases with the number of Kekulé structures, but this does not mean that each member of the set with a greater Kekulé structure count is more stable than each member with a smaller Kekulé structure count.

Most remarkable in the above stated “discovery” is that it was not stated in the 1960s or 1970s, but only at the beginning of the 21st century.

ИЗВОД

СТАБИЛНОСТ ИЗОМЕРНИХ БЕНЗЕНОИДНИХ УГЉОВОДОНИКА И БРОЈ КЕКУЛÉ-ОВИХ СТРУКТУРА

СЛАВКО РАДЕНКОВИЋ и ИВАН ГУТМАН

Природно–математички факултет Универзитета у Крагујевцу, п.бр. 60, 34000 Крагујевац

Показано је да од опште усвојеног схватања да је термодинамичка стабилност изомерних бензеноидних угљоводоника (која се процењује на основу укупне π -електронске енергије и разних енергија резонанције) тим већа што је већи број Kekulé-ових структура, постоје

бројна одступања. Најмањи примери оваквог аномалног понашања су два хексациклична перикондензована бензеноидна система формуле $C_{24}H_{14}$ и већи број парова хептацикличних катакондензованих бензеноидних система формуле $C_{30}H_{18}$.

(Примљено 10. септембра 2008)

REFERENCES

1. G. W. Wheland, *Resonance in Organic Chemistry*, Wiley, New York, 1955
2. H. C. Longuet-Higgins, *J. Chem. Phys.* **18** (1950) 265
3. M. J. S. Dewar, H. C. Longuet-Higgins, *Proc. Roy. Soc. London* **A214** (1952) 482
4. E. Heilbronner, *Helv. Chim. Acta* **50** (1962) 1712
5. P. C. Carter, *Trans. Faraday Soc.* **45** (1949) 597
6. G. G. Hall, *Int. J. Math. Educ. Sci. Technol.* **4** (1973) 233
7. G. G. Hall, *Publ. Inst. Math. Appl.* **17** (1981) 70
8. J. Cioslowski, *MATCH Commun. Math. Chem.* **20** (1986) 95
9. J. Cioslowski, *Int. J. Quantum Chem.* **31** (1987) 581
10. J. Cioslowski, *Topics Curr. Chem.* **153** (1990) 85
11. J. Cioslowski, *MATCH Commun. Math. Chem.* **25** (1990) 83
12. J. Cioslowski, O. E. Polansky, *Theor. Chim. Acta* **74** (1988) 55
13. R. Swinborne-Sheldrake, W. C. Herndon, I. Gutman, *Tetrahedron Lett.* (1975) 755
14. C. F. Wilcox, *Croat. Chem. Acta* **47** (1975) 87
15. I. Gutman, N. Trinajstić, C. F. Wilcox, *Tetrahedron* **31** (1975) 143
16. I. Gutman, S. Petrović, *Chem. Phys. Lett.* **97** (1983) 292
17. I. Gutman, *MATCH Commun. Math. Comput. Chem.* **21** (1986) 317
18. I. Gutman, S. Marković, M. Marinković, *MATCH Commun. Math. Comput. Chem.* **22** (1987) 277
19. I. Gutman, *Chem. Phys. Lett.* **156** (1989) 119
20. I. Gutman, S. Marković, *MATCH Commun. Math. Comput. Chem.* **25** (1990) 141
21. I. Gutman, G. G. Hall, *Int. J. Quantum Chem.* **41** (1992) 667
22. I. Gutman, S. Marković, G. G. Hall, *Chem. Phys. Lett.* **234** (1995) 21
23. I. Gutman, S. Marković, D. Vukićević, A. Stajković, *J. Serb. Chem. Soc.* **60** (1995) 93
24. S. Marković, I. Gutman, J. Šuković, *J. Serb. Chem. Soc.* **61** (1996) 539
25. I. Gutman, *Int. J. Quantum Chem.* **74** (1999) 627
26. I. Gutman, S. Radenković, *Chem. Phys. Lett.* **423** (2006) 382
27. I. Gutman, *Topics Curr. Chem.* **162** (1992) 29
28. I. Gutman, *J. Serb. Chem. Soc.* **70** (2005) 441
29. I. Gutman, S. Radenković, *J. Serb. Chem. Soc.* **71** (2006) 1039
30. I. Gutman, S. Gojak, B. Furtula, S. Radenković, A. Vodopivec, *Monatsh. Chem.* **137** (2006) 1127
31. J. Đurđević, B. Furtula, I. Gutman, S. Radenković, *Kragujevac J. Sci.* **28** (2006) 57
32. I. Gutman, B. Furtula, R. Kovačević, *J. Serb. Chem. Soc.* **72** (2007) 663
33. S. Gojak, I. Gutman, S. Radenković, A. Vodopivec, *J. Serb. Chem. Soc.* **72** (2007) 673
34. J. Đurđević, S. Radenković, I. Gutman, *J. Serb. Chem. Soc.* **73** (2008) 989
35. I. Gutman, N. Trinajstić, *Z. Naturforsch.* **29a** (1974) 1238
36. I. Gutman, O. E. Polansky, *Mathematical Concepts in Organic Chemistry*, Springer-Verlag, Berlin, 1986, pp. 151–153.



J. Serb. Chem. Soc. 74 (2) 159–169 (2009)
JSCS–3819

Spectrophotometric determination of the acidity constants of calcon in water and mixed water–organic solvents

MOHAMMAD MAZLOUM-ARDAKANI^{1*}, SHAHRAM LOTFI², JAHANBAKHSH GHASEMI³, ALAHDAD SHABABI² and MOHAMMAD NOROOZI⁴

¹Department of Chemistry, Faculty of Science, Yazd University, Yazd, ²Department of Chemistry, Payame Noor University, Gilane Gharb Unit, Gilane Gharb, ³Department of Chemistry, Faculty of Science, Razi University, Kermanshah and ⁴Research Institute of Petroleum Industry, Kermanshah Research Center of Oil and Engineering, Kermanshah, Iran

(Received 27 November 2007, revised 19 July 2008)

Abstract: The acid–base properties of calcon (1-(2-hydroxy-1-naphthylazo)-2-naphthol-4-sulfonic acid) in water and mixed water–organic solvents at 25 °C at an ionic strength of 0.10 M are studied by a multiwavelength spectrophotometric method. The organic solvents used were the amphiprotic (methanol), dipolar aprotic (dimethylsulfoxide), and low basic aprotic (acetonitrile). To evaluate the pH absorbance data, a resolution method based on the combination of soft- and hard-modeling was applied. The acidity constants of all related equilibria were estimated using the whole spectral fitting of the collected data to an established factor analysis model. The data analysis program Datan was applied for determination of the acidity constants. The corresponding pK_a values were determined in water and mixed water–organic solvents. Linear relationship between the acidity constants and the mole fraction of the different solvents in the mixtures exist. The effect of solvent properties on acid–base behavior is discussed.

Keywords: calcon; Datan; spectrophotometry; organic solvents; acidity constants.

INTRODUCTION

The accurate determination of acidity constant values is often required in various chemical and biochemical areas. These are of vital importance in understanding the distribution, transport behavior, binding to receptors and mechanism of action of certain pharmaceutical preparation.^{1,2} The acidity constants of organic reagents play a very fundamental role in many analytical procedures, such as acid–base titrations, solvent extractions and complex formation. However, in determining of acidity constants of these molecules, several drawbacks, such as low

* Corresponding author. E-mail: mazloum@yazduni.ac.ir

doi: 10.2298/JSC0902159M

solubility in aqueous solutions and the low values of the acidity constants, are encountered. Therefore, in order to enhance the acidity constants on the one hand and to increase the solubility on the other, mixed solvents have to be employed.

The widespread application of anionic azo compounds as dyes, acid–bases, drugs, metallochrome indicators and histological stains have attracted many researchers to study their acid–base and complex formation properties. However, the literature lacks studies on the acid–base properties or medium effects on the acid dissociation constants of these compounds, which are thought to be of special interest owing to their biological and therapeutic importance.^{3–7} In continuation of our studies on the acid–base properties of these compounds,^{1,8} the medium effect on the ionization constants of calcon (see Scheme 1 for structure) as a good representative was studied by the study of the electronic spectra of the compound in aqueous buffer solutions containing varying proportions of organic solvents of different polarities, *i.e.*, methanol, acetonitrile and dimethylsulfoxide. The pK_a values have been determined and discussed in terms of solvent characteristics.

The solvation of a solute in a mixed solvent is much more complex than the that in a neat single solvent and the literature offers several theories and models for this process.⁹ In general, they agree in that when a solute is dissolved in a mixed solvent, specific solvation effects determine that the proportion of the solvents in the solute sphere of solvation is different from that in the bulk solvent. The solute interacts more strongly with one or more solvents of the mixture and it is preferentially solvated by these solvents. Solute properties, such as pK_a value, depend on the composition and properties of this solvation sphere and therefore they are very sensitive to preferential solvation.

The spectroscopic instrumentation employed today almost invariably has the capacity to collect data over the full spectral range. Using a single or a few wavelengths discards most of the information in the collected spectra and requires both the presence and knowledge of such suitable wavelengths. However, in many cases, the spectral responses of the components overlap and analysis is no longer straightforward.^{10,11} A predefined model, known as hard-modeling analysis, cannot be applied if crucial information is missing. Soft modeling or model free approaches are based on much more general prerequisites, such as positive molar absorbance, positive concentration of all species, unimodality of the concentration profiles and closure (concentration of all species are the same for all solutions). Naturally, if the strengths of hard- and soft-modeling methodologies are combined, a much more powerful method of data analysis can be expected.^{12–20}

Data analysis performed by the Datan package developed by the Kubista group,^{11,20} which is called a physical constraints approach, provides a unique solution by requiring that the calculated concentrations obey an assumed equilib-

rium expression. It was demonstrated by application to the determination of the acidity constants of two and four protolytic forms of fluorescein. A possible advantage of the Kubista *et al.*¹¹ method is that it mixes a soft-modeling approach with a hard-modeling approach. This might be a better and more general strategy, since it can handle different situations, with only a partial knowledge of the chemistry of the system. The physical constraints method calculates spectral profiles, concentrations, and equilibrium constants by utilizing equilibrium expressions that are related to the components. The theory and application of the physical constraints method has been discussed by Kubista *et al.* in several papers.^{21–29}

In this work, the physical constraints approach was applied to determine the acidity constants of calcon in pure water and in different binary acetonitrile and methanol–water mixtures. Data analysis was performed in the Matlab version of the Data analysis (Datan) program developed by the Kubista group.

Theory

The theory and application of the physical constraints method was discussed by Kubista *et al.* in several papers.^{20–29} Nevertheless, the general principal will be outlined briefly.

Spectra of calcon at different pH values are digitized and arranged in a data matrix A , which is decomposed into an orthonormal basis set by Nipals or any equivalent method:¹¹

$$A = Tp^T + E \approx Tp^T = \sum_{i=1}^r t_i p_i^T \quad (1)$$

T has the same dimensions as c ; its column are referred to as target vectors, and they are orthogonal linear combinations of the columns in c , where the orthogonal target vectors t_i and orthonormal projection vectors p_i are mathematical constructs that cannot be directly related to the component spectra and concentrations, r is the number of independent spectroscopic components, which corresponds to the number of light-absorbing chemical species. It is determined by visual inspection of the t and p^T vectors or by performing statistical methods, such as, the χ^2 -test.^{30–32} E is an error matrix. By assuming linear responses, the spectra in matrix A are linear combinations of the concentrations, c , and spectral responses, V , of the chemical components:

$$A = cV + E \approx cV \quad (2)$$

If the spectral profiles of the components are known, the concentration of each component can easily be calculated, for example, by least squares minimization. If standards are not available, the common belief is that the spectral responses of the components cannot be separated, which precludes their identification. This is due to ambiguity in determining the rotation matrix, R , in the

following Equations; from Eqs. (1) and (2), it follows that there is a square matrix \mathbf{R} ($r \times r$) that satisfies:

$$T = c\mathbf{R} \quad (3a)$$

$$p = \mathbf{R}^{-1}V \quad (3b)$$

Since $A = cV = c(\mathbf{R}\mathbf{R}^{-1})V = c\mathbf{R}\mathbf{R}^{-1}V = Tp^T$

If \mathbf{R} can be determined, the spectral responses V and concentrations c of the components can be calculated from the target T and the projection p^T matrices:

$$c = T\mathbf{R}^{-1} \quad (4a)$$

$$V = \mathbf{R}p^T \quad (4b)$$

The thermodynamic expression that describes the concentration of the components is the main constraint used to determine \mathbf{R} , from which the thermodynamic parameters, and the spectral responses and concentrations of the components are calculated. Therefore, the strategy for determining the rotation matrix \mathbf{R} is as follows. The concentrations of the chemical species are calculated from the equilibrium expressions for various trial values of the equilibrium constants, and are fitted to the calculated target vectors according to Eq. (3a). The accuracy of this fit depends crucially on the trial values of the equilibrium constants and the best fit determines their values and the elements of matrix \mathbf{R} .

EXPERIMENTAL

Materials

Calcon, methanol, acetonitrile, dimethylsulfoxide, hydrochloric acid, sodium hydroxide and potassium nitrate were commercial analytical grade products (Merck, Germany). These reagents were used without further purification. A standard stock solution of 7.0×10^{-4} M of calcon was prepared by dissolving the appropriate amount of calcon in water. Stock solutions of the other materials were prepared by dissolving weighed amounts of the substances in the appropriate amounts of water. All the solutions were prepared in deionized water.

Instrumentation

A Scinco S-2000 (Korea) spectrophotometer controlled by a computer and equipped with a 1 cm path length quartz cell was used for acquisition of the UV-Vis spectra. The spectra were acquired between 350 and 765 nm. The pH values were measured using a Metrohm CH-9101 pH-meter (Switzerland) furnished with combined glass-saturated calomel electrode. To precalibrate the pH meter in the various employed binary organic + water mixtures, 0.01 M solutions of oxalate and succinate buffers were employed.

Computer hardware and software

All absorption spectra were digitized at ten data points per nanometer in the wavelength range 350–765 nm and transferred to an AMD 2000 XP (256 Mb RAM) computer for subsequent analysis by Matlab software, version 6.5 (The MathWorks) or for processing using the Datan package.

Spectrophotometric titrations

For the titrations of calcon (1.5×10^{-4} M) in pure water and (2.1×10^{-4} M) in water–organic mixtures, the absorption spectra were measured with a titration set-up consisting of a com-

puter interfaced to the spectrophotometer. Control of the pH was achieved using a modified universal buffer solution. To account for differences in acidity, basicity and ion activities for the organic–water solvent mixture relative to pure water, in which the pH-meter was standardization using aqueous buffers, the pH values in the organic–water solvent mixtures were corrected using the equation $\text{pH}^* = \text{pH}(\text{R}) - \delta$, where pH^* is the corrected reading and $\text{pH}(\text{R})$ is the reading of the pH-meter obtained in a partially aqueous organic solvent, determined by Douheret.^{33,34} After each pH adjustment, the solution was transferred to a cuvette and the absorption spectra were recorded. The ionic strength was maintained at 0.10 M by adding appropriate amounts of KNO_3 (0.10 M). All measurements were performed at a temperature of 25 °C.

RESULTS AND DISCUSSION

The absorption spectra of calcon in water and mixed water–organic solvents at various pH values in the interval 350–765 nm were recorded. Sample spectra of calcon at different pH values in pure water with the pH ranging from 0.73 to 13.76 and in water containing 30 % (w/v) of an organic solvent (methanol, acetonitrile, and dimethylsulfoxide with the pH ranging from 0.52 to 13.92, from 0.48 to 13.95 and from 0.49 to 13.85, respectively) at 0.10 M KNO_3 are shown in Figs. 1 and 2, respectively. Principal component analysis of all absorption data matrices obtained at various pH shows at least four significant factors, which is also supported by the statistical indicators of Elbergali *et al.*,²⁴ which predicted four distinguishable components in the samples. These factors could be attributed to the three dissociation equilibria of a triprotic acid such as calcon. This may not be concluded by inspection of the visible spectra of calcon.

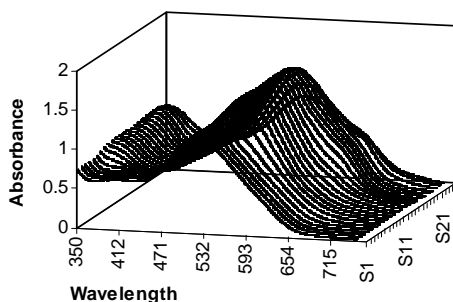


Fig. 1. Absorption spectra of calcon in pure water at 0.10 M KNO_3 at different pH values.

The $\text{p}K_a$ values of calcon were investigated spectrophotometrically in different methanol, acetonitrile, and dimethylsulfoxide + water binary mixtures at 25 °C at an ionic strength of 0.10 M. The acidity constants of calcon in several mixtures were evaluated using the computer program Datan and the corresponding spectral absorption–pH data. From inspection of the experimental spectra, it is hard to guess even the number of protolytic species involved. The four calculated most significant projection vectors, p^T , with clear spectral features (as compared to noise) indicate the presence of three spectroscopically distinguishable components. Their profiles or shapes show some order of ambiguity, (*i.e.*, they are

clearly physically meaningless and cannot be directly related to the spectral response of the four protolytic forms). After rigorous curve resolution computational steps according to a combination of hard and soft-modeling, the outputs of the program are the pK_a values and their standard deviation (derived from the error analysis plot of the program), the number of principal components, projection vectors (loadings), concentration distribution diagrams and the pure spectrum of each assumed species.

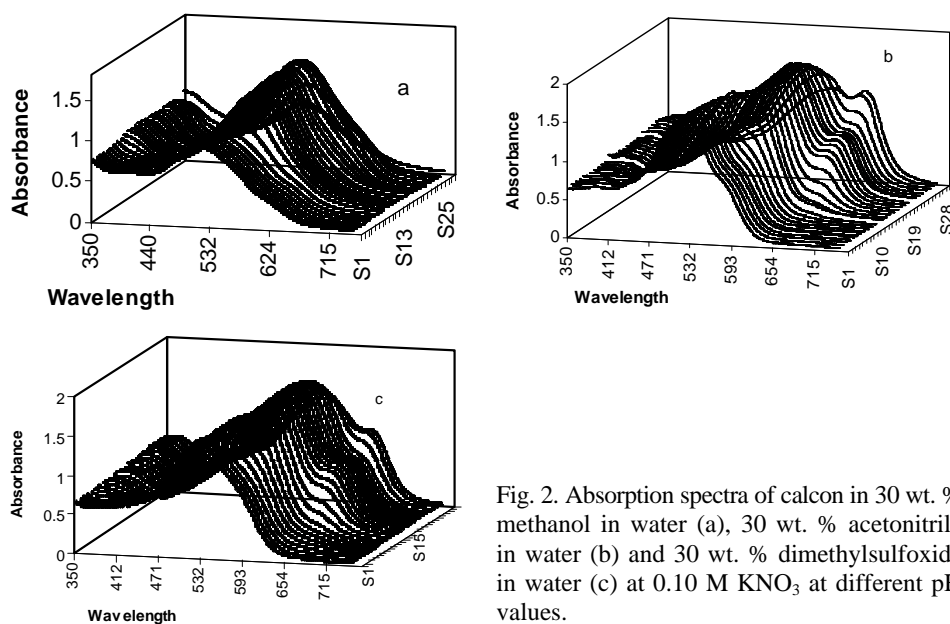


Fig. 2. Absorption spectra of calcon in 30 wt. % methanol in water (a), 30 wt. % acetonitrile in water (b) and 30 wt. % dimethylsulfoxide in water (c) at 0.10 M KNO_3 at different pH values.

The obtained pK_a values are listed in Table I. The previous reported values of the acidity constants were mainly in pure water.^{35,36} The obtained values in pure water are in good agreement with the previous values, which are also listed in Table I for comparison. The differences observed between the pK_a values are not only within the margins of experimental error but also due to the different computational strategy of the univariate methods and of newer chemometrics based methods. The manner in which noise or measurement error treatment are performed on the absorption spectra in a multivariate sense which uses the whole spectral domain, reduces considerably the level of noise and results in more precise final information. Hence, the obtained acidity constants are more reliable and precise than those obtained by previous methods. The pK_a values correspond to the pH-dependent variation of absorption spectra in all solvents mixtures. One of the very important outputs of the Datan program is the calculated spectrum of the different forms of calcon in each solvent mixture. Sample spectra of the calculated pure spectral profiles of all species in water and different organic sol-

vents/water mixtures are shown in Fig. 3. As the mole fraction of organic solvents increased, the absorption intensity changed differently for each species of calcon. It is interesting to note that the nature and the composition of the solvent have a fundamental effect on each pure spectrum. As is clear from Fig. 3, this effect is greater for H_3L and L^{3-} than for H_2L^- and HL^{2-} . The spectrum of the L^{3-} species has a larger λ_{max} than the other species which shows a splitting pattern in high weight percents of methanol, acetonitrile and dimethylsulfoxide. The splitting of the absorption peak at λ_{max} of L^{3-} is more obvious than that of the other species. This can be described using the non-electrostatic (H-bonding) property of the stabilization and/or destabilization of the ground and excited states of the $n \rightarrow \pi^*$ and $\pi \rightarrow \pi^*$ transitions. The appearance and disappearance of some shoulder and absorption peaks of each species is related to the type and mass percent of the organic solvent.

TABLE I. Acidity constants of calcon in pure water and in different percentage of MeOH, AN, DMSO (w/v) at 25 °C and at constant ionic strength (0.10 M KNO_3)

wt. %	Methanol			Acetonitrile			Dimethylsulfoxide		
	pK_1	pK_2	pK_3	pK_1	pK_2	pK_3	pK_1	pK_2	pK_3
0	1.05	7.21	13.43	—	—	—	—	—	—
0 ^a	1	7.3	13.5	—	—	—	—	—	—
10	0.96	7.38	13.55	0.93	7.45	13.58	0.91	7.12	13.45
20	0.88	7.54	13.68	0.79	7.61	13.71	0.77	7.50	13.54
30	0.69	7.76	13.76	0.62	7.90	13.83	0.61	7.68	13.61

^aRef. 35

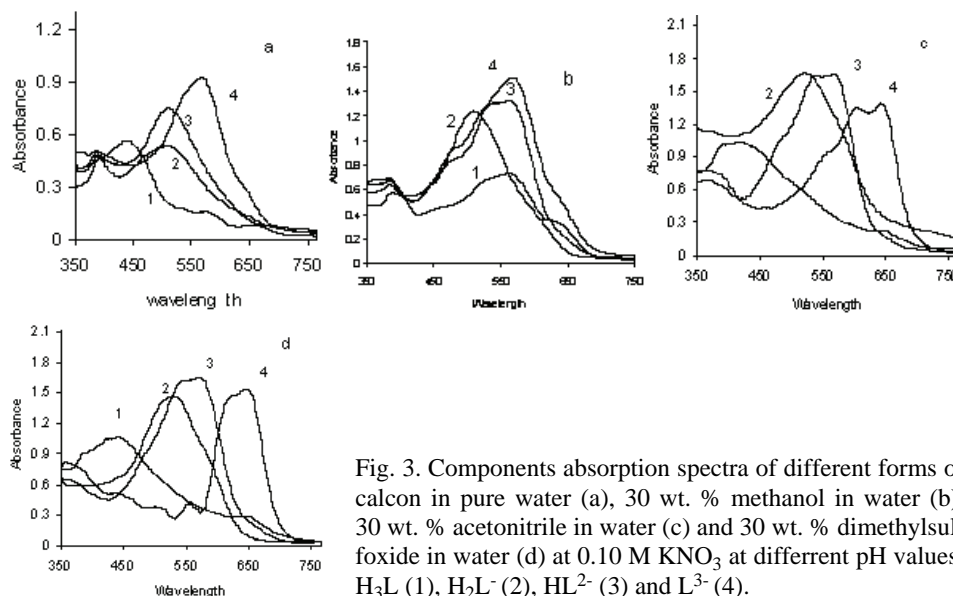


Fig. 3. Components absorption spectra of different forms of calcon in pure water (a), 30 wt. % methanol in water (b), 30 wt. % acetonitrile in water (c) and 30 wt. % dimethylsulfoxide in water (d) at 0.10 M KNO_3 at different pH values; H_3L (1), H_2L^- (2), HL^{2-} (3) and L^{3-} (4).

The most important features of the distribution diagrams are the pH limit of the evolution and disappearance of the components. Hence, according to distribution diagrams, it could be concluded that the spectra at pH lower than 1 is attributable to the H_3L form because this form is dominant in this pH range. In the pH 1.0–7.0 interval, the H_2L^- form is dominant and, hence, the spectra are mostly attributed to this form. The HL^{2-} and L^{3-} forms appeared in the pH intervals 7.0–13.5 and $pH > 13.5$, respectively. Samples of the obtained distribution diagrams are shown in Figs. 4 and 5. The data shown in Table I clearly illustrate the important influence of the nature of the solvent on the dissociation reaction. The acidity constants of the second and third dissociation steps of calcon decreased with increasing the mole fraction of methanol in the mixed solvents. It has been shown that the solvating ability³⁷ (as expressed by the Gutmann donicity scale) and dielectric constant of the solvent play a fundamental role in dissociation reactions. Water is a solvent of high solvating ability (*i.e.*, donor number $DN = 33$, dielectric constant $\epsilon = 87.3$), which can dissociate the acid and stabilize the produced anion and hydrogen ion. Thus, it is expected that addition of methanol ($DN = 19$, $\epsilon = 32.6$), acetonitrile ($DN = 14$, $\epsilon = 36$), and dimethylsulfoxide ($DN = 26.5$, $\epsilon = 46.6$) with lower donor numbers and dielectric constants relative to water decreases the extent of interaction between the acid anion and proton with the solvent, which decreases the acidity constants of calcon.

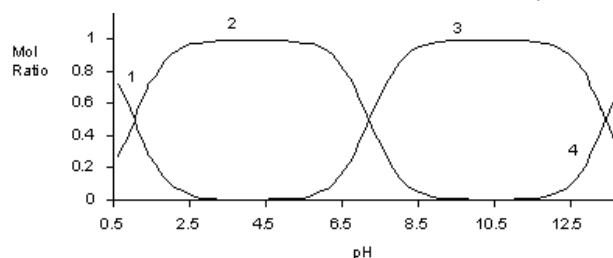


Fig.4. Distribution of major species of calcon, 1) H_3L , 2) H_2L^- , 3) HL^{2-} and 4) L^{3-} , as a function of pH for the spectral data in Fig. 1.

It is interesting to note that there is actually a linear relationship between the pK_a of the three dissociation steps (the first step decreases whereas the second and third steps increase) and the mole fraction of methanol (x_{solvent}) in the employed binary mixed solvents, as can be seen in Fig. 6.

It is clear that the dissociation of an uncharged acid in a solvent requires the separation of two ions of opposite charges. The work required to separate these charges is inversely proportional to the dielectric constant of the solvent. The energy required for dissociation is supplied by solvation of the ions and also proton transfer from the acid to the solvent molecule supplies additional energy. If the dielectric constant and the solvating ability of the solvent are decreased, more energy will be required to separate the anion and cation and, consequently, the extent of dissociation of the acid will be lowered. Therefore, the increase in first

step and the decrease in second and third steps of the dissociation constants are due to the increasing mole fraction of methanol, acetonitrile and dimethylsulfoxide in the binary mixed solvents.

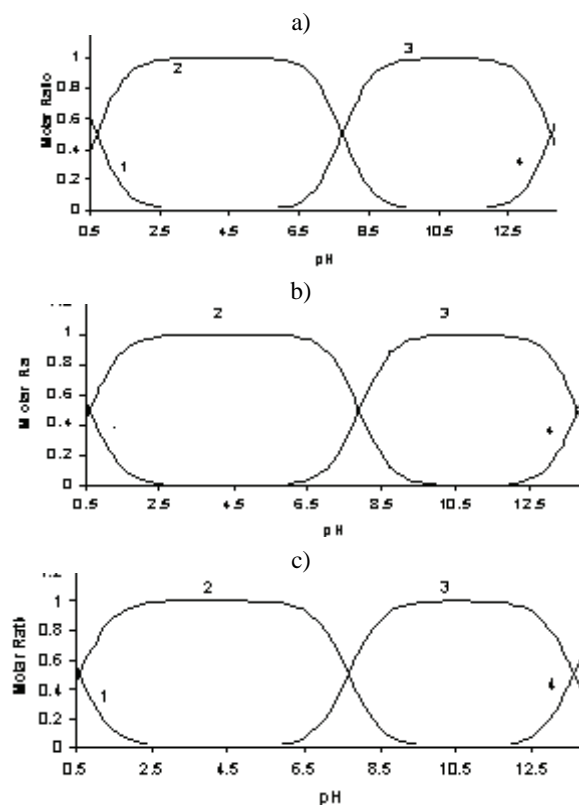


Fig. 5. Distribution of major species of calcon, 1) H_3L , 2) H_2L^- , 3) HL^{2-} and 4) L^{3-} , as a function of pH for the spectral data in Fig. 2.

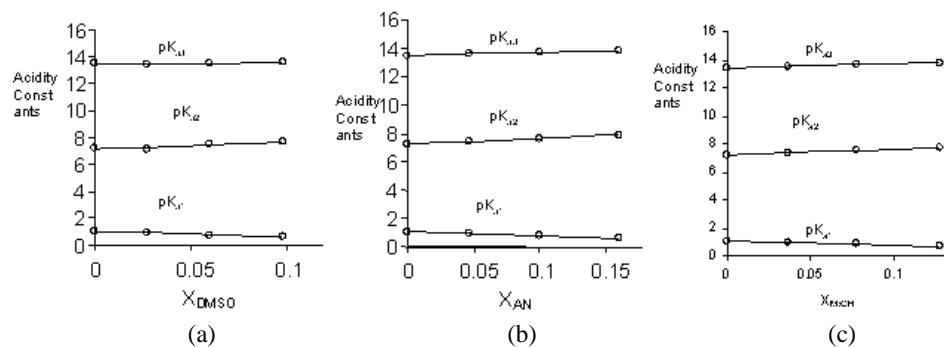


Fig.6. Variation of the values of the acidity constants of calcon with mole ratio of different organic solvents.

CONCLUSIONS

In this study, the acidity constants of calcon in different and mixed solvents were determined. The Data Analysis (Datan) program was employed to analyze correlated spectroscopic data. The pK_a values of calcon were determined in methanol, acetonitrile and dimethylsulfoxide–water mixtures. The pK_a values correspond to the pH-dependent variation of the absorption spectra in all solvent mixtures. A linear relationship was found between the pK_a values of the three dissociation steps (the first step decreases and the second and third steps increase) and the mole fraction of the organic solvents in the binary mixed solvents.

Acknowledgement. The authors are thankful to the Payam University Research Council (Ardakan Center), the IUT Research Council and Excellence in Sensors for financial support of this research.

ИЗВОД

СПЕКТРОФОТОМЕТРИЈСКО ОДРЕЂИВАЊЕ КОНСТАНТЕ КИСЕЛОСТИ КАЛКОНА У ВОДЕНИМ И ВОДА–ОРГАНСКИМ РАСТВОРАЧИМА

МОХАММАД МАЗЛОУМ АРДАКАНИ¹, ШАХРАМ ЛОТФИ², ЈАХАНБАКХШ ГХАСЕМИ³, АЛАХДАД ШАБАБИ² и МОХАММАД НОРООЗИ⁴

¹Department of Chemistry, Faculty of Science, Yazd University, Yazd, ²Department of Chemistry, Payame Noor University, GilaneGharb Unit, Gilane Gharb, ³Department of Chemistry, Faculty of Science, Razi University, Kermanshah u ⁴Research Institute of Petroleum Industry, Kermanshah Research Center of Oil and Engineering, Kermanshah, Iran

Кисело–базна својства калкона (1-(2-хидрокси-1-нафтилазо)-2-нафтол-4-сулфонске киселине) у води и растворима вода–органски растварачи на 25 °С при јонској јачини 0,10 М су испитивана спектрофотометријски. Коришћени су органски растварачи метанол, диметилсулфоксид и ацетонитрил. Константе киселости у случају свих равнотежних система су одређиване у целом спектралном региону коришћењем факторске анализе применом програма Datan. Одговарајуће вредности pK_a су одређене у води и растворима вода–органски растварач. Добијена је линеарна зависност киселости и молске фракције различитих растварача. Дискутован је утицај својстава растварача на кисело–базна својства.

(Примљено 27. новембра 2007, ревидирано 19. јула 2008)

REFERENCES

1. D. Almasifar, F. Forghaniha, Z. Khojasteh, J. Ghasemi, H. Shargi, M. Shamsipur, *J. Chem. Eng. Data* **742** (1999) 1212
2. M. Shamsipur, J. Ghasemi, F. Tamaddon, H. Shargi, *Talanta* **40** (1992) 697
3. G. A. Qureshi, G. Svehla, M. A. Leonard, *Analyst* **104** (1979) 705
4. R. H. Thomson, *Naturally Occurring Quinones*, 2nd Ed., Academic Press, New York, 1971
5. F. Arcamone, *Med. Res. Rev.* **14** (1984) 153
6. M. Lucker, *Secondary Metabolism in Microorganism, Plants and Animals*, Springer Verlag, New York, 1984
7. N. J. Lowe, R. E. Ashton, H. Koudsi, M. Verschoore, H. Schaefer, *J. Am. Acad. Dermatol.* **10** (1984) 69

8. M. Shamsipur, J. Ghasemi, F. Tamadon, H. Sharghi, *Talanta* **40** (1993) 697
9. F. Rived, I. Canals, E. Bosch, M. Roses, *Anal. Chim. Acta* **439** (2001) 315
10. K. Y. Tam, M. Hadley, W. Patterson, *Talanta* **49** (1999) 539
11. M. Kubista, R. Sjoback, B. Albinsson, *Anal. Chem.* **65** (1993) 994
12. A. de Juan, M. Maeder, M. Martínez, R. Tauler, *Anal. Chim. Acta* **442** (2001) 337
13. J. Ghasemi, A. Niazi, M. Kubista, A. Elbergali, *Anal. Chim. Acta* **455** (2002) 335
14. B. A. Hendriksen, M. V. Sanchez-Flix, K. Y. Tam, *Spectrosc. Lett.* **35** (2002) 9
15. J. Ghasemi, S. Ahmadi, M. Kubista, A. Forootan, *J. Chem. Eng. Data* **48** (2003) 1178
16. J. Ghasemi, S. Ghobadi, B. Abbasi, M. Kubista, *J. Korean Chem. Soc.* **49** (2005) 123
17. A. Niazi, M. Ghalie, A. Yazdanipour, J. Ghasemi, *Spectrochim. Acta, Part A* **64** (2006) 660
18. A. Niazi, A. Yazdanipour, J. Ghasemi, M. Kubista, *Collect. Czech. Chem. Commun.* **71** (2006) 1
19. J. Ghasemi, S. Lotfei, M. Safaian, A. Niazi, M. Mazloun Ardakani, M. Noroozi, *J. Chem. Eng. Data* **51** (2006) 1530
20. M. Kubista, R. Sjoback, J. Nygren, *Anal. Chim. Acta* **302** (1995) 121
21. I. Sacriminio, M. Kubista, *Anal. Chem.* **65** (1993) 409
22. R. Sjoback, J. Nygren, M. Kubista, *Spectrochim. Acta, Part A* **51** (1995) 17
23. J. Nygren, J. Andrade, M. Kubista, *Anal. Chem.* **68** (1996) 1706
24. A. Elbergali, J. Nygren, M. Kubista, *Anal. Chim. Acta* **379** (1999) 143
25. M. Kubista, J. Nygren, A. Elbergali, R. Sjoback, *Crit. Rev. Anal. Chem.* **29** (1999) 1
26. J. Nygren, N. Svanvik, M. Kubista, *Biopolymers* **46** (1998) 39
27. N. Svanvik, J. Nygren, G. Westman, M. Kubista, *J. Am. Chem. Soc.* **123** (2001) 803
28. J. Ghasemi, A. Niazi, G. Westman, M. Kubista, *Talanta* **62** (2004) 835
29. J. Ghasemi, A. Niazi, M. Kubista, *Spectrochim. Acta Part A* **62** (2005) 649
30. R. Fisher, W. Mackenzie, *J. Agric. Sci.* **13** (1923) 311
31. H. Wold, F. Daved (Ed.), *Research Papers in Statistics*, Wiley, New York, 1966, p. 441
32. K. V. Mardia, J. T. Kent, J. M. Bibby, *Multivariate Analysis*, Academic Press, London, 1979
33. G. Douheret, *Bull. Soc. Chim. Fr.* (1967) 1412
34. G. Douheret, *Bull. Soc. Chim. Fr.* (1968) 3122
35. G. P. Hildebrand, C. N. Reilley, *Anal. Chem.* **29** (1957) 258
36. D. W. Rogers, D. A. Alkens, C. N. Reilley, *J. Phys. Chem.* **66** (1962) 1582
37. V. Gutmann, *Coordination Chemistry in Nonaqueous Solutions*, Springer, New York, 1960.



J. Serb. Chem. Soc. 74 (2) 171–182 (2009)
JSCS–3820

Kinetics and mechanism of the oxidation of some substituted aldonitrones by quinolinium chlorochromate in aqueous DMF medium in the absence and presence of oxalic acid

GOVINDASAMY RAJARAJAN¹, NATESAN JAYACHANDRAMANI², SUBRAMANIAN MANIVARMAN¹, JAYARAMAN JAYABHARATHI¹ and VENUGOPAL THANIKACHALAM^{1*}

¹Department of Chemistry, Annamalai University, Annamalainagar - 608 002, Tamil Nadu and ²Department of Chemistry, Pachaiyappa's College, Chennai - 600 030, India

(Received 31 December 2007, revised 16 May 2008)

Abstract: The kinetics of the oxidation of aldonitrones (nitron) by quinolinium chlorochromate (QCC) was determined in 50 % DMF–water in the absence and presence of oxalic acid in order to study the effect of oxalic acid. It was considered worthwhile to investigate whether it undergoes co-oxidation or just functions as a catalyst in the reaction. The reaction was followed iodometrically. Under the employed experimental conditions, the reaction is first order each with respect to concentration of nitron, QCC, and oxalic acid and fractional order with respect to H⁺ concentration. There was no discernible effect with increasing in ionic strength but the rate of oxidation decreased with decreasing dielectric constant of the medium. Addition of MnSO₄ had a significant and acrylonitrile no effect on the reaction rate. A mechanism involving protonated nitron and QCC as the reactive oxidant is proposed. The activation parameters were calculated and are presented.

Keywords: aldonitrones; quinolinium chlorochromate; isokinetic plot; entropy; enthalpy; free energy; oxalic acid.

INTRODUCTION

The use of quinolinium chlorochromate (QCC) as an oxidant is well documented for the oxidation of primary and secondary alcohols,^{1–3} organic sulphides,^{4,5} substituted benzaldehydes,^{6,7} benzyl alcohols,⁸ aromatic anils,⁹ lactic and glycolic acids,¹⁰ methionine,¹¹ D-fructose,¹² D-mannose,¹³ an unsaturated organic substrate,¹⁴ acrylic acid,¹⁵ 2-furaldehyde,¹⁶ D-galactose,¹⁷ etc. Quinolinium chlorochromate exists as a stable yellowish brown crystalline solid. It is freely soluble in water and aqueous solutions of QCC are stable for quite a long period.

* Corresponding author. E-mail: pvta1998@yahoo.co.in
doi: 10.2298/JSC0902171R

Oxalic acid was found to catalyse the oxidation of organic substrates by Cr(VI).^{18–20} A survey of the literature showed that there are only a few reports on the kinetic studies with nitrones (nitrone).^{21–26} There is no report on a mechanistic study of the oxidation of nitrones by QCC. Thus, in order to explore the mechanism of oxidation by QCC, the title reaction was studied in aqueous DMF medium.

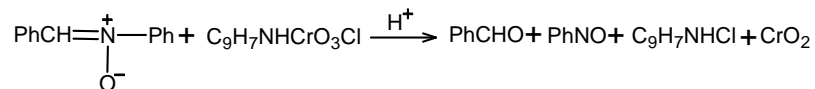
EXPERIMENTAL

Materials and methods

All the chemicals used were of high purity of mostly either AR or GR grade. Double distilled water was used throughout the work. Aldonitrones²⁷ and quinoline chlorochromate (QCC)²⁸ were prepared by known methods and recrystallized from water. The purity of the prepared QCC was checked by the iodometric method (assay 99 %). Nitrone solutions were prepared by dissolving appropriate amount of a recrystallized sample in DMF. The aqueous solution of QCC was obtained by dissolving the compound in double distilled water. Experiments were conducted in a thermostated bath which could maintain the temperature with an accuracy of ± 0.1 °C.

Kinetic studies

The kinetic studies were carried out in 50 % (v/v) DMF–water medium under pseudo-first order conditions, keeping $c(\text{nitrone}) \gg c(\text{QCC})$. The course of the reaction was followed by estimating the unreacted QCC iodometrically. The reaction was followed at four different temperatures. Pseudo-first order rate constants were evaluated from the slopes of the linear plots of $\log c(\text{QCC})$ versus time. The rate constant, k_2 was calculated using the relation $k_2 = k_{\text{obs}}/c(\text{nitrone})$. The reaction mixtures containing excess of QCC over nitrone in absence and presence of oxalic acid were kept for one day. The estimation of the unreacted QCC indicated that one mole of QCC was consumed for one mole of nitrone:



The reaction mixture was extracted with chloroform from an actual kinetic run after completion of the reaction. The reaction mixture was monitored by Co-TLC along with authentic samples of *N*, α -diphenylnitron, benzaldehyde and nitrosobenzene. Then, the products were separated into individual components by column chromatography (silica gel 60–120 mesh) with benzene–chloroform as the eluent. The melting point of the solid product obtained was found to be 67 °C, which is almost identical with the melting point of the nitrosobenzene dimer, m.p. 67.5–68 °C.²⁹ The IR spectrum was recorded in a KBr pellet, using a model Jasco 700 instrument, in the range 400–4000 cm^{-1} . Nitrosobenzene exhibits three bands at 1625, 1500 and 1019 cm^{-1} , attributed to the stretching of C–N; one sharp band at 1452 cm^{-1} , due to the stretching vibration of N–O, and one band at 530 cm^{-1} , due to ring deformation and C–N–O bending vibrations.²⁹ The liquid product was confirmed to be benzaldehyde by its semicarbazone (m.p. 221 °C; literature data: 222 °C³⁰) and 2,4-dinitrophenylhydrazone (m.p. 238 °C; literature data: 239 °C³⁰) derivatives.

RESULTS AND DISCUSSION

The kinetics of oxidation of nitrones by QCC was performed in 50 % aqueous DMF in the absence and presence of oxalic acid in order to study the be-

haviour of oxalic acid. It was considered worthwhile to investigate whether it undergoes co-oxidation or just functions as a catalyst in the reaction.¹⁸⁻²⁰ The reaction was followed iodometrically. In both the cases, *i.e.*, in the absence and presence of oxalic acid, the reaction is first order with respect to QCC. Furthermore, the pseudo-first order rate constant k_{obs} was found to be independent of the initial concentration of QCC.

The substrate, aldonitrone, was varied in the concentration range of 5×10^{-3} to 15×10^{-3} mol dm⁻³ at 308 K in the absence of oxalic acid and 5×10^{-3} to 20×10^{-3} mol dm⁻³ at 308 K in the presence of oxalic acid, keeping all other constituents and conditions constant (Tables I and II). The k_{obs} values increased with increasing concentration of nitrones. The plot of $\log k_{\text{obs}}$ versus $\log c(\text{nitrone})$ was a straight line with a slope of unity and a plot of k_{obs}^{-1} versus $c(\text{nitrone})^{-1}$ was also linear ($r = 0.999$), passing through the origin, which indicates a first order dependence on $c(\text{substrate})$. No complex formation occurred before the rate-determining step in absence of oxalic acid, whereas complex formation occurred before rate-determining step in its presence.

TABLE I. Effect of the variation of $c(\text{QCC})$, $c(\text{nitrone})$ and $c(\text{H}^+)$ on the oxidation of nitrones by QCC in the absence oxalic acid at 308 K

$c(\text{QCC}) \times 10^3$ mol dm ⁻³	$c(\text{nitrone}) \times 10^2$ mol dm ⁻³	$c(\text{HClO}_4) \times 10^3$ mol dm ⁻³	% DMF (v/v)	$k_{\text{obs}} \times 10^3$ s ⁻¹
0.50	1.00	6.00	50	1.530
0.75	1.00	6.00	50	1.480
1.00	1.00	6.00	50	1.527
1.25	1.00	6.00	50	1.519
1.50	1.00	6.00	50	1.536
1.00	0.50	6.00	50	0.756
1.00	0.75	6.00	50	1.141
1.00	1.00	6.00	50	1.529
1.00	1.25	6.00	50	1.918
1.00	1.50	6.00	50	2.308
1.00	1.00	1.50	50	1.184
1.00	1.00	3.00	50	1.364
1.00	1.00	6.00	50	1.529
1.00	1.00	7.50	50	1.705
1.00	1.00	9.00	50	1.852
1.00	1.00	6.00	30	1.650
1.00	1.00	6.00	40	1.592
1.00	1.00	6.00	50	1.529
1.00	1.00	6.00	60	0.844
1.00	1.00	6.00	70	0.642
1.00	1.00	6.00	80	0.546

The influence of H^+ on the reaction rate was studied by varying the acidity from 1.5×10^{-3} to 9×10^{-3} mol dm⁻³ while maintaining the ionic strength constant

at $\mu = 0.10 \text{ mol dm}^{-3}$ with sodium perchlorate. The concentration of hydrogen ions was found to increase the reaction rate (Tables I and II). It was previously observed that the reaction showed a fractional order dependence on the hydrogen ion concentration in the presence and absence of oxalic acid.^{31,32}

TABLE II. Effect of the variation of $c(\text{QCC})$, $c(\text{nitron})$, $c(\text{H}^+)$ and $c(\text{H}_2\text{C}_2\text{O}_4)$ on the oxidation of nitrones by QCC in the presence of oxalic acid at 308 K

$c(\text{QCC}) \times 10^3$ mol dm ⁻³	$c(\text{nitron}) \times 10^2$ mol dm ⁻³	$c(\text{HClO}_4) \times 10^3$ mol dm ⁻³	$c(\text{H}_2\text{C}_2\text{O}_4) \times 10^2$ mol dm ⁻³	% DMF (v/v)	$k_{\text{obs}} \times 10^3$ s ⁻¹
0.50	1.00	6.00	1.00	50	2.325
0.75	1.00	6.00	1.00	50	2.285
1.00	1.00	6.00	1.00	50	2.323
1.25	1.00	6.00	1.00	50	2.310
1.50	1.00	6.00	1.00	50	2.245
1.00	0.50	6.00	1.00	50	1.080
1.00	0.75	6.00	1.00	50	1.751
1.00	1.00	6.00	1.00	50	2.323
1.00	1.25	6.00	1.00	50	2.657
1.00	1.50	6.00	1.00	50	3.645
1.00	2.00	6.00	1.00	50	4.621
1.00	1.00	3.00	1.00	50	2.140
1.00	1.00	6.00	1.00	50	2.323
1.00	1.00	7.50	1.00	50	2.450
1.00	1.00	8.50	1.00	50	2.608
1.00	1.00	9.01	1.00	50	2.725
1.00	1.00	6.00	0.50	50	1.108
1.00	1.00	6.00	0.75	50	1.821
1.00	1.00	6.00	1.00	50	2.323
1.00	1.00	6.00	1.50	50	3.550
1.00	1.00	6.00	2.00	50	4.712
1.00	1.00	6.00	1.00	40	2.640
1.00	1.00	6.00	1.00	50	2.323
1.00	1.00	6.00	1.00	60	2.102
1.00	1.00	6.00	1.00	70	1.848
1.00	1.00	6.00	1.00	80	1.624

The effect of oxalic acid on the reaction at 308 K was studied by varying its concentration from 5×10^{-3} to $20 \times 10^{-3} \text{ mol dm}^{-3}$ at constant concentrations of QCC, nitron and HClO_4 . The reaction rate increased with increasing concentration of oxalic acid. The results are collected in Table II. The plot of $\log k_{\text{obs}}$ versus $\log c(\text{H}_2\text{C}_2\text{O}_4)$ was linear with a slope of unity (*ca.* 1.03; $r = 0.998$) and the order with respect to oxalic acid was one. When the experiment was repeated with oxalic acid in the absence of nitron, there was no oxidation of oxalic acid under these experimental conditions. However, the addition of oxalic acid enhanced the rate of oxidation of nitron. This observation clearly establishes that oxa-

lic acid does not undergo co-oxidation under the experimental conditions employed in this investigation and that it acts only as a catalyst.

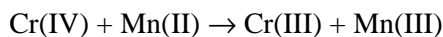
Effect of ionic strength was studied by varying the sodium perchlorate concentration from 0 to 0.15 mol dm⁻³. There was no discernible effect with increasing $c(\text{NaClO}_4)$ (Table III).

TABLE III. Effect of ionic strength on the oxidation of nitron by QCC in the presence/absence of oxalic acid ($c(\text{QCC}) = 1.0 \times 10^{-3}$ mol dm⁻³; $c(\text{nitron}) = 1.0 \times 10^{-2}$ mol dm⁻³; $c(\text{H}^+) = 6.0 \times 10^{-3}$ mol dm⁻³; $c(\text{H}_2\text{C}_2\text{O}_4) = 1.0 \times 10^{-2}$ mol dm⁻³; 50 % v/v DMF)

$c(\text{NaClO}_4) / \text{mol dm}^{-3}$	$^a k_{\text{obs}} \times 10^3 / \text{s}^{-1}$	$^b k_{\text{obs}} \times 10^3 / \text{s}^{-1}$
0.00	1.529	2.323
0.050	1.439	2.001
0.075	1.387	1.800
0.100	1.256	1.743
0.125	1.100	1.525
0.150	0.918	1.304

^aAbsence of oxalic acid; ^bpresence of oxalic acid

A variation in $c(\text{Mn(II)})$ in both systems decreased the rate of reduction of Cr(VI) in the HClO₄ medium. The values of k_{obs} are listed in Table IV. Manganese(II) has an inhibitory,³³ catalytic³⁴ or no effect^{35,36} in the redox chemistry of Cr(VI) in the presence of organic reductants. The decrease in the rate of Cr(VI) reduction on addition of Mn(II) was attributed to the removal of Cr(IV) by reaction with Mn(II):³⁷



Thus, the observed inhibitory effect was due to the one-step, two-electron reduction of Cr(VI).

TABLE IV. Effect of $c(\text{MnSO}_4)$ on the oxidation of nitron by QCC in the presence/absence of oxalic acid ($c(\text{QCC}) = 1.0 \times 10^{-3}$ mol dm⁻³; $c(\text{nitron}) = 1.0 \times 10^{-2}$ mol dm⁻³; $c(\text{H}^+) = 6.0 \times 10^{-3}$ mol dm⁻³; $c(\text{H}_2\text{C}_2\text{O}_4) = 1.0 \times 10^{-2}$ mol dm⁻³; 50 % v/v DMF)

$c(\text{MnSO}_4) \times 10^3 / \text{mol dm}^{-3}$	$^a k_{\text{obs}} \times 10^3 / \text{s}^{-1}$	$^b k_{\text{obs}} \times 10^3 / \text{s}^{-1}$
0.00	1.529	2.323
1.00	1.248	2.014
2.00	1.093	1.921
3.00	0.973	1.850
4.00	0.856	1.542

^aAbsence of oxalic acid; ^bpresence of oxalic acid

Acrylonitrile added to both the reaction mixtures did not show any polymerization, thereby ruling out the possibility of a free radical mechanism.³⁸ The effect of dielectric constant on the rate of oxidation was also studied and the rate decreased moderately with decreasing dielectric constant of the medium. This result also supports the involvement of an ion-dipole species in the slow step.³⁹

The reactions were also performed at four different temperatures (303, 308, 313 and 318 K) in the absence and presence of oxalic acid (298, 303, 308 and 313 K). The thermodynamic parameters, namely the entropy and enthalpy of activation,⁴⁰ were calculated from the linear plot of $\ln(k_2/T)$ versus $1/T$. The calculated values are summarized in Tables V and VI.

TABLE V. Rate constants and activation parameters for the oxidation of nitrones with QCC in the absence of oxalic acid ($c(\text{QCC}) = 1.0 \times 10^{-3} \text{ mol dm}^{-3}$; $c(\text{nitron}) = 1.0 \times 10^{-2} \text{ mol dm}^{-3}$; $c(\text{H}^+) = 6.0 \times 10^{-3} \text{ mol dm}^{-3}$; $c(\text{NaClO}_4) = 0.100 \text{ mol dm}^{-3}$; 50 % v/v DMF)

R	$k_2 \times 10^2 / \text{dm}^3 \text{ mol}^{-1} \text{ s}^{-1}$				ΔH^\ddagger kJ mol ⁻¹	$-\Delta S^\ddagger$ J K ⁻¹ mol ⁻¹	ΔG^\ddagger kJ mol ⁻¹	r
	T / K							
	303	308	313	318				
H	10.90	15.30	19.84	24.63	40.82	129.38	80.67	0.996
<i>p</i> -Me	11.18	18.39	23.66	30.29	49.49	99.40	80.10	0.984
<i>p</i> -OMe	12.45	18.94	24.95	33.30	49.18	90.71	79.92	0.995
<i>p</i> -F	8.31	14.20	18.23	24.63	53.76	87.77	80.79	0.985
<i>p</i> -Cl	8.09	13.79	16.47	23.25	51.09	96.79	80.91	0.980
<i>p</i> -Br	7.92	12.94	15.26	22.43	50.15	100.26	80.03	0.983
<i>p</i> -NO ₂	4.67	8.43	11.21	13.96	54.80	88.88	82.17	0.973
<i>m</i> -F	5.33	10.12	14.23	18.63	63.21	60.03	81.70	0.960
<i>m</i> -Cl	5.91	10.77	14.47	18.99	58.42	75.04	81.53	0.980
<i>m</i> -Br	5.44	10.91	14.23	18.43	60.54	68.47	81.63	0.966
<i>m</i> -NO ₂	4.93	8.53	12.23	14.80	56.61	83.92	82.45	0.978

TABLE VI. Second-order rate constants and activation parameters for the oxidation of nitrones by QCC in the presence of oxalic acid ($c(\text{QCC}) = 1.0 \times 10^{-3} \text{ mol dm}^{-3}$; $c(\text{nitron}) = 1.0 \times 10^{-2} \text{ mol dm}^{-3}$; $c(\text{H}^+) = 6.0 \times 10^{-3} \text{ mol dm}^{-3}$; $c(\text{H}_2\text{C}_2\text{O}_4) = 1.0 \times 10^{-2} \text{ mol dm}^{-3}$; $c(\text{NaClO}_4) = 0.100 \text{ mol dm}^{-3}$; 50 % v/v DMF)

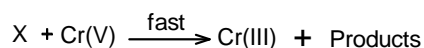
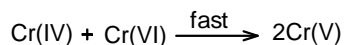
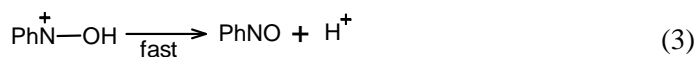
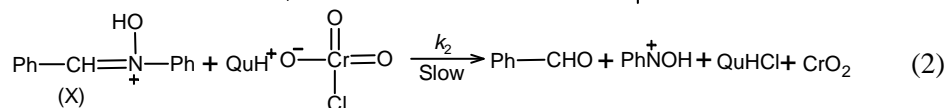
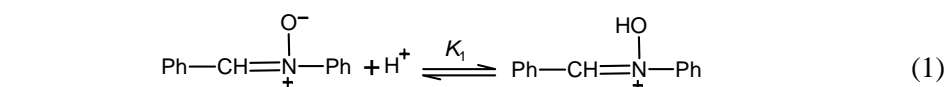
R	$k_2 \times 10^2 / \text{dm}^3 \text{ mol}^{-1} \text{ s}^{-1}$				ΔH^\ddagger kJ mol ⁻¹	$-\Delta S^\ddagger$ J K ⁻¹ mol ⁻¹	ΔG^\ddagger kJ mol ⁻¹	r
	T / K							
	298	303	308	313				
H	16.17	18.77	23.23	26.66	24.30	179.50	79.57	0.996
<i>p</i> -Me	16.24	18.94	23.65	27.06	26.17	172.32	79.23	0.997
<i>p</i> -OMe	16.37	19.23	24.32	28.88	27.50	167.78	79.17	0.997
<i>p</i> -F	16.08	18.70	22.16	25.87	22.21	185.64	79.39	0.999
<i>p</i> -Cl	15.70	18.12	21.40	24.83	21.36	188.69	79.48	0.999
<i>p</i> -Br	15.44	18.44	20.42	24.37	20.27	192.39	79.53	0.993
<i>p</i> -NO ₂	14.84	15.81	16.59	19.07	9.83	227.92	79.74	0.950

TABLE VI. Continued

R	$k_2 \times 10^2 / \text{dm}^3 \text{ mol}^{-1} \text{ s}^{-1}$				ΔH^\ddagger kJ mol ⁻¹	$-\Delta S^\ddagger$ J K ⁻¹ mol ⁻¹	ΔG^\ddagger kJ mol ⁻¹	r
	T / K							
	298	303	308	313				
<i>m</i> -F	15.80	16.50	18.54	20.71	16.83	200.37	73.53	0.973
<i>m</i> -Cl	15.58	16.20	18.44	20.35	11.86	220.77	79.86	0.970
<i>m</i> -Br	15.63	16.00	18.26	20.27	11.56	221.81	79.88	0.953
<i>m</i> -NO ₂	14.98	15.92	18.13	19.32	11.31	222.84	79.94	0.983

Mechanism and rate law

The kinetics of oxidation of nitrones by QCC was investigated in 50 % DMF–water in the absence of oxalic acid. The reaction was found to be first order with respect to both $c(\text{QCC})$ and $c(\text{nitrone})$. The reaction was catalysed by H^+ . The addition of the radical scavenger acrylonitrile had no effect on the rate. The observed salt and solvent effects shows that the rate determining step of did not involve ionic species. Due to the above reasons, the nitrone can be protonated before the rate determining step and it can then react with QCC in the slow step. A plausible mechanism is given below:



The rate law for the suggested mechanism is:

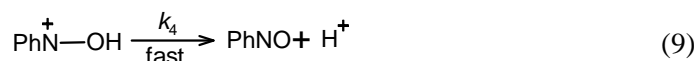
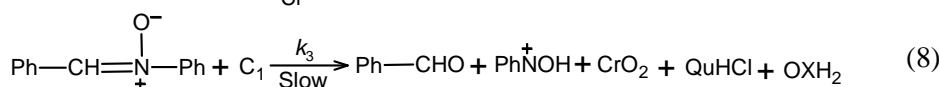
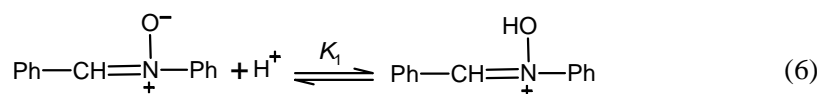
$$-\frac{dc(\text{QCC})}{dt} = \frac{K_1 k_2 c(\text{QCC})c(\text{S})c(\text{H}^+)}{1 + K_1 c(\text{H}^+)} \quad (4)$$

$$k_{\text{obs}} = \frac{K_1 k_2 c(\text{S})c(\text{H}^+)}{1 + K_1 c(\text{H}^+)} \quad (5)$$

where $c(\text{S}) = c(\text{nitrone})$.

Presence of oxalic acid

The increase in the oxidation rate with acidity suggests the participation of protonated nitrene prior to the rate-limiting step. No polymerisation of acrylonitrile was observed, indicating that free radicals were not involved in the reaction. The order with respect to $c(\text{substrate})$ and $c(\text{H}_2\text{C}_2\text{O}_4)$ was found to be unity. The following mechanism is proposed to explain the observations:



The rate law for the mechanism is:

$$-\frac{dc(\text{QCC})}{dt} = \frac{K_1 K_2 k_3 c(\text{QCC}) c(\text{S}) c(\text{H}^+) c(\text{H}_2\text{C}_2\text{O}_4)}{1 + K_1 c(\text{H}^+)} \quad (10)$$

$$k_{\text{obs}} = \frac{K_1 K_2 k_3 c(\text{S}) c(\text{H}^+) c(\text{H}_2\text{C}_2\text{O}_4)}{1 + K_1 c(\text{H}^+)} \quad (11)$$

where $c(\text{S}) = c(\text{nitrene})$.

Effect of substituents

The rate of oxidation of a number of *m*- and *p*-(α -phenyl)-substituted *N*, α -diphenylnitrenes was studied at different temperatures in the presence and absence of oxalic acid and the activation parameters were calculated (Tables V and VI). The electron releasing groups enhanced and the electron with-drawing groups retarded the oxidation rate. The log k_2 values were plotted against the σ values in a Hammett plot (Fig. 1). The small negative ρ values obtained indicate only a small structural influence on the rate. The negative ρ value (Table VII) was attributed to the development of a positively charged transition state. The entropies of activation were largely negative, as expected for bimolecular reactions.⁴¹ The variation in ΔH^\ddagger should be linearly related to the change in ΔS^\ddagger ($\Delta H^\ddagger = \Delta H_0^\ddagger + \beta \Delta S^\ddagger$).⁴² A plot of ΔH^\ddagger versus ΔS^\ddagger gave a straight line with a good correlation coefficient ($r = 0.994$, $\beta = 332$ K) in the absence of oxalic acid. The isokinetic temperature lies above the experimental temperature, showing thereby that these oxidations are enthalpy controlled and $\beta = 296$ K, $r = 0.990$, $SD = 0.07$ in the

presence of oxalic acid. The isokinetic temperature lies within the experimental temperature showing thereby that these oxidations are entropy controlled. If this linearity between enthalpies and entropies is true, it should predict a meaningful correlation between $\log k_2$ and σ .⁴³

$$\log k_2(T_2) = a + b \log k_2(T_1) \quad (12)$$

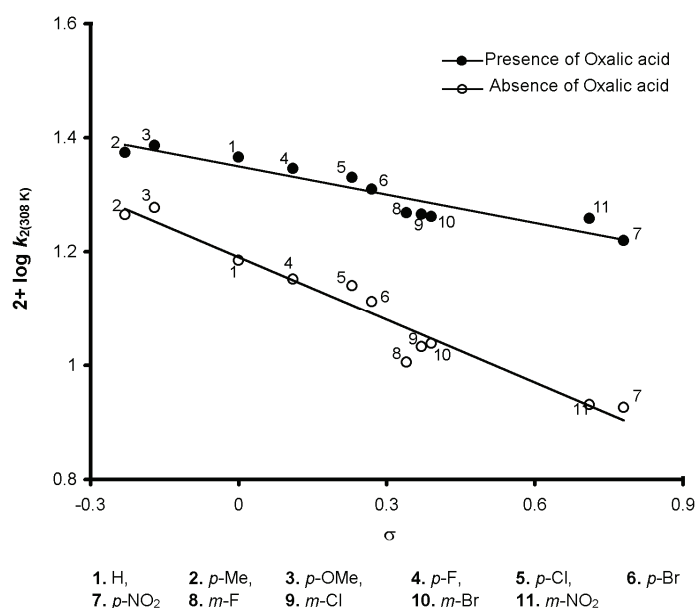


Fig. 1. Hammett plot of $(2 + \log k_2(308 \text{ K}))$ versus σ .

TABLE VII. Reaction constants for the oxidation of *N*, α -diphenylnitrones by QCC in the absence and presence of oxalic acid

<i>T</i> / K	Absence of oxalic acid			Presence of oxalic acid		
	Reaction constant (ρ^-)	<i>r</i>	<i>SD</i>	Reaction constant (ρ^-)	<i>r</i>	<i>SD</i>
298	—	—	—	0.041	0.966	0.03
303	0.441	0.940	0.05	0.096	0.900	0.01
308	0.361	0.974	0.03	0.161	0.950	0.02
313	0.333	0.980	0.02	0.195	0.944	0.02
318	0.356	0.984	0.02	—	—	—

Using Equation (12), a good correlation coefficient for QCC ($r = 0.980$) was obtained when $\log k_2(T_2)$ was plotted against $\log k_2(T_1)$ (Fig. 2).⁴⁴ This shows that the reaction under investigation follows a common mechanism. The ΔG^\ddagger values were almost constant for all the investigated substituted nitrones, which confirmed the operation of a common mechanism. Irregularity in the values of either ΔH^\ddagger or ΔS^\ddagger may be due to solute – solvent interactions, which could affect both ΔH^\ddagger and ΔS^\ddagger in a compensating manner. A negative value of entropy of ac-

tivation (ΔS^\ddagger) suggests the formation of an activated complex with a reduction in the degree of freedom of the reacting molecules.⁴⁵

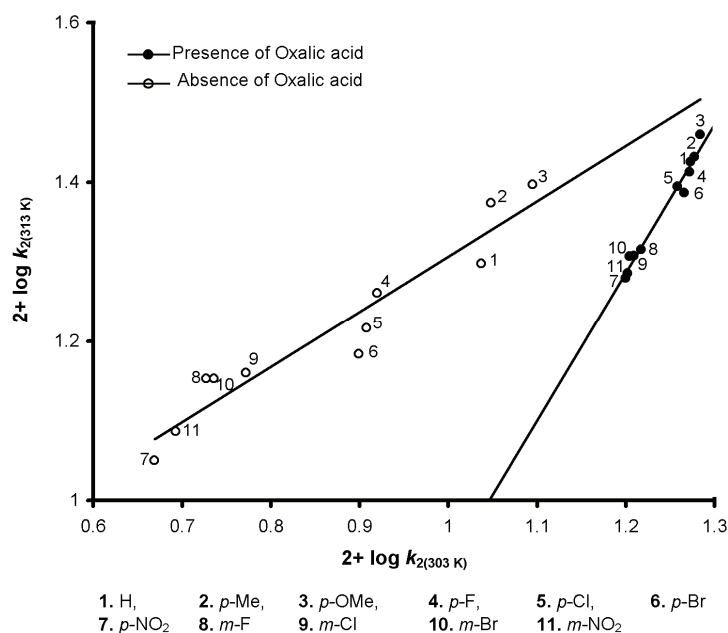


Fig. 2. Exner plot of $(2 + \log k_2(313\text{ K}))$ versus $(2 + \log k_2(303\text{ K}))$.

CONCLUSIONS

Based on the above facts, it is concluded that all the studied substituted nitrones follow the same mechanism when subjected to QCC oxidation in the presence and absence of oxalic acid under the conditions employed in the present study. The overall rate of reaction was greater in the presence than in the absence of oxalic acid.

ИЗВОД

КИНЕТИКА И МЕХАНИЗАМ ОКСИДАЦИЈЕ НЕКИХ СУБСТИТУИСАНИХ АЛДОНИТРОНА СА ХИНОЛИНИЈУМ-ХЛОРХРОМАТОМ У ПРИСУСТВУ И ОДСУСТВУ ОКСАЛНЕ КИСЕЛИНЕ У ВОДЕНИМ DMF СРЕДИНАМА

GOVINDASAMY RAJARAJAN¹, NATESAN JAYACHANDRAMANI², SUBRAMANIAN MANIVARMAN¹, JAYARAMAN JAYABHARATHI¹ и VENUGOPAL THANIKACHALAM¹

¹Department of Chemistry, Annamalai University, Annamalaiagar- 608 002, Tamil Nadu u ²Department of Chemistry, Pachaiyappa's College, Chennai- 600 030, India

Кинетика оксидације алдонитрона (нитрона) хинолинијум-хлорхроматом (QCC) је праћена у 50 % DMF у води у присуству и одсуству оксалне киселине. Испитивано је да ли оксална киселина има каталитички ефекат или је кооксиданс. Реакција је праћена јодометријски. Реакција је првог реда у односу на нитрон и оксалну киселину, а разломљеног реда у односу на H⁺. Није уочен пораст брзине реакције са порастом јонске јачине раствора, а

брзина опада са смањењем диелектричне константе раствора. Додатак $MnSO_4$ значајно утиче на брзину реакције, док додатак акрилонитрила нема утицаја. Предпостављен је механизам који укључује протонизацију нитрона и QCC као оксидационог средства. Израчунати су активациони параметри реакције.

(Примљено 31. децембра 2007, ревидирано 16. маја 2008)

REFERENCES

1. R. Iqbal, N. H. Rama, A. R. Ahmed, *J. Chem. Soc. Pakistan* **14** (1992) 118
2. R. Srinivasan, C. V. Ramesh, W. Madhulatha, K. Balasubramanian, *Indian J. Chem.* **35B** (1996) 480
3. J. Singh, G. L. Kad, S. Vig, M. Sharma, B. R. Chhabra, *Indian J. Chem.* **36B** (1997) 272
4. R. Gurumurthy, K. Karunakaran, *J. Indian Chem. Soc.* **72** (1995) 349
5. R. Gurumurthy, M. Gopalakrishnan, B. Karthikeyan, M. Selvaraju, *Asian J. Chem.* **10** (1998) 476
6. K. P. Elango, K. Karunakaran, *Asian J. Chem.* **7** (1995) 798
7. A. Jameel, J. Abdul, *J. Indian Chem. Soc.* **75** (1998) 439
8. B. Özgün, N. Değirmenbaşı, *Monatsh. Chem.* **135** (2004) 483
9. G. Karthikeyan, K. P. Elango, K. Karunakaran, A. Balasubramanian, *Oxid. Commun.* **21** (1998) 51
10. R. Gurumurthy, B. Karthikeyan, *Oriental J. Chem.* **14** (1998) 435
11. M. Pandeewara, B. John, D. S. Bhuvaneshwari, K. P. Elango, *J. Serb. Chem. Soc.* **70** (2005) 1
12. J. V. Singh, K. Mishra, A. Pandey, *Oxid. Commun.* **26** (2003) 235
13. J. V. Singh, K. Mishra, A. Pandey, *Oxid. Commun.* **26** (2003) 80
14. K. Mishra, J. V. Singh, A. Pandey, *Bull. Polish Acad. Sci.* **51** (2003) 25
15. K. Mishra, J. V. Singh, A. Pandey, *Bull. Polish Acad. Sci.* **51** (2003) 15
16. G. S. Chaubey, B. Kharsyntiew, M. K. Mahanti, *J. Phys. Org. Chem.* **17** (2003) 83
17. J. V. Singh, K. Mishra, A. Pandey, *Bull. Polish Acad. Sci.* **51** (2003) 35
18. G. Gopala Rao, C. R. Viswanathan, *Curr. Sci.* **11** (1942) 102; **12** (1943) 186; **13** (1944) 47
19. G. Vandergrift, J. Rocek, *J. Am. Chem. Soc.* **98** (1976) 1371
20. E. Hintz, J. Rocek, *J. Am. Chem. Soc.* **99** (1977) 132
21. M. Uma, M. Gopalakrishnan, J. Jayabharathi, V. Thanikachalam, *Indian J. Chem.* **34B** (1995) 612
22. M. Uma, M. Gopalakrishnan, J. Jayabharathi, V. Thanikachalam, *J. Indian Chem. Soc.* **73** (1996) 92
23. M. Gopalakrishnan, J. Jayabharathi, V. Thanikachalam, *Asian J. Chem.* **11** (1999) 1459
24. M. Gopalakrishnan, M. Uma, J. Jayabharathi, V. Thanikachalam, *Afinidad* **591** (2002) 688
25. M. Gopalakrishnan, J. Jayabharathi, M. Uma, V. Thanikachalam, *Oxid. Commun.* **30** (2007) 625
26. G. Rajajaran, N. Jayachandramani, S. Manivarman, J. Jayabharathi, V. Thanikachalam, *Trans. Met. Chem.* **33** (2008) 393
27. H. Staudinger, K. Niescher, *Helv. Chim. Acta* **2** (1919) 554
28. J. Singh, P. S. Kalsi, G. S. Jawanda, B. R. Chhabra, *Chem. Ind. (London)* (1986) 751
29. G. M. Bradley, H. L. Strauss, *J. Phys. Chem.* **79** (1975) 1953
30. G. Ramalingam, S. Jayanthi, *Trans. Met. Chem.* **32** (2007) 475
31. G. Mangalam, R. Gurumurthy, R. Arual, R. Karthikeyan, *Indian J. Chem.* **35B** (1995) 413

32. K. Nagarajan, S. Sundaram, N. Venkatesubramanian, *Indian J. Chem.* **18A** (1979) 335
33. J. F. Perez-Benito, C. Arias, D. Lamrhari, *J. Chem. Soc. Chem. Commun.* (1992) 472
34. C. F. Huber, G. P. Haight Jr., *J. Am. Chem. Soc.* **98** (1976) 4128
35. M. A. Olatunji, G. A. Ayoko, *Polyhedron* **7** (1988) 11
36. D. C. Gaswick, J. H. Krueger, *J. Am. Chem. Soc.* **91** (1969) 2240
37. Z. Khan, M. Y. Dar, P. S. S. Babe, *Indian J. Chem.* **42A** (2004) 1060
38. J. S. Litaler, W. A. Waters, *J. Chem. Soc.* (1959) 1299
39. (a) J. E. Quinland, E. A. Amis, *J. Am. Chem. Soc.* **77** (1955) 4187; (b) P. D. Sharma, Y. K. Gupta, *J. Chem. Soc. Dalton Trans.* (1972) 52
40. W. F. K. Wynne-Jones, H. Eyring, *J. Chem. Phys.* **3** (1935) 492
41. A. Frost, R. Pearson, *Kinetics and mechanism*, Wiley and Sons Inc., New York, 1961, p. 144
42. (a) N. R. Gilberston, G. A. Gallup, M. M. Jones, *Trans. Kansas Acad. Sci.* **57** (1954) 391; (b) J. E. Leffler, *J. Chem. Phys.* **23** (1955) 2199
43. J. March, *Advanced organic chemistry, reactions mechanisms and structure*, McGraw Hill Book Co., New York, 1968. p. 241
44. O. Exner, *Collect. Czech Chem. Commun.* **29** (1964) 1094
45. A. K. Singh, D. Chopra, S. Rahmani, B. Singh, *Carbohydr. Res.* **314** (1998) 157.



REVIEW

Hydrogen storage in complex metal hydrides

BORISLAV BOGDANOVIĆ*, MICHAEL FELDERHOFF and GUIDO STREUKENS

*Max-Planck-Institut für Kohlenforschung, Kaiser-Wilhelm-Platz 1,
45470 Mülheim a. d. Ruhr, Germany*

(Received 16 June, revised 16 October 2008)

Abstract: Complex metal hydrides such as sodium aluminohydride (NaAlH_4) and sodium borohydride (NaBH_4) are solid-state hydrogen-storage materials with high hydrogen capacities. They can be used in combination with fuel cells as a hydrogen source thus enabling longer operation times compared with classical metal hydrides. The most important point for a wide application of these materials is the reversibility under moderate technical conditions. At present, only NaAlH_4 has favourable thermodynamic properties and can be employed as a thermally reversible means of hydrogen storage. By contrast, NaBH_4 is a typical non-reversible complex metal hydride; it reacts with water to produce hydrogen.

Keywords: complex hydrides; sodium alanate; sodium aluminohydride; sodium borohydride; hydrogen storage.

CONTENTS

1. INTRODUCTION
2. SYNTHESIS OF COMPLEX METAL HYDRIDES
3. COMPLEX METAL ALUMINOHYDRIDES (ALANATES)
 - 3.1. Sodium aluminohydride
 - 3.2. Doping agents and methods
 - 3.2.1. State of titanium in doped NaAlH_4
 - 3.2.2. Mechanistic aspects of titanium doping
 - 3.3. Other alanates
 - 3.3.1. Lithium aluminohydride
 - 3.3.2. Potassium aluminohydride
 - 3.3.3. Magnesium aluminohydride
 - 3.3.4. Calcium aluminohydride
4. COMPLEX METAL BOROXYDRIDES
5. CONCLUDING REMARKS

* Corresponding author. E-mail: bogdanovic@mpi-muelheim.mpg.de
doi: 10.2298/JSC0902183B

1. INTRODUCTION

The proton exchange membrane fuel cell (PEMFC) is currently one of the most promising alternatives to internal-combustion engines on the way to zero-emission vehicles. Probably, the most crucial problem in the large-scale application of fuel cells for mobile applications is the onboard storage of hydrogen. Apart from the classical techniques, cryostorage in liquid form at $-254\text{ }^{\circ}\text{C}$ or gaseous storage under high pressure (desirable pressure: 70 MPa), chemical storage in solid-state absorbers is a well-investigated alternative. The most promising systems are the hydride complexes of borane ($\text{M}(\text{BH}_4)_n$) and alane ($\text{M}(\text{AlH}_4)_n$). The advantages of these so-called complex metal hydrides (also known as complex chemical hydrides) are their high storage capacities and rather mild decomposition temperatures and pressures.^{1–7}

The storage of hydrogen can be irreversible or reversible. Irreversible storage materials liberate the hydrogen by thermolysis or hydrolysis. Irreversible storage is problematic for mobile applications since the whole storage material must be exchanged for refuelling. By contrast, reversible storage materials can be refuelled with pressurized hydrogen. To comply with this requirement, these latter materials need to have an equilibrium pressure of around 0.1 MPa at ambient temperature and at least 0.5 MPa at $90\text{ }^{\circ}\text{C}$, which is the operating temperature of PEMFCs (targets set by the Department of Energy (DOE), USA). This restricts the flexibility of enthalpy changes for reversible storage materials. The entropy of the dehydrogenation reaction is dominated by that of gaseous hydrogen ($\approx 40\text{ kJ mol}^{-1}$), so the decomposition enthalpy of the material needs to be around 40 kJ per mol H_2 in order to result in a free enthalpy of zero at ambient temperature and pressure. An overview of the hydrogen contents of the known complex metal hydrides together with the hydrogen content of the reversible ones are given in Table I. The only complex hydrides with decomposition enthalpies approaching the required value, and are therefore reversible hydrogen storage materials, are NaAlH_4 and KAlH_4 . NaAlH_4 with a ΔH for the first decomposition step of 37 kJ

TABLE I. Hydrogenation properties of complex metal hydrides

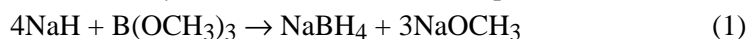
Hydride	Molecular weight g mol^{-1}	Hydrogen content wt. %	Reversibility	Reversible H_2 content, wt. %
LiBH_4	21.78	18.5	+	Unknown ⁵
NaBH_4	37.83	10.7	–	–
KBH_4	53.90	7.4	–	–
LiAlH_4	37.95	10.6	–	–
NaAlH_4	54.00	7.4	+	4.0–4.9 ⁶
KAlH_4	70.11	5.7	+	> 3.5 ⁷
$\text{Mg}(\text{AlH}_4)_2$	86.33	9.3	–	–
$\text{Ca}(\text{AlH}_4)_2$	102.01	7.8	–	–
$\text{LiMg}(\text{AlH}_4)_3$	124.28	9.7	–	–
Na_3AlH_6	102.00	5.9	+	2.1–2.3 ⁸
$\text{Na}_2\text{LiAlH}_6$	85.95	6.3	+	2.2–2.4 ⁸

mol⁻¹ is presently the most promising of the reversible complex hydrides for hydrogen storage. It has been widely studied during the last decade¹ and thus this contribution will have as its main focus recent developments concerning this material.

2. SYNTHESIS OF COMPLEX METAL HYDRIDES

The two commercially most important complex hydrides are NaBH₄ and LiAlH₄, both of which are used mainly as selective reducing agents in organic chemistry. For NaBH₄, over 100 methods of preparation have been described, but only two have reached practical significance.

In the Schlesinger process, trimethyl borate [B(OCH₃)₃] is boiled together with sodium hydride (NaH) in hydrocarbon oil at 250 °C, Eq. (1):



The addition of water hydrolyzes the NaOCH₃ to sodium hydroxide and methanol and causes the separation from the hydrocarbon oil. Methanol is recovered by distillation and recycled to form trimethyl borate. The NaBH₄ left in the sodium hydroxide solution is extracted with isopropyl amine.

The Bayer process employs the borosilicate Na₂B₄O₇·7SiO₂, which is produced by the fusion of borax and silica. The borosilicate is reacted with sodium in an atmosphere of 0.30 MPa of hydrogen at 400–500 °C. Extraction with liquid ammonia under pressure yields NaBH₄.

Sodium borohydride is the starting compound for the synthesis of all other borane-based complex hydrides. Ball-milling with lithium chloride or bromide leads to the formation of LiBH₄. The side product, *i.e.*, the corresponding sodium halide, is the thermodynamic driving force for the reaction. For the production of KBH₄, NaBH₄ is reacted with potassium hydroxide in an aqueous solution; again, the formation of side product, sodium hydroxide, is the driving force.

LiAlH₄ is industrially produced from lithium hydride (LiH) and aluminium trichloride (AlCl₃) in ether solution, Eq. (2):



Alternatively, it can be obtained metathetically from NaAlH₄ and LiCl by ball-milling. In addition, here, the formation of the side-product, sodium chloride, a thermodynamic sink, makes the procedure applicable to most of the other alanates.

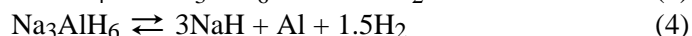
Sodium aluminohydride is usually synthesized from the elements at 100–200 °C and under 10–20 MPa of hydrogen pressure in a hydrocarbon solvent using triethyl aluminium as a catalyst.

3. COMPLEX METAL ALUMINOHYDRIDES (ALANATES)

3.1. Sodium aluminohydride

As mentioned above, sodium aluminohydride (NaAlH₄) is presently the most promising reversible complex hydride for hydrogen storage. It has a reversible

storage capacity of 5.5 wt.%, whereas its total hydrogen content amounts to 7.4 wt.%. Reversible thermal dissociation occurs in two steps *via* hexahydridoaluminate (Na_3AlH_6) as an intermediate to sodium hydride $[\text{NaH}]$ and aluminium, Eqs. (3) and (4).



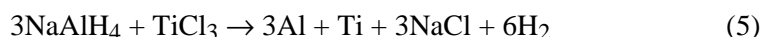
Both steps are reversible, while a third possible step, the decomposition of NaH , is possible only at much higher temperatures.

Doped sodium alanate exhibits in the first dissociation step an equilibrium pressure of 0.10 MPa at $\approx 36^\circ\text{C}$ (37 kJ/mol) and in the second at $\approx 116^\circ\text{C}$ (47 kJ/mol). Thus, NaAlH_4 is a typical low-temperature hydride, whereas Na_3AlH_6 is classified as mid-temperature hydride.^{8,9}

Although NaAlH_4 is the only known alanate with reasonable thermodynamics for use in combination with PEMFCs, it was not considered as a potential hydrogen storage material for a long time. The reported conditions for the rehydrogenation (200–400 $^\circ\text{C}$, 10–40 MPa) were simply too severe, while the kinetics were far too slow. This situation changed in 1997 with the discovery of Bogdanović and Schwickardi^{8,9} that doping NaAlH_4 with small amounts of titanium allowed rehydrogenation of the material under much milder conditions (see below). This initiated an intensive research of the material and especially the search for more efficient dopants or doping methods.

3.2. Doping agents and methods

Nowadays, titanium trichloride (TiCl_3) is generally the standard doping agent for NaAlH_4 and high-energy ball-milling, introduced in 1999, appears to be the prevalent method.¹⁰ The doping of NaAlH_4 with TiCl_3 is expressed by Eq. (5):



Titanium and aluminium are both reduced to the zero-valent state by the hydride species, which results in irreversible hydrogen evolution. For this reason, apart from the additional dead weight of the dopant, the theoretical capacity of 5.5 wt.% cannot be attained with doped samples. Therefore, the optimum doping amount is always a compromise. The more dopant that is added, the higher are the kinetic rates, but the lower is the capacity. Usually, doping levels of 2–4 mol% are considered as reasonable.

The beneficial effect of titanium on the desorption rates of alanates had been known for a long time, *i.e.*, for LiAlH_4 , but research on alternative doping materials or methods was almost non-existent. Screening of different elements as doping agents commenced only after the disclosure of the efficacy of titanium. The most investigated alternative dopants were iron and zirconium. For a long time, titanium seemed to be the most favourable doping element, as regards kine-

tics and storage capacities, so research focused mainly on different titanium precursors and doping procedures.^{11,12} In the original work, a wet chemical method was adopted and employed titanium butoxide in THF solution but today high-energy ball-milling has been demonstrated to be the more convenient preparation route and also to deliver materials with more favourable properties. For instance, the kinetic rates of NaAlH₄ doped with TiCl₃ by ball-milling are about one order of magnitude higher than those of NaAlH₄ wet chemically doped with Ti butoxide.

Therefore, apart from the doping procedure, also the nature of the titanium precursor is important for the performance of the material. Titanium halides show more favourable kinetic behaviours than those of titanium alkoxides. Titanium trifluoride shows the highest storage capacities of these halides, since the added dead weight is the lowest but, for cost reasons, titanium trichloride has emerged as the standard material. Since the use of cationic titanium sources incurs the problem that reduction to the zero valent state consumes hydrogen, which decreases the storage capacity drastically, Ti sources have been investigated. Ti₁₃ clusters, stabilized by THF, are the most prominent candidates;¹³ NaAlH₄ doped with these clusters has indeed a very high capacity and, more interestingly, extremely fast kinetics. Unfortunately, the rates decrease drastically after about five cycles and then the materials do not show any superior properties over TiCl₃-doped materials. In addition, the high costs of the clusters disqualify them for large-scale applications.

According to recent results compounds of elements other than titanium have shown good prospects as doping agents; ScCl₃ and CeCl₃ are prime examples.¹⁴ Sodium aluminohydride doped with scandium (Fig. 1) has higher kinetic rates than the titanium-doped equivalent, and also provides higher storage capacities (4.0–4.9 wt.%).

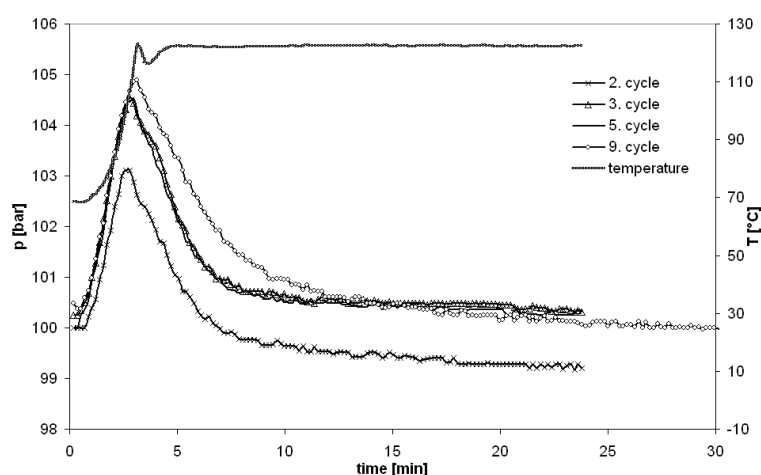


Fig. 1. Hydrogenation curves of a Sc-doped NaAlH₄ cycle test (10 MPa, 120 °C).¹⁴

With sodium aluminohydride doped with scandium (4 mol%), hydrogenations are accomplished in 4–12 min.¹⁴ The thus attained hydrogenation times approach those required for the refuelling of the future hydrogen powered fuel cell cars of 3 min. In order to check the cycle stability of the Ce-doped material, a sample (2.1 g) was tested in a 95 cycles test at 60–150 °C and 5–10 MPa (Fig. 2) and proved to be stable during this treatment. It should, however, be pointed out that removal of the hydrogenation heat by cooling in such a short time represents a tremendous technical challenge.¹⁵ In any event, both materials (Sc- and Ce-doped NaAlH₄) are extremely more expensive than titanium, hence, most probably, they will not be employed in industrial-scale applications. Accordingly, in most of the studies, TiCl₃ remains the standard doping agent.

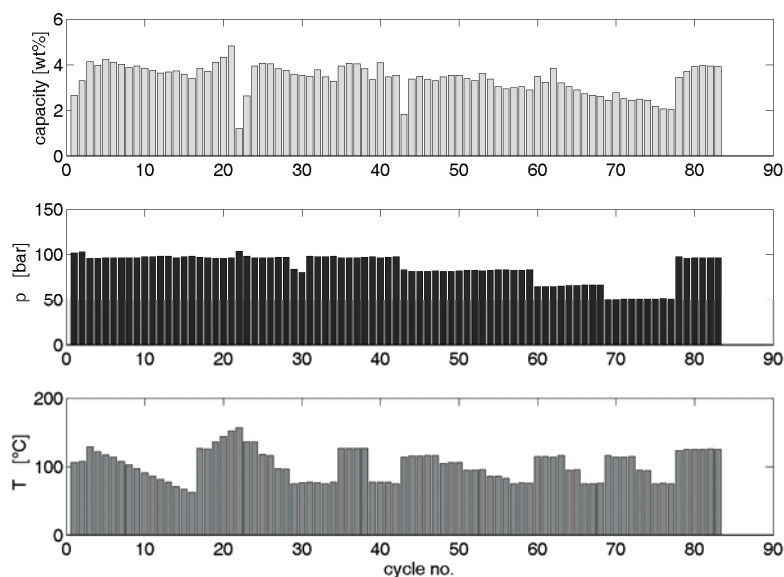


Fig. 2. Course of a 83-cycle test of Ce-doped NaAlH₄.¹⁴

3.2.1. State of titanium in doped NaAlH₄

The exact nature of titanium and its catalytic properties in the Ti–NaAlH₄ system are still not fully understood. It is even unclear whether Ti acts as a true catalyst. Nevertheless, many facts have been clarified that help to compose a clear picture of the system.

Measurements of the hydrogen evolved during ball-milling of several dopants with sodium alanate show clearly that the dopants are reduced to the zero-valent state, as formulated in Eq. (5). This finding is supported by several XRD and XAS studies. Similar studies with stoichiometric mixtures of LiAlH₄ with TiCl₃ and TiCl₄ demonstrated the formation of Ti–Al alloys. Although these alloys could not be clearly identified for NaAlH₄ reacted with TiCl₃ in sub-stoi-

chiometric amounts, some supporting evidence exists. The aluminium reflection in XRD patterns of dehydrogenated Ti-doped NaAlH_4 samples show a slight shoulder, which suggests the existence of an Al_3Ti alloy. In addition, if the remaining NaAlH_4 is leached out after ball-milling with THF and the remaining solid is treated at elevated temperatures, Al_3Ti can be detected by XRD analysis. This result corresponds to the findings from XAS experiments. Analysis of the XANES and EXAFS region of the spectra suggests an Al_3Ti -like local environment of titanium in freshly ball-milled, dehydrogenated and hydrogenated samples.^{16–18} Thus, even if an Al–Ti alloy is not formed during the doping process, probably on account of too low a temperature, there is substantial information to indicate that the titanium is reduced and dispersed into the aluminium phase and does not affect the alanate lattice. Such behaviour is also supported by XRD measurements, the NaAlH_4 lattice parameters remain exactly the same for doped and undoped materials. Additionally, TEM–EDX measurements confirm that titanium is only associated with the aluminium phase in the dehydrogenated material – hydrogenated materials would be decomposed by the electron beam and therefore cannot be evaluated by TEM. In summary, it can be concluded that titanium is reduced to the zero-valent state during doping and is dispersed in the aluminium phase. This ‘solid solution’ is a separate phase from the NaAlH_4 lattice, which is thereby unaffected by the presence of titanium.

3.2.2. Mechanistic aspects of titanium doping

Although the location of the titanium and its oxidation state in the system has been investigated very thoroughly, the mechanism of the facilitated hydrogen uptake and release has yet to be fully elucidated. The first problem in understanding the processes occurring is the spatial distance between the active species, the Ti–Al solid solution and the hydrogen-storage material (NaAlH_4). Transmission electron micrographs (TEM) of dehydrogenated samples show micrometer-sized aluminium particles decorated with NaH crystallites (Fig. 3). Since a

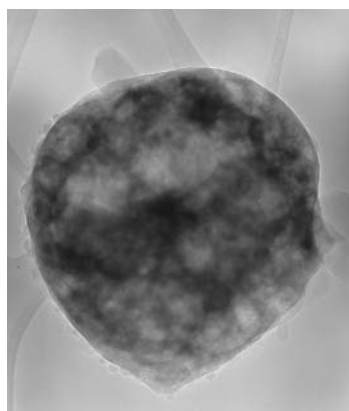


Fig. 3. TEM Microphotograph of decomposed titanium-doped sodium alanate.

complete hydrogenation of the sample takes about 5 min in optimized samples, mass transfer of sodium and/or aluminium must occur over micrometer distances during the same period of time.

Transportation *via* mobile AlH_3 was proposed as another possible explanation for the enhanced transfer rates. Indeed, inelastic neutron scattering spectroscopy experiments have shown that a volatile molecular aluminium hydride is formed during the early stage of hydrogen uptake by dehydrogenated titanium-doped NaAlH_4 .¹⁹

3.3. Other alanates

3.3.1. Lithium aluminohydride

Lithium aluminohydride (LiAlH_4), which has been studied extensively as a selective hydriding agent in organic chemistry, is an irreversible hydrogen storage material. This, together with the high cost of lithium, disqualifies the material for large-scale storage applications despite the fact that its theoretical capacity of 7.9 wt.% over the first two decomposition steps is extraordinarily high.

The alanate is thermodynamically unstable and decomposes below room temperature. The decomposition of LiAlH_4 is kinetically hindered, however, so that it is metastable at room temperature, even when ball-milled.²⁰ Interestingly, ball-milling with titanium compounds leads to a partial release of hydrogen during the doping procedure itself. This implies that the catalytic effect of titanium on the decomposition of alanates is restricted not only to NaAlH_4 but seems to be a more general phenomenon. It is deduced, therefore, that titanium acts predominantly on the $(\text{AlH}_4)^-$ or $(\text{AlH}_6)^{3-}$ species.

3.3.2. Potassium aluminohydride

Like NaAlH_4 , potassium aluminohydride (KAlH_4) is a reversible hydrogen-storage material.⁷ It even takes up and releases hydrogen without any aid of an external catalyst. This is significantly different from the reaction mechanism of NaAlH_4 or LiAlH_4 . Nevertheless, the decomposition proceeds *via* the same pathway. The hexahydride (K_3AlH_6) is formed in the first decomposition step, which further decomposes to KH and finally to potassium metal. As with the NaAlH_4 system, the last step is not reversible. The theoretical storage capacity over the first two decomposition steps of KAlH_4 amounts to 4.3 wt.%, which is only 77 % of the value for NaAlH_4 .

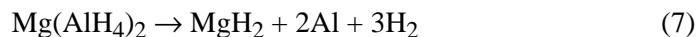
The conditions for the dehydrogenation and rehydrogenation reactions also differ significantly from NaAlH_4 . The hydrogen pressures for both steps are lower than 1 MPa, which makes the system easier to handle, but the required temperatures are in the range of 300–350 °C. A possible lowering of these temperatures by the addition of catalysts has not been reported.

3.3.3. Magnesium aluminohydride

Magnesium alanate can be easily prepared by a metathesis reaction starting from MgCl_2 and two moles of NaAlH_4 :²¹



The reaction can be performed in the solid state through ball-milling or in ether solution as a wet chemical reaction. In the latter case, etherates are the final products, which decompose at elevated temperatures under vacuum to the complex hydride. Magnesium alanate is a complex metal hydride with a high hydrogen content (7.0 wt.%) for the decomposition reaction expressed by Eq. (7):

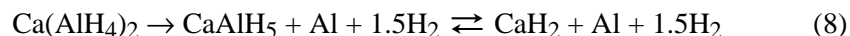


At temperatures around 130 °C, three moles of hydrogen are released in a one-step mechanism.

Compared with the alkaline alanates LiAlH_4 , NaAlH_4 and KAlH_4 , no hexahydride intermediate can be observed. The final products of the thermal decomposition are MgH_2 and aluminium metal. The decomposition enthalpy of $\text{Mg}(\text{AlH}_4)_2$ is around 0 kJ mol⁻¹, which means that the equilibrium pressure of $\text{Mg}(\text{AlH}_4)_2$ is extremely high (calculated from the Van't Hoff equation). This alanate is therefore too unstable for reversible de- and re-hydrogenation reactions and cannot be used under technical conditions in combination with a PEMFC.

3.3.4. Calcium aluminohydride

The metathesis reaction between CaCl_2 and two moles of NaAlH_4 can be employed for the preparation of calcium alanate, $\text{Ca}(\text{AlH}_4)_2$. Ball-milling produces the alanate in combination with NaCl as a by-product. Wet-chemical preparation in ether solution produces the etherate product, which decomposes at elevated temperatures under vacuum to the pure alanate.²² Three moles of hydrogen are released during the first two decomposition steps according to Eq. (8):



During both decomposition steps, 1.5 moles of hydrogen are released. The intermediate product CaAlH_5 has an octahedral structure, which is interconnected over two corners producing long chains (see Fig. 4).²³ From thermodynamic measurements, it has been shown that the first decomposition step of $\text{Ca}(\text{AlH}_4)_2$ is exothermic and cannot be used in reversible re- and de-hydrogenation reactions. The second step is endothermic and, in principle, is reversible under acceptable technical conditions.

4. COMPLEX METAL BOROHYDRIDES

Complex metal borohydrides,²⁴ of which the most commonly used is NaBH_4 , are materials with a high hydrogen content (10.8 wt.% for NaBH_4 , see Table 1),

but they mainly show unfavourable thermodynamics and can, therefore, not be used as reversible hydrogen-storage materials. The thermal decomposition reaction is different compared to the complex metal aluminohydrides and no hexahydride intermediate product has been observed. The final products of the decomposition are a binary metal hydride and elemental boron metal, Eq. (9):

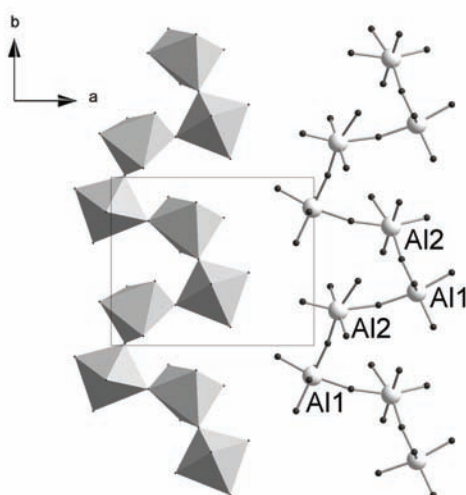
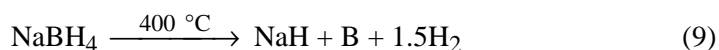


Fig. 4. Crystal structure of interconnected octahedral AlH_6 units in CaAlH_5 .

The thermal decomposition temperature of NaBH_4 is around $400\text{ }^\circ\text{C}$, *i.e.*, much too high for PEMFC applications. Traces of boron hydrogen compounds (B_xH_y) produced during the thermal decomposition are problematic because they can poison the fuel cell catalyst and also damage the membrane. Therefore, complex borohydrides are used for the production of hydrogen *via* a hydrolysis reaction with water.²⁵ In the presence of a ruthenium catalyst, dissolved NaBH_4 decomposes into hydrogen with the production of sodium metaborate, NaBO_2 , as the final product. Half of the evolved hydrogen comes from the water and thus increases the storage capacity of the system (Eq. (10)). In principle, only two moles of water are required for a complete decomposition of NaBH_4 but, in practice, the solubilities of NaBH_4 and, more importantly, of NaBO_2 are the limiting factors of the storage capacity. Sodium metaborate has a solubility of only 26 g per 100 ml in water at $20\text{ }^\circ\text{C}$. To prevent precipitation from the solution and the blocking of the active sites of the catalyst, the NaBH_4 concentration must be lower than the maximum solubility of the metaborate. A typical composition of a commercial NaBH_4 aqueous solution is 20 wt.% NaBH_4 and 1 wt.% NaOH for stabilization of the solution. This reduces the storage capacity to 4 wt.% for the whole hydride system.



The operation of a commercial NaBH₄ solution and PEMFC system is shown schematically in Fig. 5. The NaBH₄ solution is stored in a tank and converted into hydrogen when required in the catalyst chamber. The amount of hydrogen produced can be controlled by the flow of the fuel solution into the catalyst chamber. The hydrogen gas and the decomposition product (NaBO₂) are separated in the gas–liquid separator. After separation from the sodium metaborate by-product, which is stored in a second fuel tank, the hydrogen is fully humidified and can be used for the production of energy in the fuel cell. The amount of hydrogen depends on the quantity of NaBH₄ solution that is pumped into the catalyst chamber and on the electric power demanded from the fuel cell.

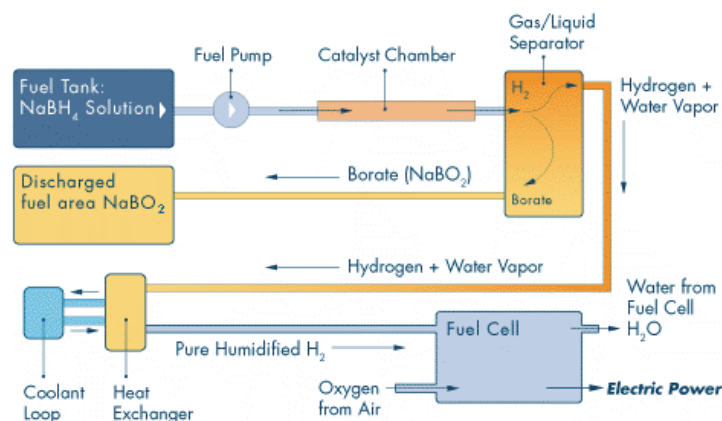


Fig. 5. Operating scheme of a commercial NaBH₄–PEMFC system (Millennium-Cell).

Significant barriers for a broad introduction of NaBH₄ as a hydrogen-releasing material are the high price for the desorbed hydrogen and the regeneration of the hydride from the metaborate solution outside the fuel cell system. Different methods have been described in the literature but several technical points have still to be resolved. Nevertheless, the storage in, and release of hydrogen from, NaBH₄ solutions is interesting for a wide range of applications.

One other borohydride with a high hydrogen content is LiBH₄, which has a capacity of more than 18 wt.% H₂.²⁶ Again, the decomposition temperature (≈ 380 °C) is too high for usage with a PEMFC and the material is not reversible under acceptable practical conditions. With the addition of a second material to the lithium borohydride, the decomposition pathway may be changed together with the thermodynamics of the system (thermodynamic tailoring).



A reaction mixture of two moles LiBH₄ and one mole MgH₂, Eq. (11), has a theoretical hydrogen storage capacity of 11.4 wt.%. This is lower than that for

pure LiBH_4 but the decomposed mixture can be re-hydrogenated at temperatures of 230–250 °C under a hydrogen pressure of 10 MPa. Unlike LiBH_4 , where elementary boron is the final product of the decomposition, the final product of the LiBH_4 – MgH_2 mixture is magnesium boride MgB_2 . This different reaction pathway stabilizes the right side of the reaction, which means that the left side is destabilized and the reaction becomes reversible. It has been shown that such a mixture could reversibly store up to 8 wt.% of hydrogen.²⁷ The hydrogenation conditions are far removed from technical requirements, but these experiments show that thermodynamic properties can be changed by the addition of a second component to the complex metal hydride.

5. CONCLUDING REMARKS

The advances in the research on complex metal hydrides for hydrogen storage over the last couple of years are remarkable. The properties of some systems are approaching the requirements for large-scale applications, set as targets by the DOE (Department of Energy).

Today, doped NaAlH_4 is still the most promising material to meet most of these targets. It decomposes sufficiently quickly to provide adequate hydrogen during all operation states of the fuel cell, which include peak power demand. The temperature required for the decomposition rates is low enough to be provided for by the waste heat of the fuel cell. In addition, the kinetics for the refueling meets the DOE-targets; re-hydrogenation times of less than five minutes have been measured for optimized systems. Additionally, the cycle stability of doped NaAlH_4 is high – no changes in performance and capacity could be observed in over 100 measured cycles.

Considering the rate of progress over recent years, a further increase of the limits is to be expected. It must be recognized, however, that the theoretical limits cannot be shifted. The theoretical hydrogen storage capacity of 5.5 wt.% is definitely considered by various organizations and industrial companies to be too low for large-scale applications. In addition, the requirements for cooling during refuelling due to the thermodynamics of the re-hydrogenation are too severe. Therefore, realistically, even NaAlH_4 , which is presently the most promising candidate material, will not meet all the criteria necessary to provide a practical means of hydrogen storage. For reversible storage capacities over 5 wt. %, other options will have to be explored.

ИЗВОД

СКЛАДИШТЕЊЕ ВОДНИКА У КОМПЛЕКСНИМ МЕТАЛНИМ ХИДРИДИМА

БОРИСЛАВ БОГДАНОВИЋ, MICHAEL FELDERHOFF и GUIDO STREUKENS

Max-Planck-Institut für Kohlenforschung, Kaiser-Wilhelm-Platz 1, 45470 Mülheim a. d. Ruhr, Germany

Комплексни метални хидриди, као што су натријум-алуминијум-хидрид (NaAlH_4) и натријум-бор-хидрид (NaBH_4), су чврсти материјали за складиштење водоника са високим капацитетом. Они се могу користити у комбинацији са горивим спрегивима као извор водоника, чиме се обезбеђује дужи рад него са класичним металним хидридима. За широку примену ових материјала најважнија је реверзибилност у умереним условима коришћења. За сада једино NaAlH_4 има задовољавајуће термодинамичке особине и може се применити као термодинамички реверзибилан вид складиштења водоника. Насупрот њему, NaBH_4 је типичан иреверзибилни комплексни метални хидрид; он реагује са водом и производи водоник.

(Примљено 16. јуна, ревидирано 16. октобра 2008)

REFERENCES

1. F. Schüth, B. Bogdanović, M. Felderhoff, *Chem. Commun.* (2004) 2249
2. M. Fichtner, *Ann. Chim.* **30** (2005) 483
3. B. Bogdanović, G. Sandrock, *MRS Bulletin* (2002) 712
4. W. Grochala, P. P. Edwards, *Chem. Rev.* **104** (2004) 1283
5. Y. Nakamori, G. Kitahara, G. Miwa, N. Ohba, S. Towata, A. Züttel, S. Orimo, *J. Alloys Compd.* **404–406** (2005) 396
6. B. Bogdanović, M. Felderhoff, A. Pommerin, F. Schüth, N. Spielkamp, *Adv. Mater.* **18** (2006) 1198
7. H. Morioka, K. Kakizaki, S. Ch. Chung, A. Yamada, *J. Alloys Compd.* **353** (2003) 310
8. B. Bogdanović, M. Schwickardi, *J. Alloys Compd.* **253–254** (1997) 1
9. B. Bogdanović, R. A. Brand, A. Marjanović, M. Schwickardi, J. Tölle, *J. Alloys Compd.* **302** (2000) 36
10. A. Zaluska, I. Zaluski, J. O. Ström-Olsen, *J. Alloys Compd.* **298** (2000) 125
11. R. A. Zidan, S. Takara, A. G. Hee, G. M. Jensen, *J. Alloys Compd.* **285** (1999) 119
12. C. M. Jensen, K. J. Gross, *Appl. Phys. A* **72** (2001) 213
13. R. Franke, J. Rothe, J. Pollmann, J. Hormes, H. Boennemann, W. Brijoux, Th. Hindenburg, *J. Am. Chem. Soc.* **118** (1996) 12090
14. B. Bogdanović, M. Felderhoff, A. Pommerin, F. Schüth, N. Spielkamp, A. Stark, *J. Alloys Compd.* (2008), doi:10.1016/j.jallcom.2008.03.106
15. M. Felderhoff, C. Weidenthaler, R. von Helmholt, U. Eberle, *Phys. Chem. Chem. Phys.* **9** (2007) 2643
16. M. Felderhoff, K. Klementiev, W. Grünert, B. Spliethoff, B. Tesche, J. M. Bellosta von Colbe, B. Bogdanović, M. Härtel, A. Pommerin, F. Schüth, C. Weidenthaler, *Phys. Chem. Chem. Phys.* **6** (2004) 4369
17. J. Graetz, J. J. Reilly, J. Johnson, A. Yu Ignatov, T. A. Tyson, *Appl. Phys. Lett.* **85** (2004) 500
18. A. Léon, O. Kircher, J. Rothe, M. Fichtner, *J. Phys. Chem. B* **108** (2004) 16372
19. Q. J. Fu, A. J. Ramirez-Cuesta, S. C. Tsang, *J. Phys. Chem. B* **110** (2006) 711
20. H. W. Brinks, B. C. Hauback, P. Norby, H. Fjellvåg, *J. Alloys Compd.* **351** (2003) 222
21. M. Mamatha, B. Bogdanović, M. Felderhoff, A. Pommerin, W. Schmidt, F. Schüth, C. Weidenthaler, *J. Alloys Compd.* **407** (2006) 76

22. M. Fichtner, C. Frommen, O. Fuhr, *Inorg. Chem.* **44** (2005) 3479
23. C. Weidenthaler, T. J. Frankcombe, M. Felderhoff, *Inorg. Chem.* **45** (2006) 3849
24. L. Laversenne, B. Bonnetot, *Ann. Chim.* **30** (2005) 495
25. S. C. Amendola, S. L. Sharp-Goldmann, M. S. Janjua, N. C. Spencer, M. T. Kelly, P. J. Petillo, M. Binder, *Int. J. Hydrogen Energy* **25** (2000) 969
26. A. Züttel, P. Wenger, S. Rentsch, P. Sudan, P. Mauron, C. Emmenegger, *J. Power Sources* **118** (2003) 1
27. J. J. Vajo, S. L. Skeith, F. Mertens, *J. Phys. Chem. B* **109** (2005) 3719.



J. Serb. Chem. Soc. 74 (2) 197–202 (2009)
JSCS–3822

SHORT COMMUNICATION

Mapping the concentration changes during the dynamic processes of crevice corrosion by digital holographic reconstruction

HENGLEI JIA¹, SHENHAO CHEN^{1,4*}, BOYU YUAN², CHAO WANG^{3,4} and LIANG LI³

¹Department of Chemistry, Shandong University, Jinan 250100, ²Department of Physics, Xuzhou Normal University, Xuzhou 221116, ³Department of Chemistry, Xuzhou Normal University, Xuzhou 221116 and ⁴State Key Laboratory for Corrosion and Protection, Shenyang 110016, P. R. China

(Received 7 July, revised 27 August 2008)

Abstract: The dynamic process of crevice corrosion during anodic dissolution of a crevice electrode in a 5.0 mmol dm⁻³ NaCl solution has been studied by digital holographic reconstruction. Digital holographic reconstruction has been proved to be an effective and *in situ* technique to detect the changes in the solution concentration because useful and direct information can be obtained from the three-dimensional images. It provides a valuable method for a better understanding of the mechanism of crevice corrosion by studying the dynamic processes of changes in the solution concentration at the interface of crevice corrosion.

Keywords: digital holography; crevice corrosion; numerical reconstruction; phase difference; concentration change.

INTRODUCTION

Crevice corrosion is a common and dangerous type of localized corrosion, which occurs within crevices or other occlusive areas on metal surfaces exposed to a corrosive environment. A crevice can be formed between metallic parts or a non-metallic part and a metallic part. For certain corrosive environments, especially in NaCl solution, crevice corrosion could be fatal to the metal.^{1–3}

Various experimental techniques and mathematical models have been presented to study crevice corrosion in the past few decades.^{4–8} Digital holography has been proved to be a versatile and rapid technique to detect concentration changes in a solution because of its non-contact, non-breakage and high precision. It has also been successfully applied in chemistry,⁹ biology^{10,11} and other

* Corresponding author. E-mail: shchen@sdu.edu.cn
doi: 10.2298/JSC0902197J

fields. In our laboratory, experiments were performed by digital holography to study dynamic electrochemical processes.

The principle of the experiments were based on the relationship between the phase of an object wave ($\Delta\phi$), the refractive index of the solution (Δn) and solution concentration (Δc), which was formulated as:¹²

$$\Delta c = k_1 \Delta n = (k_1 \lambda_0 / 2\pi d) \Delta \phi \quad (1)$$

Thus, measurement of the concentration change can be transformed into measurement of the phase difference. In the present study, the phase difference was recorded on and stored in a computer in the form of holograms. After numerical reconstruction by the Fourier analysis method, the holograms were transformed into three-dimensional images. Details about numerical reconstruction can be found in literature.^{12,13} In this study, numerical reconstruction was used to study the process of crevice corrosion.

EXPERIMENTAL

Electrochemical system

The electrochemical cell consisted of a three-electrode system. A carbon steel electrode (0.17 % C, 1.18 % Mn, 0.008 % P, 0.008 % S, 0.04 % Cr, 0.04 % Mo, 0.27 % Si), 1.6 mm × 3.7 mm in size, with a central 0.1 mm wide crevice was used as the working electrode. The electrode was carefully sealed in a glass tube with a thin layer of epoxy resin, leaving only the surface area with the crevice exposed to the solution. The crevice was positioned parallel to the laser. A large sheet of platinum was used as the counter electrode. The reference electrode was a saturated calomel electrode (SCE) with a Luggin capillary tip set 2 mm from the working electrode surface. All potentials in the experiments were measured with respect to the SCE. The electrolyte was a 5.0 mmol dm⁻³ NaCl solution. The *I-t* curve measurement was performed using a CHI660B electrochemical station. All experiments were performed at room temperature.

Holography recording system

The experimental setup of the in-line holographic recording system, which was described earlier,⁹ is shown in Fig. 1. The video signals were captured and stored in the computer. The

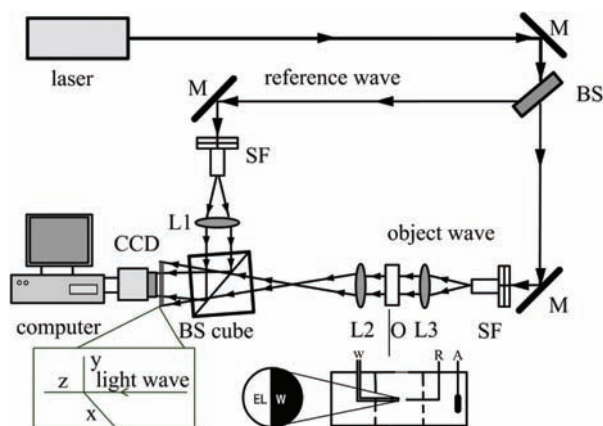


Fig. 1. Experimental setup of the in-line holographic recording system. M – mirror; BS – beam-splitter; SF – spatial filter; L1, L2 and L3 – lenses; O – object; BS Cube – beam-splitter cube; W – working electrode; R – reference electrode; A – counter electrode; EL – electrolyte.

holograms were processed by the reconstruction algorithm and the information was transformed into three-dimensional images.

RESULTS AND DISCUSSION

The $j-t$ curve of the crevice electrode in 5.0 mmol dm^{-3} NaCl solution at 0.20 V is illustrated in Fig. 2. The distribution of the phase difference in comparison with the starting time during the reaction corresponding to the points a–g in Fig. 2 are shown in Figs. 3a–3g, respectively. As shown in the images, the left sides are the solution parts and the right sides are the electrode parts, between which are the interfaces obtained by the edge detection algorithm. The color variation reflects the change of the concentration. A green area indicates that the phase difference, *i.e.*, concentration change, is zero or almost zero, while the yellow and red areas indicate that the phase differences are positive with the concentration changes increasing from yellow to red. The value of Z (phase difference) reflects how much the phase has changed. The larger is the value of Z (phase difference), the more evident are the color changes, that is to say, the more severely the concentration changes.

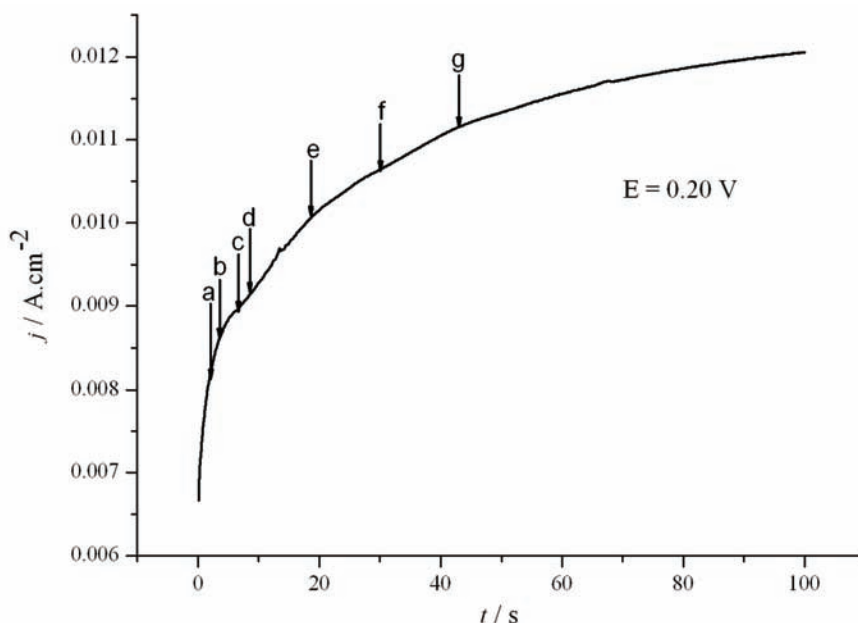


Fig. 2. The $j-t$ curve of the crevice electrode in 5.0 mmol dm^{-3} NaCl solution, with the electrode potential controlled at 0.20 V .

Figure 3a shows the distribution of the phase difference at 2 s , in which a change at the interface can hardly be seen. With increasing time, the appearance of a yellow area in Fig. 3b at a time of 4 s indicates that the concentration had increased. This change can be clearly seen in Fig. 3c at 6 s . It can also be observed

from Fig. 3c that the change of the concentration at the interface was not uniform and the concentration change at the crevice mouth is most obvious. This pheno-

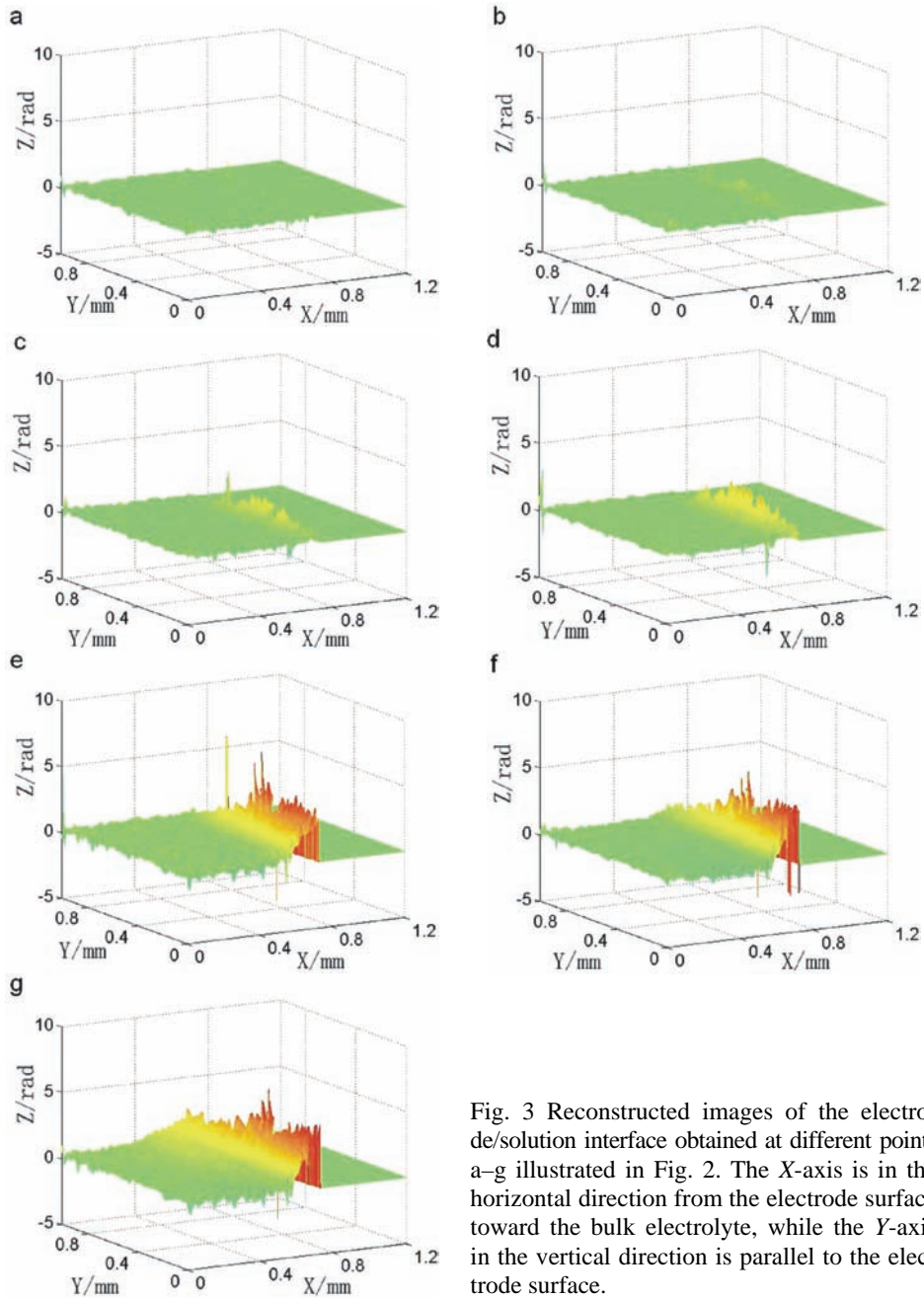


Fig. 3 Reconstructed images of the electrode/solution interface obtained at different points a–g illustrated in Fig. 2. The X -axis is in the horizontal direction from the electrode surface toward the bulk electrolyte, while the Y -axis in the vertical direction is parallel to the electrode surface.

menon becomes more visible in Fig. 3d at 8 s, with the first appearance of a red area at the crevice mouth, which indicates that phase difference or concentration continued increasing. The red area in Figs. 3e, 3f and 3g are very evident. This proves that many more ions had been produced in the crevice and transported out. Metal ions produced in the crevice moved to the bottom of the electrode because of gravity, which is in accordance with the red areas in Figs. 3e, 3f and 3g.

CONCLUSIONS

Digital holographic reconstruction was employed to study the change of the concentration at the interface of crevice corrosion. The reconstructed images provide visual results, from which more useful information about the change of concentration at the interface can be obtained. The results show that the changes of concentration at the interface are not uniform and that the concentration increase at the crevice mouth was the most obvious. The reconstructed images supply more visual information for a better analyzes and understanding of the dynamic processes of solution concentration change.

Acknowledgement. The authors thank the Special Funds for the Major State Basic Research Projects (No. 2006CB605004).

ИЗВОД

МАПИРАЊЕ ПРОМЕНЕ КОНЦЕНТРАЦИЈЕ ТОКОМ ДИНАМИЧКОГ ПРОЦЕСА КОРОЗИЈЕ У ПУКОТИНАМА КОРИШЋЕЊЕМ ДИГИТАЛНЕ ХОЛОГРАФСKE РЕКОНСТРУКЦИЈЕ

HENGLEI JIA¹, SHENHAO CHEN^{1,4}, BOYU YUAN², CHAO WANG^{3,4} и LIANG LI³

¹Department of Chemistry, Shandong University, Jinan 25010089, ²Department of Physics, Xuzhou Normal University, Xuzhou 221116, ³Department of Chemistry, Xuzhou Normal University, Xuzhou 221116 и

⁴State Key Laboratory for Corrosion and Protection, Shenyang 110016, P. R. China

Динамички процес корозије у пукотинама током анодног растварања у раствору 5,0 mmol dm⁻³ NaCl праћен је дигиталном холографском реконструкцијом. Дигитална холографска реконструкција се показала као ефикасна *in situ* техника за детекцију промене концентрације, јер даје корисне и директне информације у виду тродимензионих слика. Она омогућава боље разумевање механизма корозије у пукотинама испитивањем динамике промене концентрације раствора уз површину пукотине.

(Примљено 7. јула, ревидирано 27. августа 2008)

REFERENCES

1. J. A. Wharton, K. R. Stokes, *Electrochim. Acta* **53** (2008) 2463
2. X. He, D. S. Dunn, A. A. Csontos, *Electrochim. Acta* **52** (2007) 7556
3. Z. Li, F. Gan, X. Mao, *Corros. Sci.* **44** (2002) 689
4. R. C. Wolfe, K. G. Weil, H. W. Pickering, *J. Phys. Chem. B.* **108** (2004) 14298
5. A. H. Goff, S. Joiret, D. Abourazzouk, *Electrochim. Acta* **43** (1998) 53
6. F. Loëte, B. Vuillemin, R. Oltra, D. Chaumont, E. Bourillot, *Electrochem. Commun.* **8** (2006) 1016

7. B. Vuillemin, R. Oltra, R. Cottis, D. Crusset, *Electrochim. Acta* **52** (2007) 7570
8. G. Salvago, L. Magagnin, M. Bestetti, *Electrochim. Acta* **47** (2002) 1787
9. X. Yang, S. Chen, C. Wang, L. Li, *Electrochem. Commun.* **6** (2004) 643
10. F. Charrière, N. Pavillon, T. Colomb, C. Depeursinge, *Opt. Express.* **14** (2006) 7005
11. B. Rappaz, P. Marquet, E. Cuche, Y. Emery, C. Depeursinge, P. J. Magistretti, *Opt. Express.* **13** (2005) 9361
12. B. Yuan, S. Chen, X. Yang, C. Wang, L. Li, *Electrochem. Commun.* **10** (2008) 392
13. L. Li, C. Wang, S. Chen, X. Hou, X. Yang, *J. Serb. Chem. Soc.* **73** (2008) 561.



J. Serb. Chem. Soc. 74 (2) 203–212 (2009)
JSCS–3823

Titanium diffusion coatings on austenitic steel obtained by the pack cementation method

MIRELA BRITCHI^{1*}, NICULAE ENE¹, MIRCEA OLTEANU¹
and CONSTANTIN RADOVICI²

¹Romanian Academy, Institute of Physical Chemistry “Ilie Murgulescu”, Splaiul
Independentei, 202, Bucharest and ²ICECHIM, Splaiul Independentei,
202, Bucharest, Romania

(Received 21 March, revised 25 June 2008)

Abstract: The surface of specimens made of 316L austenitic steel was modified by titanium diffusion. The diffusion coatings were obtained by packing in a powder mixture consisting of titanium powder, NH_4Cl and Al_2O_3 powder. The procedure required high temperatures, over 900 °C, and long durations. Atomic titanium was formed in the muffle during the process. Titanium atoms from the metallic part surfaces diffuse towards the interior and a diffusion layer is formed as a function of the steel composition. Titanium diffusion into the surface of 316L austenitic steel determines the formation of a complex coating: a thin layer of TiN at the exterior and a layer consisting of compounds containing Ti, Ni and Fe in the interior of the coating. The obtained coatings were continuous, adherent and had a hardness higher than that of the substrate material. The diffusion coatings were investigated by optical and electron microscopy, X-ray diffraction and Vickers microhardness tests.

Keywords: titanium diffusion coatings on 316L austenitic steel; pack cementation method.

INTRODUCTION

In addition to a very broad field of other applications, 316L austenitic steel with a high content of chromium (16–18 wt. %) and nickel (10–14 wt. %)¹ is employed for the manufacture of bone implants, such as hip, knee and femur prostheses. This type of steel is well tolerated by the human organism but after a long period of time in contact with human fluids metallic ions leach from the prostheses. It has been proved that hexavalent chromium ions are very toxic or even cancerous.^{2,3} Such a drawback can be overcome if the surface of the implant is coated with a biovitroceramic layer. The biovitroceramic material previously stu-

* Corresponding author. E-mail: iuliab40@yahoo.com
doi: 10.2298/JSC0902203B

died^{4,5} possessed a thermal dilatation coefficient much lower than that of 316L austenitic steel and close to that of TiN ($\alpha = 90 \times 10^{-7} \text{ }^\circ\text{C}^{-1}$).⁶

In order to achieve a better adherence between the previously studied biovitroceramic and the steel, the thermal dilatation coefficients of the two materials have to be as similar to each other as possible. This can be achieved by modifying the composition and the surface structure of samples made of 316L austenitic steel by diffusion layers. As a function of covering elements and substrate material, the surface layers obtained by diffusion processes can be of the solid solution type with wide miscibility domains or, otherwise, a sequence of phases can be formed progressively according to the equilibrium diagrams. Two concurrent diffusion processes occur, *i.e.*, the diffusion of the covering element or elements towards the bulk of the metallic substrate is accompanied by the diffusion towards the surface of elements from the substrate material. Within the layer, the mass transport is characterized by the diffusion coefficients, while layer increase occurs according to kinetic laws specific to each phase.⁷ Formation of these layers offers several advantages, *i.e.*, very good adherence to the substrate, chemical and mechanical properties superior to those of the substrate material and only minimal dimensional changes occur. There are several methods for obtaining diffusion layers. The one employed in this work, much studied in previous papers, is that of powder packing using ammonium chloride as an activator.^{8–10} Using the pack cementation method, diffusion coatings with different elements, Cr,^{11–13} V,^{13,14} Al,^{15–17} B,¹⁸ Cr–V,^{12,13,19} Al–Cr,^{20–22} Cr–Si,^{23,24} and Ti,^{25–28} can be obtained.

Diffusion layers are formed in two different stages. In the first stage, the diffusive element is brought in contact with the surface of the substrate material and in the second one, the diffusion process which follows consists of the gradual adsorption of the diffusive element into the base material network of the substrate. In the case of the powder mixture packing method with NH_4Cl as the activator, the diffusive element is formed as a result of a chemical reaction in the gaseous state. In general, the mechanism for supplying the diffusive element is as follows. The gaseous phase consists of halides, especially chlorides. Several types of reactions can occur in which a BX_2 halide of a metal frees the diffusive element B so that it can diffuse into the substrate metal A. These reactions can be represented schematically as:¹⁰

Change reaction:



Reducing reaction:



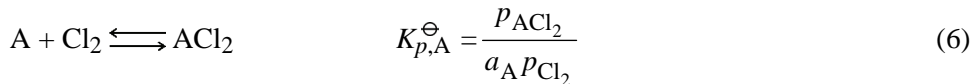
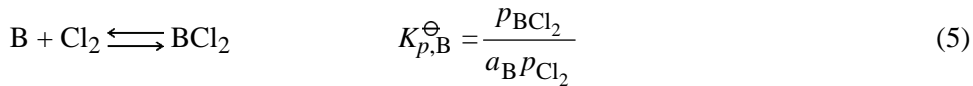
Thermal decomposition reaction:



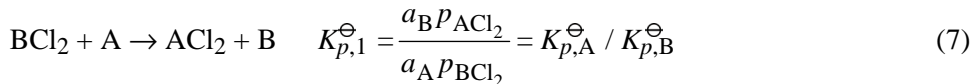
The change reaction implies the removal or displacement of an A atom from the surface of the base material for each deposited B atom. For A and B atoms with similar atomic masses, this reaction produces only minimal changes of the sample weight regardless of the thickness of the diffusion layer. The other two reactions lead to a weight increase of the treated material. The possibility for these reactions to occur can be inferred from some thermodynamic considerations. The concentration of the B element deposited on the metallic substrate A depends on the partial pressure of the gaseous compounds at the treatment temperature, P_i , and activities, a_i , of both the deposited material B and the base metal A. If the equilibrium condition for free energy, ΔG^\ominus , is applied:

$$\Delta G^\ominus = -2.303RT \log K_p^\ominus \quad (4)$$

for the formation of BCl_2 and ACl_2 halides, reactions (5) and (6), then the equilibrium constants, K_p^\ominus , are:



and for the interchange reaction (1):



$$\text{Log } K_{p,1}^\ominus = \text{log } K_{p,\text{A}}^\ominus - \text{log } K_{p,\text{B}}^\ominus \quad (8)$$

For layers where $a_{\text{A}} \approx a_{\text{B}}$ at the surface, a difference of -1 units in equation (8) means that $\approx 10\%$ of the metal chloride vapors are converted into the covering metal in an atomic state. A difference of -2 units represents a conversion of $\approx 1\%$, which is the minimum for a practical interchange reaction.¹⁰

The goal of this work was to obtain titanium diffusion layers on the surface of 316L austenitic steel specimens by the pack cementation procedure. The diffusion layers obtained in this manner modify the surface properties of the steel.

EXPERIMENTAL

The 316L austenitic steel samples used as substrates were in the form of small plates with dimensions of $10 \text{ mm} \times 10 \text{ mm} \times 3 \text{ mm}$. The chemical composition of 316L steel is given in Table I. Prior to the thermochemical treatment, all the plates were ground on a set of 240–280 mesh emery papers and degreased in acetone. There were weighted before and after the treatment with a precision to the fourth decimal (10^{-4} g).

The powder mixtures consisted of the following substances: 99.9% (Merck purity) titanium powder with a $150 \mu\text{m}$ granulation, 99.5% aluminum oxide with a $125 \mu\text{m}$ granulation and p. a. ammonium chloride. The ammonium chloride was dehydrated and finely ground be-

fore preparation of the mixtures. 3 wt. % NH_4Cl was used in all the experiments. The titanium and aluminum oxide powders were employed in various concentrations. The working conditions for the sample treatment are shown in Table II.

TABLE I. Composition and thermal dilatation coefficients of 316L austenitic steel

Composition wt. %	C	Cr	Ni	Mn	Mo	Si	P	S	N	Fe
	0.03	16–18	10–14	2.0	2–3	0.75	0.045	0.03	0.10	Up to 100
Thermal dilatation coefficient, $\alpha \times 10^7 / ^\circ\text{C}^{-1}$					159 (0–100 $^\circ\text{C}$) 162 (0–315 $^\circ\text{C}$) 175 (0–538 $^\circ\text{C}$)					

TABLE II. Working conditions for different treatments

Powder mixture composition, wt. %			$t / ^\circ\text{C}$	τ / h
Ti	Al_2O_3	NH_4Cl		
77	20	3	1000; 1125; 1150; 1200	2; 5; 7.5

Powder mixtures together with the samples were placed in refractory steel crucibles with a 25 mm diameter and 50 mm height. Only one sample, placed exactly in the middle of the crucible, was treated at a time. The powder mixture was compacted carefully around the sample so that the latter was uniformly covered. The crucible was filled up to the upper end, covered with a metallic lid and placed in a ceramic crucible in order to protect the ceramic wall of the furnace. A L-1206 M type furnace with a horizontal hearth and a Kanthal electrical resistance provided with a Chromel–Alumel thermocouple with a precision of the maintaining the temperature in a stability regime of ± 2 $^\circ\text{C}$ was employed.

After treatment, the samples were cleaned, degreased in acetone and prepared for examination. They were mounted in methacrylate in the cross section and ground on 240–1200 mesh emery papers and a felt impregnated with Al_2O_3 emulsion (0.75 and 0.25 μm). The surfaces prepared in such a manner were etched with Vilella reagent (1.0 g picric acid, 5.0 cm^3 concentrated HCl and 95 cm^3 ethanol).

Optical microphotographs were taken by means of an optical M.C.1.M. microscope provided with an Exacta Vares camera.

An SEM Hitachi-S 2600 instrument equipped with a dispersive energy spectroscope (EDS) was used for qualitative and quantitative analysis. Images of secondary electrons (SEM) and $\text{XK}\alpha$ -rays for Ti, Cr, Ni and Fe were obtained.

In order to identify the phases and compounds formed within the diffusion layer, the samples were examined by X-ray diffraction with a DRON-20 instrument using $\text{CuK}\alpha 1$ radiation ($\lambda = 1.54178$ \AA).

Vickers microhardness values of both the layer and the metal substrate were measured with a Hannemann hardness meter provided with a diamond pyramid with an angle of 136° between the facets²⁹ and calculated using the Relation:

$$HV_p = 1854.4 \frac{P}{\varepsilon^2 d^2} \quad (9)$$

where P is the penetration force (in the present case, $P = 100$ gf), ε is a transforming factor (a micrometric division is equal to 0.2907 μm) and d represents the number of micrometric divisions corresponding to the microhardness indent diagonal. The values of the Vickers microhardness, HV_p , are expressed in Kgf/mm^2 .

RESULTS AND DISCUSSION

The samples titanized under conditions when the powder mixture contained 77 wt. % titanium and treated at temperatures of 1000, 1150 and 1200 °C for 5 h are shown in Figs. 1–3, respectively. The diffusion layers were continuous, uniform, very adherent to the metallic substrate and had a thickness between 30 and 350 µm.

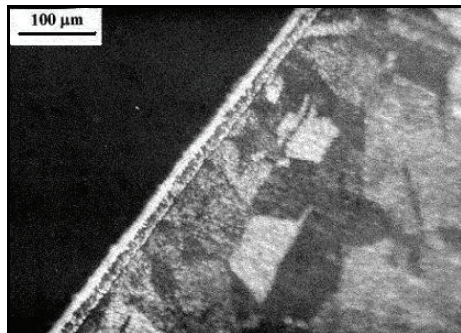


Fig. 1. Optical microphotograph of a cross section of a sample titanized in a powder mixture with 77 wt. % Ti at 1000 °C for 5 h; Vilella metallographic etchant.

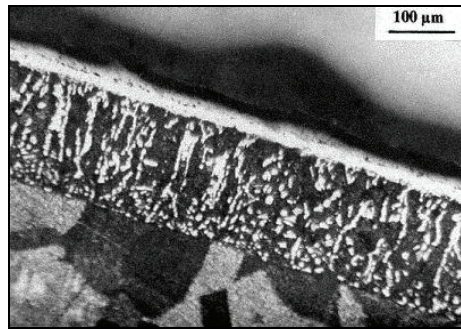


Fig. 2. Optical microphotograph of a cross section of a sample titanized in a powder mixture with 77 wt. % Ti at 1150 °C for 5 h; Vilella metallographic etchant.

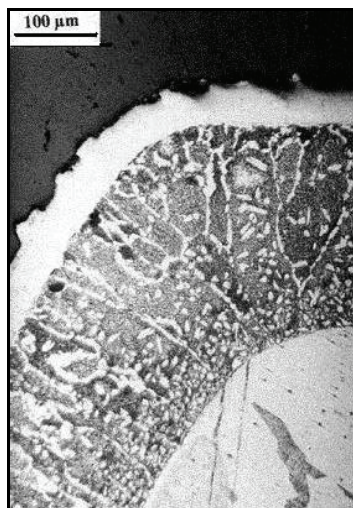


Fig. 3. Optical microphotograph of a cross section of a sample titanized in a powder mixture with 77 wt. % Ti at 1200 °C for 5 h; Vilella metallographic etchant.

The variation of the layer thickness with temperature is shown in Fig. 4, from which it can be seen that the variation follows an exponential law typical for a diffusion process. The variation of the layer thickness with time at a constant temperature, 1000 °C, follows a parabolic law, as can be seen from Fig. 5, this being another proof for the fact that the layers formed with the participation of a diffusion process.

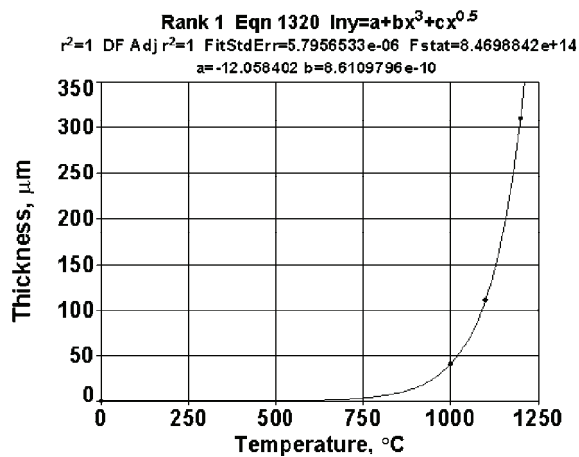


Fig. 4. Variation of the layer thickness with temperature (diffusion time 5 h; 77 wt. % Ti).

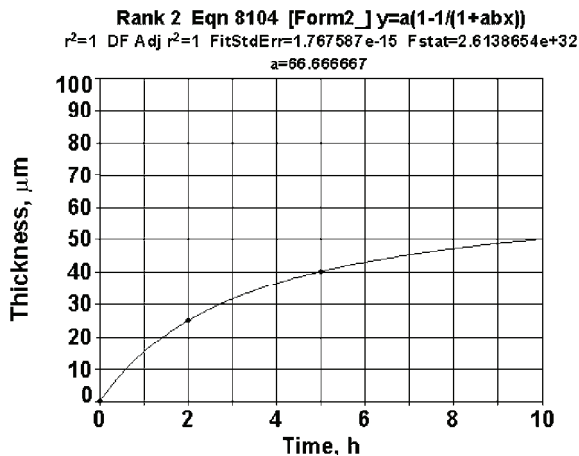


Fig. 5. Variation of the layer thickness with time (temperature 1000 °C; 77 wt. % Ti).

Vickers microhardness measurements are listed in Table III. The indent size on the layers was much smaller than that on the austenitic steel substrate (Fig. 6).

The distribution of titanium within the layer and the main elements, Cr, Ni and Fe, that underwent thermochemical treatment of the sample at 1150 °C for 5 h was well evidenced by SEM and EDS (Figs. 7–11).

From Fig. 7, it can be seen that titanium diffused not only into the coating, but, in a lower concentration, also into the substrate.

TABLE III. Vickers microhardness (average of at least 5 measurements) of different layers and substrate (77 wt. % Ti; 1200 °C; 5 h)

Zone	$HV_P / \text{Kgf mm}^{-2} (P = 100 \text{ gf})$
Layer (exterior zone, thin, light color)	849
Layer (interior zone, thicker)	475
Substrate of 316L austenitic steel	158
Untreated 316L austenitic steel	203

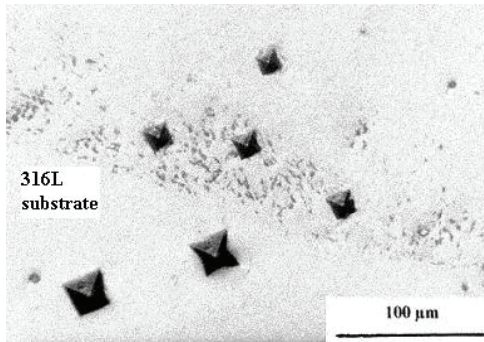


Fig. 6. Vickers microhardness imprints on a cross section coating-substrate, penetration force $P = 100 \text{ gf}$ (77 wt. % Ti; 1200 °C; 5h).

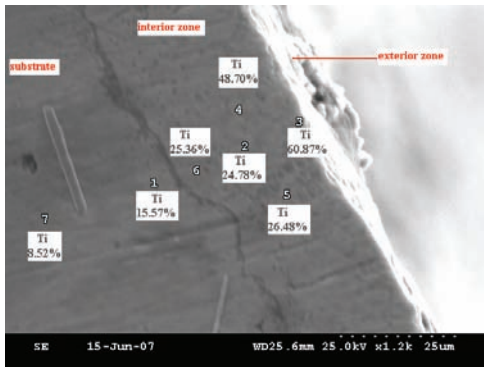


Fig. 7. SEM Secondary electron image of a cross section of a sample titanized in a powder mixture with 77 wt. % Ti at 1150 °C for 5 h.

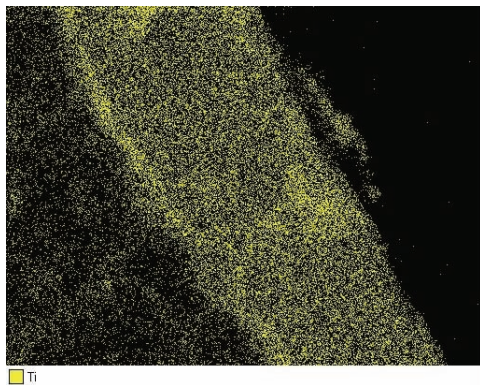


Fig. 8. Image of X- ray $K\alpha\text{Ti}$; $\times 1200$; (77 wt. % Ti; 1150 °C; 5h).

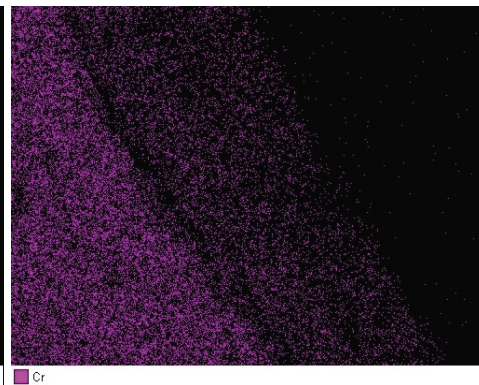


Fig. 9. Image of X- ray $K\alpha\text{Cr}$; $\times 1200$; (77 wt. % Ti; 1150 °C; 5h).

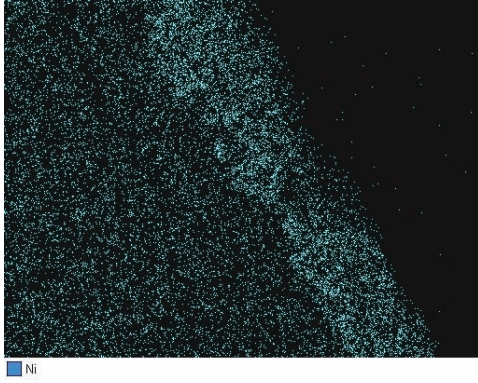


Fig.10. Image of X- ray $K\alpha$ Ni; $\times 1200$;
(77 wt. % Ti; 1150 °C; 5h).

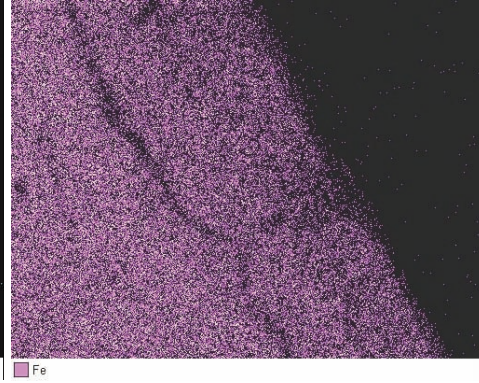


Fig. 11. Image of X- ray $K\alpha$ Fe; $\times 1200$;
(77 wt. % Ti; 1150 °C; 5h).

It may be seen by examining Figs. 8 and 9 that titanium almost replaced chromium in the coating. Figure 10 shows that nickel concentrates in the inner layer. The distributions of iron in the coating and substrate do not differ significantly (Fig. 11).

The X-ray diffraction analysis of the surfaces of the samples proved the formation of the TiN compound (Fig. 12), a fact that is in concordance with the high Vickers hardness value, $HVP = 100 \text{ gf} = 849 \text{ Kgf/mm}^2$, obtained for the exterior layer which was formed by diffusion with the reaction process. The TiN compound was distributed into the matrix of the layer. If the exterior layer would be formed only of the TiN compound, it would be thinner and much harder. The inner layer is much thicker and possesses a Vickers hardness lower than that of the outer one, but higher than that of the metallic substrate (Table III). The value of the hardness was constant through the entire thickness of the inner layer. This fact proved that this layer was formed also by diffusion with the reaction process.

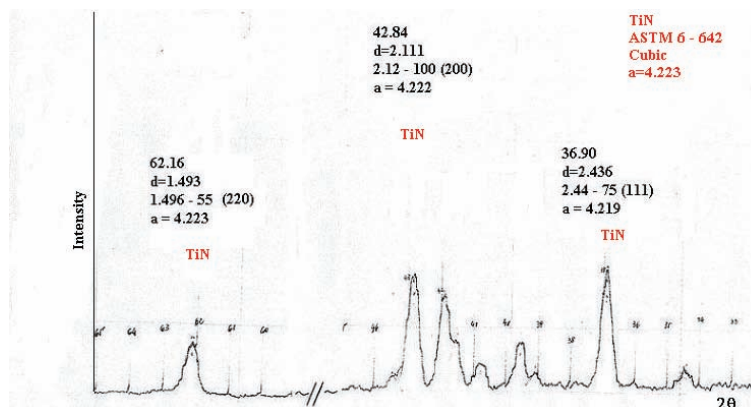


Figure 12. Diffractogram of the exterior layer of a sample titanized at 1150 °C for 5 h;
77 wt. % Ti. (d and a in Å).

The nature of the compound was different from that in the outer layer. By corroborating the data of the optical micrograph (Fig. 2), electron micrographs (Figs. 8–11) and the microhardness measurements (Fig. 6), it was concluded that the interior layer is formed of a Ti–Ni–Fe compound.

CONCLUSIONS

1. Specimens of 316L austenitic steel used in implantology for manufacturing prostheses were subjected to thermochemical treatment by titanium diffusion in order to obtain surface coatings.

2. As a function of the variation of the process parameters, temperature and duration, diffusion layers with a thickness between 30 and 350 μm were obtained.

3. All coatings obtained at temperatures higher than 900 °C consisted of two zones:

– an exterior zone, thin and lightly colored, formed of TiN and with a hardness approximately 5 times higher than that of the metallic substrate;

– a thicker inner zone formed of a Ti–Ni–Fe compound. The hardness value of this layer was approximately 3 times higher than that of the metallic substrate with the constant value throughout the whole thickness.

Acknowledgement. The authors thank Mr. Gabriel Dumitrescu for performing the optical and electron photo images.

ИЗВОД

ПРЕВЛАКЕ НА АУСТЕНИТНОМ ЧЕЛИКУ НАСТАЛЕ ДИФУЗИЈОМ ТИТАНА ПАКУЈУЋОМ ЦЕМЕНТАЦИЈОМ

MIRELA BRITCHI¹, NICULAE ENE¹, MIRCEA OLTEANU¹ и CONSTANTIN RADOVICI²

¹Romanian Academy, Institute of Physical Chemistry “Ilie Murgulescu”, Splaiul Independentei, 202, Bucharest u ²ICECHIM, Splaiul Independentei, 202, Bucharest, Romania

Површина узорака аустенитног челика 316L модификована је дифузијом титана. Превлаке настале дифузијом добијене су паковањем из смеше прахова која се састојала од прахова титана, NH_4Cl and Al_2O_3 . Процедура је дуготрајна и захтева високе температуре, преко 900 °C. На почетку процеса формира се атомски титан. Атоми титана дифундују из металних делова површине ка унутрашњости, чиме се формира дифузиони слој у зависности од саптава челика. Дифузија титана у површину аустенитног челика одређује формирање комплексне превлаке: танак слој TiN у површинским деловима превлаке и слој у унутрашњости превлаке који се састоји од једињења која садрже Ti, Ni и Fe. Добијене превлаке су континуалне, добро пријањајуће и тврдоће која је већа од оне коју има материјал подлоге. Дифузионе превлаке су испитиване оптичком и електронском микроскопијом, дифракцијом x-зрака и Vickers-овим тестом микротврдоће.

(Примљено 21. марта, ревидирано 25. јуна 2008)

REFERENCES

1. C. J. Smithells, *Metals Reference Book*, 3rd Ed., Butterworth, London, 1962, p. 705
2. D. H. Kohn, *Curr. Opin. Solid State Mater. Sci.* **3** (1998) 309

3. L. E. Eiselstein, D. M. Proctor, T. C. Flowers, *Mater. Sci. Forum* **539–543** (2007) 698
4. M. Britchi, M. Olteanu, N. Ene, *Int. J. Mater. Prod. Technol.* **25** (2006) 267
5. M. Britchi, M. Olteanu, N. Ene, *Adv. Mater. Res.* **23** (2007) 217
6. J. D. Lee, Y. M. Choi, O. S. Lee, S. H. Lee, US Patent 6018142 (1998)
7. P. G. Shewmon, *Diffusion in Solids*, 2nd Ed., TMS-AIME, Warrendale, PA, 1989
8. K. Rafferty, B. Rowe, US Patent 5334417 (1994)
9. M. Britchi, M. Olteanu, N. Ene, *Proceedings of METAL 2005, the 14th International Metallurgical and Material Conference*, Hradec and Moravici, Czech Republic, 2005, p. 1
10. N. A. Lockington, *Principles of Applying Coatings by Diffusion*, Corrosion, 2nd Ed., Newnes – Butterworths, London, 1976, p. 58
11. C. H. Koo, T. H. Yu, *Surf. Coat. Technol.* **126** (2000) 171
12. N. Petrescu, M. Petrescu, M. Britchi, *Int. J. Mater. Prod. Technol.* **8** (1993) 273
13. M. Britchi, M. Olteanu, D. Gheorghe, M. Branzei, *Surface Modification Technologies XV*, T. S. Sudarshan, J. J. Stiglich, M. Jeandin, Eds., ASM International, Materials Park Ohio and IOM Communications Ltd., London, 2002, p. 287
14. V. I. Pokhmurskii, S. V. Tolstova, A. M. Mokrova, *Mater. Sci.* **9** (1975) 630
15. Z. D. Ziang, P. K. Datta, *Mater. Sci. Technol.* **22** (2006) 1177
16. Z. D. Xiang, P. K. Datta, *Acta Mater.* **54** (2006) 4453
17. C. Houngninou, S. Chevalier, J. P. Larpin, *Mater. Sci. Forum* **461–464** (2004) 273
18. N. Ueda, T. Mizukoshi, K. Demizu, T. Sone, A. Ikenaga, M. Kawamoto, *Surf. Coat. Technol.* **126** (2000) 25
19. M. Britchi, N. Petrescu, M. Petrescu, *Sci. Bull. P. I. B. Chem. Mater. Sci.* **53** (1991) 147
20. Z. D. Xiang, S. R. Rose, P. K. Datta, *Mater. Sci. Technol.* **18** (2002) 1479
21. M. T. Kim, N. H. Heo, J. H. Shim, C. Y. Kim, *Surf. Coat. Technol.* **123** (2000) 227
22. M. Zheng, R. A. Rapp, *Oxid. Met.* **49** (1998) 19
23. X. P. Guo, L. X. Zhao, P. Guan, K. Kusabiraki, *Mater. Sci. Forum* **561–565** (2007) 371
24. M. A. Harper, R. A. Rapp, *Oxid. Met.* **42** (1994) 303
25. S. Hirai, S. Ueda, *J. Japan Inst. Metals* **51** (1987) 1039
26. S. Hirai, S. Ueda, *J. Japan Inst. Metals* **51** (1987) 1030
27. M. Moradi, *Trans. Mater. Heat Treat.* **25** (2004) 661
28. M. Britchi, M. Momirlan, I. Pencea, *Int. J. Mater. Prod. Technol.* **13** (1998) 400
29. H. Colan, M. Filipescu, E. Bicsak, *Studiul Metalelor*, Ed.: Didactica si Pedagogica, Pedagogica, Bucuresti, Bucharest, 1968, p. 117 (in Romanian).



J. Serb. Chem. Soc. 74 (2) 213–221 (2009)
JSCS–3824

Mesophilic leaching of copper sulphide sludge

VLADIMIR B. CVETKOVSKI^{1*}, VESNA T. CONIĆ¹, MILOVAN VUKOVIĆ^{2#}
and MILENA V. CVETKOVSKA³

¹Mining and Metallurgy Institute, Bor, ²Technical Faculty, University of Belgrade, Bor
and ³Faculty of Chemistry, University of Belgrade, Belgrade, Serbia

(Received 16 May, revised 24 June 2008)

Abstract: Copper was precipitated using a sodium sulphide solution as the precipitation agent from an acid solution containing 17 g/l copper and 350 g/l sulphuric acid. The particle size of nearly 1 μm in the sulphide sludge sample was detected by optical microscopy. Based on chemical and X-ray diffraction analyses, covellite was detected as the major sulphide mineral. The batch bioleach amenability test was performed at 32 °C on the Tk31 mine mesophilic mixed culture using a residence time of 28 days. The dissolution of copper sulphide by direct catalytic leaching of the sulphides with bacteria attached to the particles was found to be worthy, although a small quantity of ferrous ions had to be added to raise the activity of the bacteria and the redox potential of the culture medium. Throughout the 22-day period of the bioleach test, copper recovery based on residue analysis indicated a copper extraction of 95 %, with copper concentration in the bioleach solution of 15 g/l. The slope of the straight line tangential to the exponential part of the extraction curve gave a copper solubilisation rate of 1.1 g/l per day. This suggests that a copper extraction of 95 % for the period of bioleach test of 13.6 days may be attained in a three-stage bioreactor system.

Keywords: copper; acid solutions; hydrogen sulphide; sulphide sludge; bioleaching.

INTRODUCTION

The ecological hazards caused by uncontrolled release of the Bor mining and metallurgical effluent streams have not been addressed for a long time. Acidic effluent streams from industrial activities are traditionally treated by the process of lime neutralization. This treatment method is expensive, and produces a gypsum sludge which requires dewatering and disposal.¹

* Corresponding author. E-mail: vladimirc@ibb-bor.co.yu

Serbian Chemical Society member.

doi: 10.2298/JSC0902213C

Over the course of time, the Bor Mining and Metallurgical Company has developed several projects for copper extraction and neutralization of the mine water and acid solutions, but not one of them gave a sufficiently good result. These processes were as follows: copper sulphate production from tank house bleed electrolyte, copper cementation from mine water, improvement of cementation on scrap iron,^{2,3} neutralization of mine acid water in a tailing pond^{4,5} and electrowinning of copper from acid solutions.⁶⁻⁸

The low recovery and the low grade of the copper produced in these plants meant that further smelting was required, which is often not economically justified. The present situation in the mining and metallurgical complex Bor is that copper losses with mine water are nearly 300 tons per year, with a concentration of copper from 0.3 to 1 g/l and a pH ranging from 1.8 to 3.5. Moreover, losses with metallurgical acid solutions are nearly 50 tons per year, with a concentration of Cu of 3 to 20 g/l with that of sulphuric acid ranging between 20 to 400 g/l.

Successful treatment of tank house acid solution was performed by the Cerro Copper Product, which includes solvent extraction, electrowinning, evaporation, crystallization and filtration processes for copper and nickel sulphate production.⁹

The object of this study was to attempt to solve the problem of copper recovery from acid effluent streams by new biohydrometallurgical processes and, at the same time, to decrease the environmental hazards in the area of East Serbia. It has already been demonstrated that the particle size distribution can dramatically affect the bioleaching efficiency when using extreme thermophilic bacteria.¹⁰⁻¹² The sulphide sludge was produced from metallurgical effluent streams (tank house, copper sulphate plant, copper powder plant and dore plant) by conventional hydrogen sulphide precipitation followed by mesophilic leaching, solvent extraction and electrowinning of the obtained leach solution.

EXPERIMENTAL

Bacterial inoculum

A mesophilic acidophiles culture provided by Mining and Smelting Company Bor was used as the inoculum. This culture (named Tk31) originates from the underground copper mine Tilva Ros. The bacterial strains were identified as a mixed culture of acidithiobacillus ferrooxidans and acidithiobacillus thiooxidans. Their optimum growth temperature was in the range between 30 and 35 °C, and their tolerance to copper and iron was attained naturally in the existing underground copper mine.¹³

Sulphide materials

The laboratory scale study was performed using copper sulphide sludge obtained by conventional hydrogen sulphide precipitation from an acid solution received from the copper sulphate plant.

A sodium sulphide solution was used as the precipitation agent from an acid solution with a copper content of 17 g/l and a concentration of sulphuric acid of 350 g/l.

Mineralogical analysis

The relative proportions of the minerals present in a sample were determined by the X-ray diffraction analysis.

Nutrient

The composition of the nutrition medium used during the test was (in g/l): $(\text{NH}_4)_2\text{SO}_4$, 3.0; KCl, 0.10; K_2HPO_4 , 0.50; $\text{MgSO}_4 \cdot 7\text{H}_2\text{O}$, 0.50; $\text{Ca}(\text{NO}_3)_2 \cdot 4\text{H}_2\text{O}$, 0.010 and ferrous irons, 2.2.

Batch bioleach test

The laboratory-scale unit consisted of 4-litre glass reactors with 2.9 l of culture media. The operating temperature was maintained at around 32 °C. The bioleach culture medium consisted of sulphide sludge with a low solids concentration, concentrated nutritive medium (1.5 \times) and Tk31 inoculum, which was stirred with a magnetic stirrer. The operating conditions were as follows: solids concentration 3 % (w/w), air flow 20 Nl/h, with a 21 % (v/v) oxygen content and a 0.03 % (v/v) carbon dioxide content, and a residence time of 28 days. Existence of free bacteria in leach solution was detected using sample of bioleach medium as inoculum in 9 K solution. The pH value was maintained at approximately 1.7 by adjusting the pH of the culture medium during the leach test.

At the end of the bioleach test, after centrifugation of the solution at 3000 rpm for 5 min, microscopic observations revealed a high amount of mesophilic acidophiles.

Analytical technique

The copper and total iron concentrations in the solution were measured by atomic absorption spectrophotometry, PE-403. The pH of the leach solution was measured with a combined glass electrode at ambient temperature. The copper dissolution rates and final copper recovery were calculated by material balance using the copper concentrations in the culture medium and in the sludge residue.

RESULTS AND DISCUSSION

The results of the chemical analysis of the sulphide sludge sample are given in Table I.

TABLE I. Chemical analyses of the sulphide sludge

Element	Content (w/w)
Cu	62.10
Fe	0.18
S ^{tot}	24.00
Mg	0.02
Ca	0.03
Zn	0.01
Pb	0.02
Ni	0.02

A particle size of the sludge was $\approx 1 \mu\text{m}$ as detected by optical microscopy.

The result of X-ray analysis, presented in Fig. 1, shows covellite (CuS) as the major phase in the sample.

The sulphide mineral component of the sulphide sludge was $\approx 99 \%$. According to the chemical and X-ray analyses of the sample, the extent of copper sul-

phides was about 98 %, the rest were traces of other metal sulphides. It should be noted that the X-ray analysis could not distinguish between covellite and chalcocite (Cu_2S), due to their finely intergrown nature. Consequently, these two species are designated as Cu-sulphides in which, according to chemical analysis, due to lower content of sulphur, the amount of covellite and chalcocite was approximately 65 and 35 %, respectively. The fine material was used as the feed material in the test work programme.

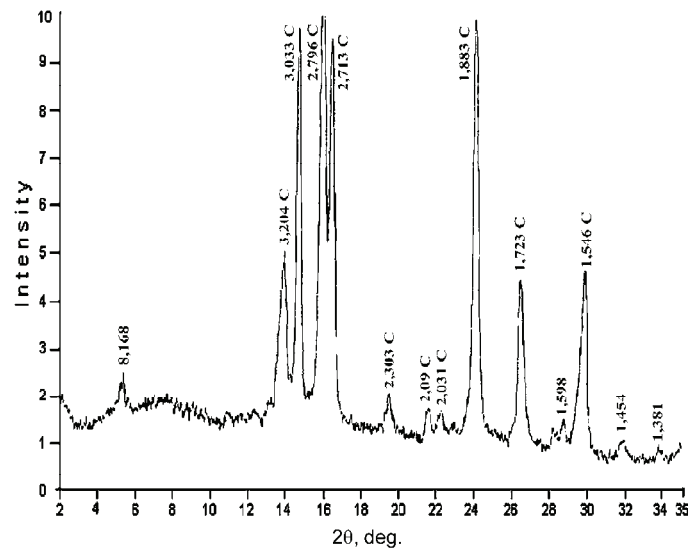


Fig. 1. X-Ray diffraction pattern of the sample (C – covellite).

The variation of pH monitored in the culture medium during the test is presented in Fig. 2. The pH, initially adjusted to 1.7 with sulphuric acid, always attained a value over 2 because of the neutralization of some quantity of sodium remaining in sample and the chemical dissolution of copper generated during the direct bioleaching of chalcocite.

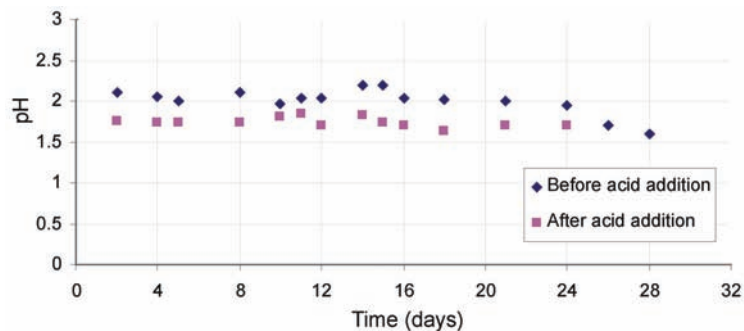


Fig. 2. pH Values as a function of time.

The results of copper extraction obtained in terms of biochemical leaching of the sample are presented in Fig. 3 as a plot of the copper content vs. time. The plot shows a pronounced “S”-shaped curve. The section of this curve corresponds to the lag, exponential and asymptotic growth regions, respectively. Through a series of inoculations, the bacteria will adapt to the sulphide sludge, and the lag phase will be considerably decreased, and the bacterial growth and leaching rate increased.¹⁴

Throughout the 22-day bioleach test, the copper recovery based on residue analysis indicated a copper extraction of 95 %, with copper concentration in the bioleach solution of 15 g/l (corresponding to the maximum content of copper in Fig. 3, representing the highest value of copper in g/l). The bioleach solution obtained of 15 g/l and pH 1.7 is convenient for down stream processes, which includes three stages of extraction, two stages of stripping and electrowinning for cathodic copper production.

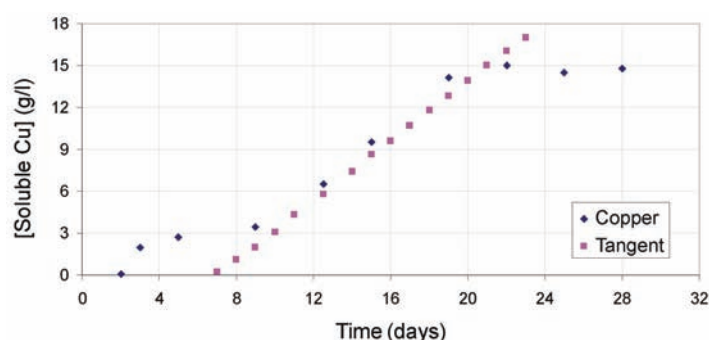


Fig. 3. Content of Cu as a function of time.

A summary of the extractions based on residue analysis is presented in Table II.

TABLE II. Summary of the results obtained from the batch bioleach test during 22 days

Element	Amount extracted, %
Cu	95
S ²⁻	96

Gericke¹⁵ suggested that in a multi-stage reactor system, an acceptable copper solubilisation rate should be achievable in line with those demonstrated by the mesophilic batch bioleach test. The slope of the straight line tangential to the exponential part of the curve, which is a measure of the copper solubilisation rate, was 1.1 g/l per day. This indicates that at a high redox potential it is possible to achieve a copper extraction of 95 % for the period of bioleach test of 13.6 days in a three-stage bioreactor system.

The dissolution of a copper sulphide sludge by bacteria involves direct and indirect leaching. Recently, some authors¹⁶ disregarded the difference between

the direct and indirect leaching, combining these mechanisms into a single process. For the present purposes, the direct/indirect model is still useful for the introduction of the basic chemical reactions arising in the process.

It is supposed that the dissolution of covellite and chalcocite by bacteria was involved in the direct leaching; the bacteria attached to the particles catalyse the oxidation of the covellite and chalcocite crystals into soluble sulphates, thereby dissolving copper in the sulphuric acid solution.^{17–19} Direct leaching includes the oxidation by *T. ferrooxidans* of covellite into copper sulphate (CuSO_4), and chalcocite (Cu_2S) into copper sulphate and copper. These processes are illustrated by the following chemical Reactions:



Moreover, according to the electrochemical principle, it is necessary for the dissolution of a mineral that a distinct difference between the redox potential (E_h) of the medium solution and the electrostatic potential of the sulphide mineral condition should exist.²⁰

In the present work, in order to improve the bioleaching process, a small quantity of 2.5 g/l of ferrous ions was added to the leach solution. A better optimization of the culture conditions by adding different oxidants, such as pure pyrite or a higher content of ferric ions, as well as nutrient requirements and carbon dioxide, would improve the overall bioleaching performances.

The variation of the iron content in the culture media is illustrated in Fig. 4. Initially, the added 2.5 g/l of ferrous iron was oxidized during the bioleaching process to ferric iron, increasing the $\text{Fe}^{3+}/\text{Fe}^{2+}$ ratio, *i.e.*, the redox potential of the culture medium up to approximately 18 g/l.

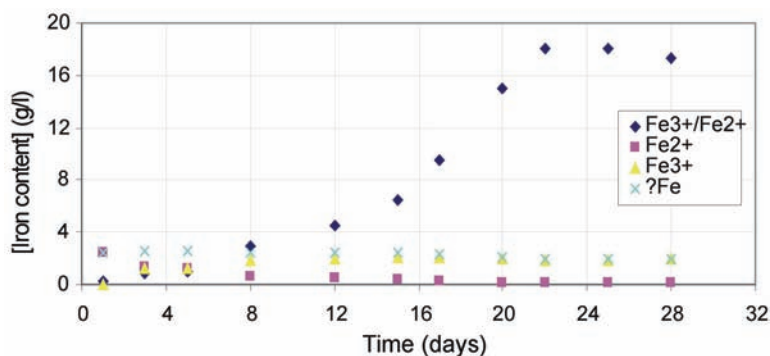
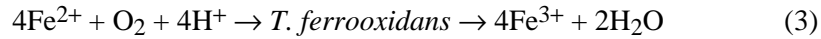
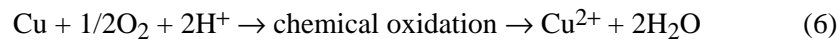
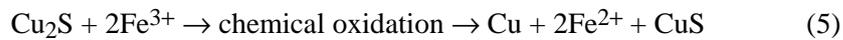


Fig. 4. Ferric/ferrous ratio as a function of time.

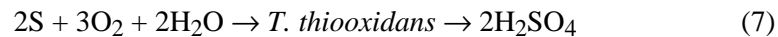
Direct bacterial oxidation of ferrous iron (Fe^{2+}) compounds present in the leach solution to ferric iron (Fe^{3+}) may be described by the following chemical Reaction:



In the indirect leaching, the oxidation of the metal sulphide crystals is mediated by ferric iron (Fe^{3+}) originating from the direct bacterial oxidation of ferrous iron (Fe^{2+}) compounds present in the culture medium, as shown in Eq. (3). Thus, the ferric iron produced in Eq. (3) can leach copper as copper sulphate from covellite and copper and copper sulphide (covellite) from chalcocite, as shown below:



The sulphur resulting from Eq. (4) can, in turn, be recycled by *T. thiooxidans* into sulphuric acid, Eq. (7), where sulphuric acid is used as a reactant in Eq. (3) when only ferrous sulphate is available in the process for the generation of ferric sulphate:



The Cu extraction data (based on the residue analyses) presented in Table II indicates that the amounts of copper and sulphur extracted from the copper sulphide sludge over a period of 22 days were 95 of 96 %, respectively.

An ongoing batch amenability ferric leach test at 70 °C that a 95 % copper recovery was attained with a 3-day residence time, *i.e.*, the result attainable in tests with thermophilic bacteria.

CONCLUSIONS

The starting point of this study was to provide appropriate operating parameters for the industrial application and to increase the copper recovery from secondary raw materials and improve environmental protection. The result achieved during the mesophilic bioleaching of sulphide sludge that the dissolution of sulphide copper from the sulphide sludge with mesophilic mixed culture is technically feasible. Over the period of the batch bioleach amenability test of 22 days, copper recovery (based on residue analysis) indicated a copper extraction of 95 %, with a copper concentration in the leach solution of 15 g/l. In a three-stage reactor system, an acceptable copper solubilisation rate should be achievable in line with those demonstrated by the mesophilic batch bioleach test. The slope of the straight line tangential to the exponential part of the curve, which is a measure of the copper solubilisation rate of 1.1 g/l per day, indicates a copper extraction of 95 % over the period of 13.6 days in the three-stage bioreactor system. Better optimization of the culture conditions by the addition of different oxidants, such as pure pyrite or higher amounts of ferric ions, as well as nutrient requirements and carbon dioxide, would improve the overall bioleaching performances.

Acknowledgements. This work was carried out in the frame of BioMinE (European project contract NMP1-CT-500329-1). The authors acknowledge the financial support given to this project by the European Commission under the Sixth Framework Programme for Research and Development. We also wish to thank our various partners on the project for their contributions to the work reported in this paper.

ИЗВОД

ЛУЖЕЊЕ БАКАР-СУЛФИДНОГ МУЉА МЕЗОФИЛНИМ БАКТЕРИЈАМА

ВЛАДИМИР Б. ЦВЕТКОВСКИ¹, ВЕСНА Т. ЦОНИЋ¹, МИЛОВАН ВУКОВИЋ² и МИЛЕНА В. ЦВЕТКОВСКА³

¹Институт за бакар, Бор, ²Технички факултет у Бору, Универзитет у Београду
и ³Хемијски факултет, Универзитет у Београду

Преципитација бакра остварена је употребом воденог раствора натријум-сулфида реагенса за преципитацију бакра из раствора који садржи 17 g/l бакра и 350 g/l сумпорне киселине. Величина честица у узорку, која се кретала око 1 µm, одређена је оптичком микроскопијом. Хемијском и рендгено дифракционом анализом установљено је присуство ковелина као главног сулфидног минерала. Лабораторијски биолужни тест је остварен на температури од 32 °C коришћењем Тк31 рударске мезофилне културе. Растварање сулфида бакра је остварено директним каталитичким растварањем сулфида са бактеријама на површини честица, али је незнатна количина феро-јона додата у раствор у циљу развоја бактерија и редокс потенцијала. У лабораторијском биолужном експерименту у периоду од 22 дана, растворено је 95 % бакра, и при томе остварен садржај бакра у лужном раствору 15 g/l. На основу нагиба праве линије, тј. тангенте на експоненцијални део криве растварања бакра, која представља брзину растварања бакра од 1,1 g/l на дан, одређено је растварање 95 % бакра у биолужном експерименту за време од 13,6 дана у систему континуалног рада три биореатора у серији.

(Примљено 16. маја, ревидирано 24. јуна 2008)

REFERENCES

1. S. Foucher, F. Battaglia-Brunet, D. M. Ignatiadis, *Chem. Eng. Sci.* **56** (2001) 639
2. G. Nedeljković, V. Cvetkovski, G. Đurašević, D. Milosavljević, *Copper (Bakar)* **23** (1998) 47 (in Serbian)
3. R. Marković, S. Živković Nikolić, V. Cvetkovski, in *Proceedings of 7th International Mineral Processing Symposium*, Istanbul, Turkey, (1998), p. 469
4. T. Stefanović, V. Cvetkovski, R. Lekovski, in *Proceedings of 2nd Symposium on Chemistry and Environment Protection*, V. Banja, FR Yugoslavia, (1993), p. 441 (in Serbian)
5. V. Cvetkovski, G. Djurašević, R. Lekovski, *Erzmetall*, No. 3 (2000) 178
6. Ž. Gojković, V. Cvetkovski, in *Proceedings of International conference for waste water and waste solid*, Monastery Prohor Pčinjski, FR Yugoslavia, (1994), p. 89 (in Serbian)
7. Ž. Gojković, V. Cvetkovski, R. Stanojević, R. Marković, in *Proceedings of 14th Yugoslav Symposium on Electrochemistry*, Bečići, FR Yugoslavia, (1998), p. 157 (in Serbian)
8. G. Đurašević, *Copper (Bakar)* **24** (2001) 2 (in Serbian)
9. J. L. Sundstrom, *Residues and Effluents – Processing and Environmental Considerations*, R. G. Reddy, W. P. Imrie, P. B. Queneau, Eds., The Mineral, Metals & Materials Society, 1991, p.p. 525–538
10. E. B. Lindstrom, S. Wold, N. Kettaneh-Wold, S. Saaf, *Appl. Microbiol. Biotechnol.* **38** (1993) 702

11. M. Gericke, A. Pinches, *Min. Eng.* **12** (1999) 893
12. M. Nemat, J. Lowenadler, S. T. L. Harrison, *Appl. Microbiol. Biotechnol.* **53** (2000) 173
13. V. Cvetkovski, S. Stanković, K. Pavlović, M. Šteharik, in *Proceedings of 36th IOC on Mining and Metallurgy*, Bor, Serbia and Montenegro, (2004), p. 430 (in Serbian)
14. G. I. Karavaiko, G. Rossi, A. D. Agate, S. N. Groudev, Z. A. Avakyan, *Biogeotechnology of Metals, Manual*, Centre for International Projects GKNT, Moscow, 1988, Ch.1, p. 10
15. M. Gericke, *Bioleaching of the Majdanpek and Veliki Krivelj Concentrates*, 2007 EU FP6, Biotechnology for metall bearing material in Europe, 2007
16. H. Brandl, *Microbial Leaching of Metals*, Vol. 10, Wiley-VCH, Weinheim, 2001, Ch. 8, p. 191
17. M. Boon, J. J. Heijnen, G. S. Hansford, *Mine. Proc. Extr. Metall. Rev.* **19** (1998) 107
18. L. Falco, C. Pogliani, G. A. Curutchet, *Hydrometallurgy* **71** (2003) 31
19. S. Gabriel, *Hydrometallurgy* **75** (2004) 99
20. A. Sanhueza, I. J. Ferrer, T. Vargas, *Hydrometallurgy* **51** (1999) 115.